BENTHIC ANCHIALINE HABITAT VARIABILITY IN KARST SUBTERRANEAN ESTUARIES OVER SPACE AND TIME

A Dissertation

by

JACQUELYN NICOLE CRESSWELL

Submitted to the Office of Graduate and Professional Studies of
Texas A&M University
in partial fulfillment of the requirements for the degree of

DOCTOR OF PHILOSOPHY

Chair of Committee,	Peter J. van Hengstum
Committee Members,	Anja Schulze
	Gilbert Rowe
	Karl Kaiser
Interdisciplinary Faculty Chair	Jaime R. Alvarado-Bremer

December 2019

Major Subject: Marine Biology

ABSTRACT

Diverse benthic and pelagic habitats develop in coastal estuarine settings from land-to-ocean physicochemical gradients, such as variations in salinity, dissolved oxygen, nutrients like carbon, and water circulation. Understanding the environmental controls of benthic habitat variability and how flora and fauna in those habitats respond to external environmental pressures, is of great ecological interest. Karst subterranean estuaries (KSEs) are globally distributed along coastal carbonate platforms wherein anchialine ecosystems exist that populate unique habitats. However, the environmental drivers of benthic anchialine habitat variability within karst subterranean estuaries is poorly understood. This dissertation explores benthic foraminiferal distributions in modern surface sediments and sediment cores to identify benthic anchialine habitat variability over time and space. The first study presents evidence for modern benthic anchialine habitat variability within KSEs using benthic foraminiferal distributions in caves of Bermuda. Benthic foraminiferal communities are controlled by provenance of organic matter (i.e., marine vs. terrestrial), and secondarily by other physical variables (i.e., tidal exposure, sediment grain size, light). The next study identifies developmental succession of benthic anchialine habitats in response to Holocene sea-level rise and vertical migration of a karst subterranean estuary since the last ice age in Bermuda. This study illuminates how sea-level rise can force subsurface aquatic island fauna to experience a previously unknown bottleneck event. Finally, the last study reveals that benthic anchialine habitat development over the last 10,000 years is driven initially by water mass (meteoric lens vs. saline groundwater) and secondarily by organic matter quantity and quality. This provides further evidence that sea-level rise influences benthic anchialine habitat development within KSEs. Overall, findings from this dissertation

provide multiple pieces of evidence that benthic anchialine habitat variability, over time and space, is present within KSEs. Importantly, anchialine benthic habitat variability should be considered within marine ecosystem risk assessments, as the coastal zone in particular will face dramatic changes from coastal urbanization and marine climate changes during the 21st century, which will impact coastal faunal.

ACKNOWLEDGEMENTS

I would like to thank my committee chair, Dr. Pete van Hengstum. His support and guidance over the years have been instrumental in completing my research. He has been an outstanding mentor, role model, counselor, and leader. I have been extremely fortunate to have been given the opportunity to learn from him over these years and for this I will be forever grateful.

Thanks to my committee members, Dr. Anja Schulze, Dr. Gil Rowe, and Dr. Karl Kaiser, for their guidance and support throughout the course of this research. I would like to thank Gil Nolan and Bruce Williams for help and expertise in the field. Thanks to Jason Richards for his outstanding cave survey and mapping support. I would like to thank Dr. Tim Dellapenna for use of the Malvern Mastersizer and to Kevin Kelley, Meghan Horgen, and Shawna Little for support and assistance with labwork.

Thanks also to the faculty, staff and graduate students at Texas A&M University at Galveston for their friendship and guidance over the years as well as for assistance to acquire my degree.

Finally, thanks to my family for their support and to Jake Emmert for his patience, love, and constant encouragement.

CONTRIBUTORS AND FUNDING SOURCES

Contributors

This work was supervised by a dissertation committee consisting of Dr. Pete van Hengstum of the Department of Marine Sciences and Oceanography, Dr. Anja Schulze of the Department of Marine Biology, Dr. Gil Rowe of the Department of Marine Biology, and Dr. Karl Kaiser of the Department of Marine Sciences and Oceanography.

The work for the dissertation was completed by the student, with field support from Gil Nolan and Bruce Williams (Bermuda Zoological Society). Cave surveys and maps were completed by Jason Richards. Lab work for Chapter 3 and 4 was supported by Kevin Warner and Meghan Horgen. The relative sea-level rise modeling for Chapter 3 was conducted by Dr. Glenn Milne (University of Ottawa).

Funding Sources

Graduate study was supported by Graduate student Teaching Assistantship from Texas A&M University.

This work was also made possible in part by the following funding sources: Geological Society of America, The Bermuda Zoological Society, and American Academy of Underwater Sciences.

NOMENCLATURE

KSE	Karst Subterranean Estuary
POC	Particulate Organic Carbon
MBSL	Meters Below Sea Level
Cal yrs BP	Calendar years Before Present

TABLE OF CONTENTS

Page

LIST OF FIGURES

Page

LIST OF TABLES

Page

CHAPTER I

INTRODUCTION

Introduction to karst subterranean estuaries and the anchialine habitat continuum

On carbonate platforms and islands, groundwater mixes with oceanic water in the subsurface to form karst subterranean estuaries (Gonneea et al. 2014) that are environmentally similar to subaerial estuaries (Moore et al., 1999). These environments have a global distribution, since ~25% of the world's coastlines are on carbonate terrain (Ford and Williams, 2013). Humans access and observe karst subterranean estuaries (KSE) through groundwater wells, or physically explore them through often horizontally expansive flooded cave systems. In comparison to the subaerial counterparts, our knowledge on the biology, biogeochemistry, and environmental functioning of KSE is limited.

The groundwater masses that comprise the KSE provide habitat to ecosystems and fauna that have been associated with the adjective "anchialine" (Holthuis, 1973; Iliffe et al., 1983; Stock et al., 1986; Santoro et al., 2008; Gerovasileiou et al., 2015). KSEs have an upper meteoric lens that is typically brackish to freshwater, and this water mass is stratified from the lower saline groundwater that is broadly circulating with the ocean (Garman and Garey, 2005; Santos et al., 2008; Menning et al., 2015; Moore, 1999). The mixing of groundwater masses in the subsurface, from tidal pumping and groundwater flow (Martin et al, 2004, Beddows et al., 2007), creates additional groundwater masses known as mixing zones. The presence, or absence, of meteoric lenses and mixing zones is dictated by multiple local control factors, such as antecedent geology, conduit size and geometry, rainfall, and regional topography. Nevertheless, the differences in groundwater masses create physicochemical gradients that contribute to the

development of diverse benthic and pelagic habitats. Understanding the drivers of subsurface habitat variability, and biodiversity, remain ongoing areas of scientific inquiry.

Problematically, these groundwater mass divisions mean that coastal flooded caves and their fauna are often classified as freshwater (meteoric lens only), anchialine (stratified water column), or marine or submarine (marine water mass only). This approach has significant limitations, including: (a) cave passages naturally grade across different groundwater masses (e.g., Green Bay Cave, Bermuda or Ox Bel Ha, Mexico), (b) some anchialine taxa have an evolutionary history across both water masses (Sanz and Platvoet, 1995; Alvarez et al., 2005; Hunter et al., 2008), (c) the habitat requirements of the archetypal anchialine predator remepedia does not require a meteoric lens (Mejía–Ortíz et al., 2007; Neiber et al., 2011), (d) it promotes researcher disagreement on the correct appreciation of the word "anchialine" itself, and (e) modern groundwater conditions cannot explain global anchialine biodiversity patterns, since climate, sea level, and regional geologic change impact groundwater conditions over geologic time.

The term "anchialine" was originally developed to describe land-locked ponds in Hawaii (Holthuis, 1973). However, the ecological load of this term was expanded just 11 years later, after the development of cave diving approaches, to include environments that have marine and terrestrial influences, subterranean connections to the sea, and restricted exposure to open air (Stock et al., 1986). Most recently, "anchialine" was proposed to constitute only sharp physical and chemical stratification in groundwater as the marine system at the coast merges with the groundwater system inland (Bishop et al., 2017). However, it is difficult to reconcile the Bishop et al. (2017) ideas of "anchialine" with observations of the archetypal anchialine predator remipede in offshore marine karst caves in Belize (Yager, 2013), or that meteoric lens

development is transient across geographic areas over geologic times (e.g., Lanzarote, Canary Islands, Spain). So, what is the meaning of the adjective anchialine?

Here we consider that karst subterranean estuaries (KSEs) are populated by an anchialine habitat continuum that spans, but does not strictly define, groundwater mass variability from the ocean to the terrestrial realm on a carbonate landscape (Fig. 1). Importantly, this framework highlights the well-known significance of groundwater variability to the environment, but imparts flexibility to water mass changes (e.g., elevational changes with sea-level change, loss of meteoric lens from increased aridity) over geologic time. In this framework, the karst subterranean estuary (KSE) is considered a discrete coastal environment along carbonate platforms and islands, which is biologically, hydrographically, and physically different from other coastal environments (e.g., estuaries, calettas, mangrove swamps, carbonate tidal flats). This is just an application of what theoretically constitutes an environment or a depositional environment, which inherently includes provisions for analysis of ecospace over geologic time.

Drivers of anchialine habitat variability

Anchialine habitat variability is initially driven by water (i.e., meteoric lens, mixing zone, saline groundwater), as the density stratified water masses provide unique habitat divisions for anchialine fauna. Remipedes, for example, are classic anchialine fauna that exist only in the saline groundwater, below the meteoric lens (Yager, 1981), while another characteristic fauna, *Typhlatya*, is a genus that largely occurs in freshwater, with a few select species inhabiting the brackish to fully marine water masses (Sanz and Platvoet, 1995; Alvarez et al., 2005). Indeed, the water mass characteristics have been given such importance as to be used to define habitats in the anchialine habitat continuum. In the classic work of Palmer et al. (1997), for example,

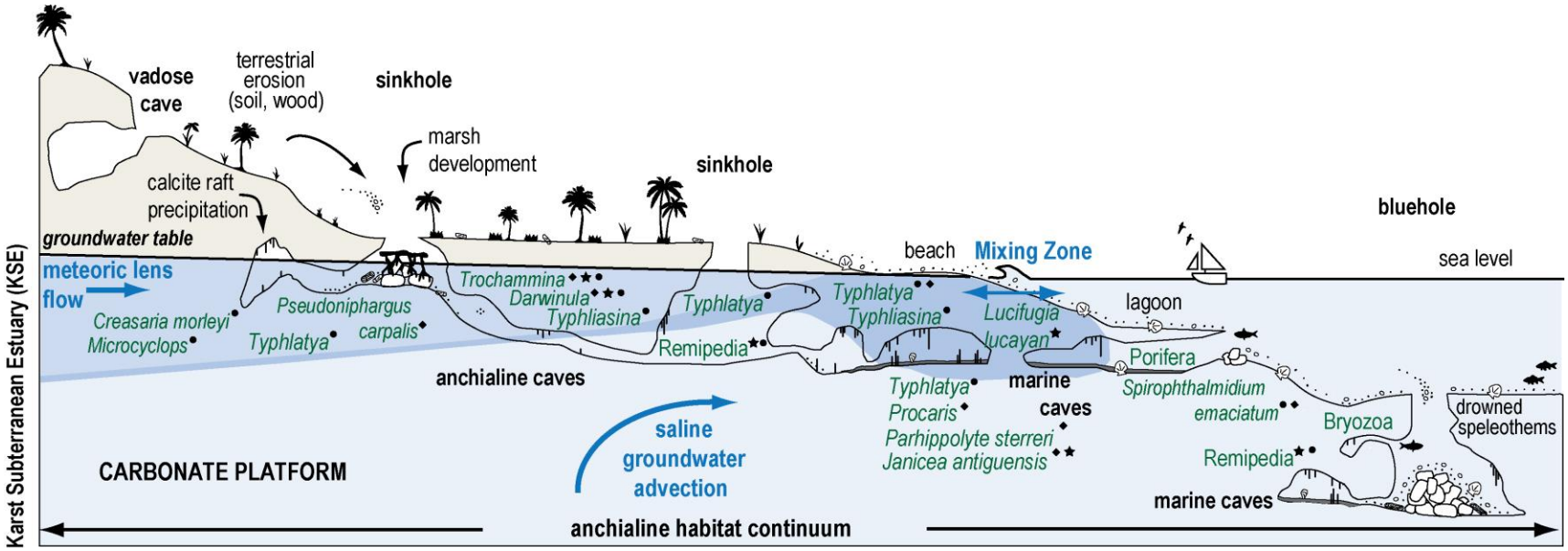

Figure 1. Conceptual model of a karst subterranean estuary and the anchialine habitat continuum created by subsurface groundwater variability. Western North Atlantic anchialine fauna (e.g., fish, shrimps, decapods, ostracodes, foraminifera, marine Porifera and Bryozoa) are positioned in their typical groundwater habitat based on observations from several localities, including The Bahamas (★), Yucatan Peninsula (●), and Bermuda (◆).

flooded cave habitats were designated with a bias towards the pelagic zone: arena, vestibule, transition, and deep cave. However, meiofaunal benthic habitat variability has received less attention.

Limited research has highlighted the importance of salinity (van Hengstum and Scott, 2011; Radolovic et al., 2015; Riera et al., 2018; Romano et al., 2018) and nutrient supply (Fichez, 1990; Fichez, 1991; Ape et al., 2016) on meiofaunal communities (i.e., nematodes, crustaceans, polychaeta), while loss of biomass and diversity from outer to inner regions of KSEs of suspension and filter feeders (i.e., sponges, cnidarians, bryozoans, and tunicates) has been shown to be the result of light attenuation (Harmelin et al., 1985; Marti et al., 2004; Coombes et al., 2015), reduced tidal activity, and decreasing sediment size (Navarro-Barranco et al., 2013).

Importantly, the paleoecological interpretation of benthic anchialine habitat variability depends on an understanding of the ecological processes operating at the present. For example, van Hengstum and Scott (2012) demonstrate the role of sea-level rise on anchialine habitat development over time while recent research suggests allogenic succession due to relative sea-level rise is the link between these habitats (Chapter 3, this study). The concept of allogenic succession is relevant to KSEs because, arguably, the most significant environmental event to such cave habitats is their inundation by sea-level rise. Additionally, previous research documents how the vertical elevation of the mixing zone is controlled by sea level forcing on millennial timescales (Gabriel et al., 2009; van Hengstum et al., 2011). However, little is known about how sea-level rise impacts developmental succession patterns of KSEs benthic habitats.

The **primary goal of this work** is to better understand benthic habitat variability in the anchialine continuum across recent geologic time (last 10,000 years) and geographic space (a

single island: Bermuda), using a model organism (benthic foraminifera) that is represented in statistically-significant populations in both the modern and sub-fossil environment.

Introduction to benthic foraminifera

Benthic foraminifera are single-celled protists, the majority of which secrete a calcium carbonate shell or test that remains in the sediment long after the organism has died (Gooday et al., 1992; Lea, 2003). Benthic foraminifera readily colonize most marine and transitional habitats, form discrete assemblages in different coastal environments (i.e., reefs, lagoons, marshes), and respond rapidly to external pressures such as salinity, dissolved oxygen, temperature, and organic matter supply (Boltovskoy et al., 1991; Dissard et al., 2010; Kaiho, 1994; Martine et al., 2002; Murray, 2001; Waelbroeck et al., 2002). As such, their fossil remains are widely used to reconstruct environmental change in the marine realm (Murray, 2001) and investigate environmental and ecosystem dynamics in the coastal zone (Gooday et al., 1992; Murray, 2011; Sen Gupta and Machain- Castillo, 1993).

Benthic foraminifera are also known from KSEs worldwide. Romano et al. (2018) used benthic foraminifera as a tool to recognize distinct ecological zones in Mediterranean KSEs, while previous research from caves in Mexico suggest benthic foraminifera are useful salinity proxies (van Hengstum et al., 2009). Alternatively, Omori et al. (2010), used benthic foraminiferal fossil records from the Daidokutsu Cave in Japan to delineate loss of light and nutrient supply over the past 7,000 years.

Previous research in Bermuda indicates widespread colonization of diverse populations of benthic foraminifera. The earliest documentation identifies general benthic foraminiferal colonization of shallow-waters on the Bermuda carbonate platform (Carman, 1927), while more

recent surveys identify foraminifera from specific coastal environments (i.e., reefs, lagoons, caves, mangroves, ponds; Javaux and Scott, 2003). Importantly, benthic foraminifera from Bermuda's KSEs have been used to delineate both modern and prehistoric environmental change, specifically in response to salinity change (van Hengstum and Scott, 2011; van Hengstum et al., 2011).

Research field area: Bermuda

Bermuda's karst has emerged as a global epicenter of underwater cave research (Bowman and Iliffe, 1985; Iliffe et al., 2011; Kornicker and Iliffe, 1989; Maddocks and Iliffe, 1986). The island of Bermuda is an excellent natural laboratory to study benthic habitat variability within KSEs because they are locally abundant and most are in final marine stage, allowing for entire sea-level transgression to be recorded in sediments. Most of the research on Bermuda's KSEs have focused on the aquatic cave fauna (Sket and Iliffe, 1980) which has included some hydrogeologic study as an ecological framework for the endemic cave fauna (e.g., Maddocks and Iliffe, 1986). Some superficial descriptions of Bermudian cave sediments have been published (Iliffe, 1987), providing evidence that Bermuda is a suitable location to test the hypotheses.

Previous research from Bermuda suggests there are temporal and spatial variations within KSE benthic habitats (van Hengstum and Scott, 2011; van Hengstum et al., 2011; van Hengstum and Scott, 2012). Benthic foraminifera are particularly suitable to characterize the process linking benthic habitat development to sea-level rise (van Hengstum and Scott, 2012), and consequently allogenic succession. Given their statistically significant and diverse populations in small sediment samples, benthic foraminifera are particularly useful microfossils for environmental monitoring in coastal environments (Gooday et al., 1992; Gupta and Machain-

Castillo, 1993; Murray, 2006). In areas with sufficient sedimentation, subfossil benthic foraminifera in the stratigraphic record can document centennial-scale changes in groundwater conditions (e.g., oxygen, salinity) (van Hengstum et al., 2010; van Hengstum and Scott, 2012; Kovaks et al., 2017) and reconstruct anchialine and submarine environments in response to sea-level forcing (van Hengstum et al., 2011; van Hengstum and Scott, 2012).

In general, the research for this study is concentrated in the Palm Cave System, located on the isthmus between Harrington Sound and Castle Harbour. The ~1,500 m long Palm Cave System has been extensively explored and mapped, with at least seven entrances interconnected by an extensive network of underwater conduits, and the cave geometry extends to a maximum depth of 23 m below modern sea level (Kornicker and Iliffe, 1989). Collapse entrances provide physical openings to a subterranean habitat, allowing influx of terrestrial nutrients sediments, and non-cave dwelling organisms (Denitto et al., 2007; van Hengstum and Scott, 2011). Hydrographically, the Palm Cave System is a marine cave flooded by oxygenated saline groundwater that tidally circulates with seawater from the adjacent coastal lagoons. Hydrographic measurements from the 2015 summer months found the saline groundwater in the Palm Cave had a pH of 7.8 ± 0.2, temperature of 28.5 ± 0.2 C, and salinity of 38.7 ± 0.4 psu (Stoffer, 2013). The Palm Cave System is also connected to the adjacent Harrington Sound through subterranean conduits, which provide a source for direct tidal exchange with the adjacent lagoon (i.e., marine) environments (Maddocks and Iliffe, 1991).

The Green Bay Cave, Cow Cave, and Deep Blue cave were also study sites within Chapter II, addressing modern benthic habitat variability. The Green Bay Cave is a large anchialine cave in Bermuda with more than two kilometers of underwater passages. There are two primary entrances into the system: a subaerial sinkhole-based entrance (Cliff Pool Sinkhole)

and a submarine entrance at the end of Green Bay lagoon, part of the restricted Harrington Sound. Hydrographically, Green Bay Cave is currently flooded by well-oxygenated saline groundwater that is tidally circulated through the oceanic entrance at the Harrington Sound shoreline. A local brackish meteoric lens can be observed only in a few locations (e.g., Cliff Pool Sinkhole, Letter Box, and Air Dome), and can completely disappear during prolonged periods of drought.

Cow Cave and Deep Blue are located on the same isthmus between Harrington Sound and Castle Harbour as the Palm Cave System. Cow Cave is more proximal to Castle Harbour, located approximately 170 meters away from the shoreline. Both Cow Cave and Deep Blue have shallow, benthic areas that progressively deepen (Little & van Hengstum, 2019). Deep Blue is a single, large, crescent-shaped entrance that extends into the spatially extensive Walsingham Cave System, which is one of the largest underwater caves in Bermuda (van Hengstum et al., 2015). Cow Cave has one terrestrial entrance that opens into a completely roofed cave chamber. Both caves are inundated by oxygenated seawater.

Dissertation structure

This dissertation is successively organized into chapters to investigate the following research questions and themes:

Chapter 2: What controls modern benthic foraminiferal assemblages across multiple caves in Bermuda? Hypothesis: the source of sedimentary organic carbon (terrestrial versus marine) plays a primary environmental control. To test this hypothesis, a *new* database was generated that combined benthic foraminiferal distributions and environmental variables (i.e., sediment grain size, particulate organic carbon provenance using a $\delta^{13}C_{org}$ analysis with a 2-end

member mixing analysis, and C:N ratio) from the Palm Cave, with previously compiled data from Green Bay Cave, Deep Blue Cave, and Cow Cave (van Hengstum and Scott, 2011; Little and van Hengstum, 2019). This creates the largest database yet available of modern benthic foraminifera from a single area.

The results document that the source of particulate organic matter (terrestrial versus marine) is a fundamental driver of benthic foraminiferal distributions, while light, tidal exposure, and water mass are secondary. One caveat, however, is that water mass salinity is largely constant in our study area, which is a local characteristic of the study site and not representative of all global locations. These results suggest that changes in particulate organic matter flux, as a result of anthropogenic modifications of coastlines, may alter benthic habitats and their meiofaunal populations.

Chapter 3. How do benthic anchialine habitats in a carbonate cave change and develop in response to sea-level forced vertical migration, and cave inundation, of a karst subterranean estuary since the last glacial maximum (~20,000 years ago). Hypothesis: benthic anchialine habitat onset is driven by deglacial sea-level rise, with subsequent habitat change influenced by the impacts of carbonate platform flooding and regional coastal circulation. I test the hypothesis using sediment cores from the Palm Cave System. Environmental change in the Palm Cave System over the last 10,000 years was documented by analyzing cave-wide stratigraphic patterns and emplacement age of sediments, organic matter provenance analysis, along with a qualitative assessment of preserved benthic meiofauna (e.g., foraminifera, ostracodes, bryozoans) and vertebrate remains (e.g., fish bones).

The results document the most complete record yet known of developmental succession in anchialine habitats in response to concomitant relative sea-level rise and vertical migration of

a karst subterranean estuary since the last ice age in Bermuda. In addition, the results illuminate how sea-level rise can force subsurface aquatic island fauna to experience a previously unknown bottleneck event. It is highly likely that this process impacted the evolutionary history of global subsurface aquatic island fauna during the Phanerozoic, and problematically, 21st century island-based marine ecosystem risk assessments are incomplete if this process is not regionally evaluated.

Chapter 4: What do benthic foraminifera reveal about drivers of benthic habitat development as groundwater mass changes in a karst subterranean estuary since the last ice age? Hypothesis: the source and quantity of organic carbon (terrestrial versus marine) is a primary control of benthic foraminifera communities. In Chapter 4, I test the hypothesis that changes in organic carbon quantity and quality contribute to benthic habitat development over the last 10,000 years in response to Holocene sea-level rise. Using the same sediment cores as Chapter 3, additional environmental analysis was used to investigate the environmental variables contributing to benthic habitat development in the Palm Cave System over the last 10,000 years.

The results document a shift from benthic habitats that were first controlled by fresh to slightly brackish condition of a paleo meteoric lens, when the subaerial island of Bermuda had a greater geographic extent. With island shrinkage associated with continual Holocene sea-level rise, the paleo meteoric lens eventually vanished in northeastern Bermuda, and gave rise to caves only flooded by saline groundwater that was circulated with the ocean. These results further indicate how sea-level rise and groundwater variability are not static through geologic time, in which fauna in the anchialine habitat continuum must become adapted to, or are locally extirpated.

CHAPTER II

SEDIMENTARY ORGANIC CARBON (SOURCE AND QUANTITY), PARTICLE SIZE AND TIDAL EXPOSURE CONTROL BENTHIC ANCHIALINE HABITAT VARIABILITY IN KARST SUBTERRANEAN ESTUARIES

Introduction

On global carbonate platforms and islands, groundwater mixes with oceanic water in the subsurface to form karst subterranean estuaries (Gonneea et al. 2014) that are environmentally similar to subaerial estuaries (Moore, 1999). Biologically, karst subterranean estuaries now flood extensive cave systems that host diverse and ancient aquatic ecosystems and fauna that have traditionally been described with the adjective "anchialine" (Bishop et al., 2015; Stock et al., 1986). Early research in this unique environment was focused on creating taxonomic inventories of unknown animals, but attention is increasingly focused on environmental analysis (Zabala et al., 1989; Fichez, 1990; Santos, 2006; García et al., 2009; Radolović et al., 2015), ecosystem functioning (Pohlman et al., 1997, Brankovits et al., 2018), and molecular biogeographical approaches (Porter, 2007; Botello et al., 2013; Jurado-Rivera et al., 2017). Similar to other estuarine settings, complex physico-chemical gradients develop in a land-to-ocean transect that impacts biodiversity and biogeochemical cycling. Indeed, researchers often categorize caves, and their fauna, based on groundwater mass characteristics alone, such as freshwater (meteoric lens water mass), anchialine (multiple water masses), and marine or submarine (saline groundwater only), since water column variability is a well-known driver of anchialine habitat variability.

In this study we refer to the ecospace created in the karst subterranean estuary as a continuum of diverse benthic and pelagic anchialine habitats (Fig. 1). Fauna and ecosystem

processes must be properly compared within the anchialine habitat continuum to fully understand their broader significance within the karst subterranean estuary. For example, this framework allows for the habitat colonized by rempiedes in saline groundwater mass (e.g., Yager, 1981; Daenekas et al. 2009; Olesen et al., 2017) to be effectively quantified and contrasted against the habitat colonized by anchialine atyid shrimps and decapods colonizing the upper low salinity meteoric lens water mass (Sanz and Platvoet, 1995; Alvarez et al., 2005; Moritsch et al., 2014). However, much is unknown about the quantitative drivers of benthic and pelagic habitats variability in karst subterranean estuaries. Previous research documents the importance of groundwater mass salinity (van Hengstum and Scott, 2011; Radolovic et al., 2015; Riera et al., 2018; Romano et al., 2018) and nutrient supply (Fichez, 1990; Fichez, 1991; Ape et al., 2016) on meiofaunal communities (i.e., nematodes, crustaceans, polychaeta). In caves that transect the lower saline groundwater mass from the ocean inland, there is a well-documented decrease in biomass and diversity of suspension and filter feeders (i.e., sponges, cnidarians, bryozoans, and tunicates) from light attenuation, reduced tidal activity, and decreasing sediment size (Navarro-Barranco et al., 2013; Marti et al., 2004; Coombes et al., 2015).

Increasing attention is now shifting to the supply, transport and utility of carbon sources through anchialine food webs, and its impact on biodiversity and habitat variability. Early work suggested that sedimentary organic carbon was not a primary source of carbon to pelagic animals in Yucatan anchialine caves (Pohlman et al., 1997), with further work indicating the significance of dissolved organic carbon and methane for pelagic communities (Brankovits et al., 2018). Fichez (1990) provides evidence that decreasing particulate organic input from the entrance to the inner, dark parts of the cave results in increasingly oligotrophic conditions and a decline in hard substrate and soft bottom communities. This suggests the flux of particulate organic carbon

to the benthos may be relevant to habitat variability in some areas of the karst subterranean estuary. Similarly, previous work in Bermuda's flooded caves (e.g., Green Bay Cave, Cow Cave, and Deep Blue) indicate that benthic foraminifera define discrete habitats in response to changing sedimentary organic carbon, most of which is likely delivered to the benthos as particulate organic carbon (POC) from the adjacent terrestrial and marine realms.

Considering anchialine habitat variability on geologic timescales presents a further complication, since groundwater hydrography and elevation respond to climatic, geologic, and glacio-isostatic sea-level changes. For example, the Yucatan Peninsula has a geographically widespread upper meteoric lens water mass (salinity < 10 psu) that is mostly separated from dysoxic to anoxic saline groundwater below. This groundwater configuration has most likely persisted throughout Quaternary sea-level changes (Chapter 3, this study). In contrast, western Bermuda (where most of its well-studied flooded caves are) and many well-studied Mediterranean systems have only very localized to non-existent meteoric lens development and are flooded by well oxygenated saline groundwater circulated with the ocean. During lower sea-levels on geologic timescales, Bermuda was a larger landmass that likely had a larger meteoric lens akin to the Yucatan-style cave systems (van Hengstum et al., 2011).

Here we use benthic foraminifera in flooded Bermudian caves to better understand the broad drivers of benthic habitat variability in the marine sector of karst subterranean estuaries. Benthic foraminifera are unicellular protists that are highly sensitive to environmental gradients. Benthic foraminifera can be broadly divided into epifaunal taxa that utilize resources at the sediment-water interface, versus the infaunal taxa that live within the upper ~5 cm of sediment (Jorissen et al., 1995). Advantageously, the preservation of their simple test (or shell) remains in the sediment after death to record statistically-significant populations that can probe spatial

patterns of biodiversity and delineate benthic habitat variability, and its potential drivers, across the entirety of water mass variability in karst subterranean estuaries. This study analyzes recent benthic foraminiferal distributions throughout the expansive Palm Cave in Bermuda, and compares this new population assessment in Palm Cave with previous results on benthic foraminiferal populations in other Bermudian caves (i.e., Green Bay Cave, Deep Blue, and Cow Cave).

Research design and study site

The archipelago of Bermuda is a basalt core overlain by alternating wind-blown carbonates and paleosols that accumulated during Quaternary sea-level highstands and lowstands, respectively (Fig. 2)(Bretz, 1960; Land et al., 1967; Vacher and Rowe, 1997). The local carbonate has since weathered into a mature karst landscape from limestone dissolution and cave collapse events in both phreatic and vadose settings (Palmer et al., 1977). Caves are especially abundant between Castle Harbour and Harrington Sound (e.g., Palm Cave: 32.34º, –64.71º, Deep Blue: 32.347º, –64.711º, and Cow Cave: 32.34º, –64.71º), and between North Shore Lagoon and Harrington Sound (e.g., Green Bay Cave: 32.33º, –64.74º, Palmer and Queen, 1977; Fig. 2). Interestingly, the apex anchialine crustacean predator *Remipedia* has not been observed in Bermuda's caves. Bermuda's caves are ideal for investigating habitat variability in the marine sector of the karst subterranean estuary because the saline groundwater is well circulated with the ocean, which limits the confounding influence of dissolved oxygen in the water column on habitat variability. Consistent marine salinity in the ground water masses (normal marine conditions) and well-oxygenated conditions (>3 mg/L) throughout eastern Bermudian caves make them well suited for investigating benthic habitat variability in karst

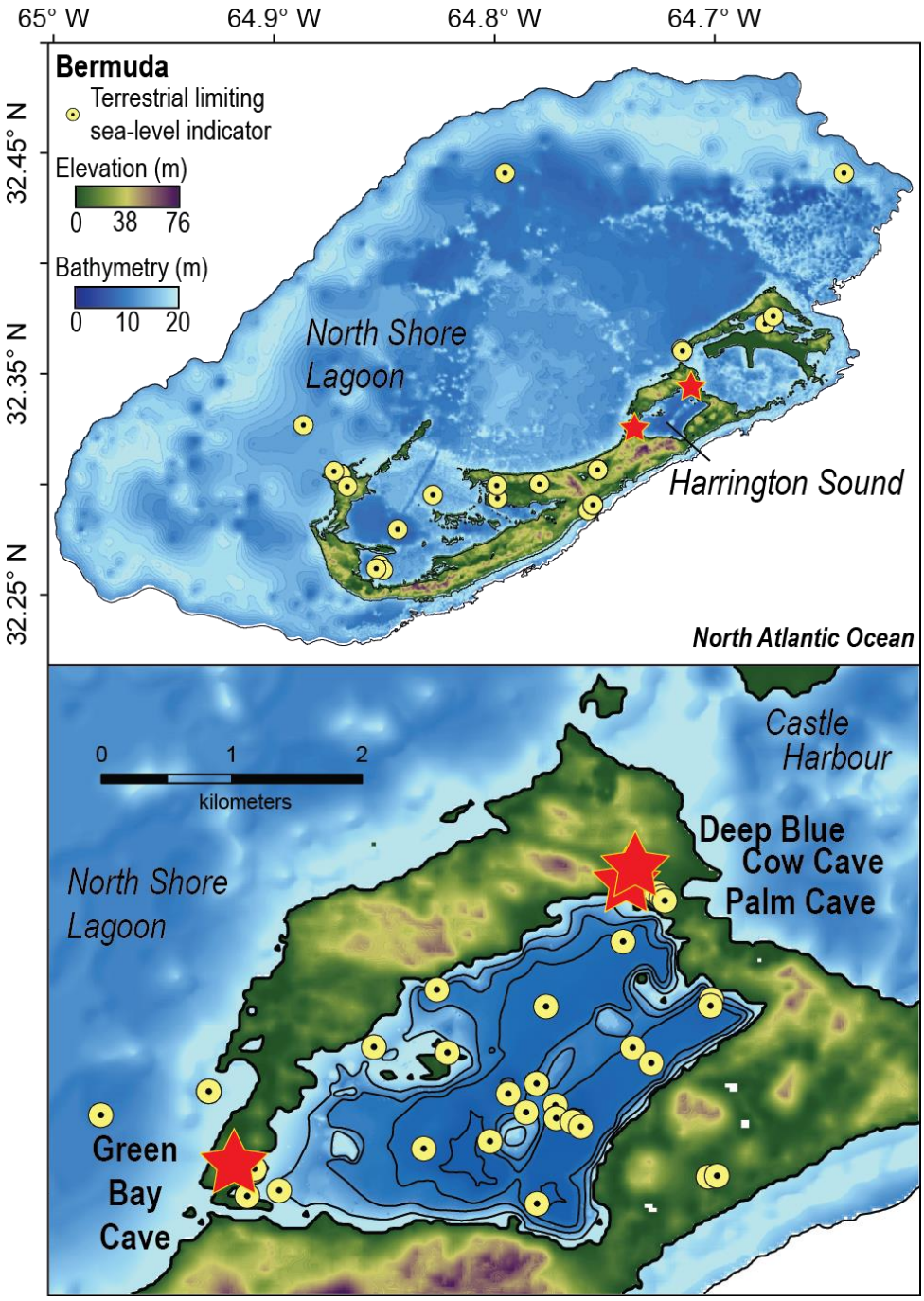

Figure 2. Palm Cave System in Bermuda. (Top) Digital elevation model of Bermuda in the North Atlantic Ocean. (Bottom) Detailed map of Harrington Sound plotted in ArcGIS. Yellow markers identify locations of geological sea-level indicators from Bermuda (peat, *n*=113, Appendix A). Red stars indicate locations of study sites.

subterranean estuaries, independent of salinity changes (e.g., Bel Torrente Cave, Mediterranean; Romano et al., 2018) or decreasing dissolved oxygen changes in an overlying water mass. The physical process of tidal pumping (Martin et al., 2004) causes microtidal variability (<0.5 m) in the local groundwater level (i.e., water table), which can be observed in the cave pool entrances to the flooded caves (Palmer et al., 1977; van Hengstum et al., 2015, Little and van Hengstum, 2019). Sedimentation in the Bermuda caves is dominated by silt to sand-sized carbonate particles, with common shells from the bivalve *Barbatia domingensis*.

Palm Cave is located on the isthmus between Harrington Sound and Castle Harbour (Fig. 3, 32.34º, –64.71º), which are marine carbonate lagoons (Neumann, 1965; Volbrecht 1996). The ~1,500 m long Palm Cave System has been extensively explored and mapped, with an extensive network of underwater conduits accessed by seven known, at least human-sized entrances and exits. The maximum depth observed in cave passages is 23 m below modern sea level (mbsl). Geomorphologically, cave entrances provide physical openings to the subterranean habitats, and allow for the influx of terrestrial nutrients, sediments and non-cave dwelling organisms to an otherwise marine environment. There is currently a direct, but narrow, connection between Harrington Sound and Palm Cave through the passage 'Cripple Gate'. At the current position of sea level, Cripple Gate allows for direct tidal exchange of seawater and nutrients between Palm Cave and the adjacent Harrington Sound (Fig. 3).

Hydrographically, Palm Cave is entirely flooded by well-oxygenated saline groundwater that tidally circulates with seawater from the adjacent coastal lagoons. Some Bermudian caves have localized development of small or thin brackish water lenses (e.g., Letter Box and Cliff Pool areas of Green Bay Cave; see van Hengstum and Scott, 2011), but Palm Cave does not have similar hydrographic characteristics. The narrow landmass width (<300 m) near Palm Cave

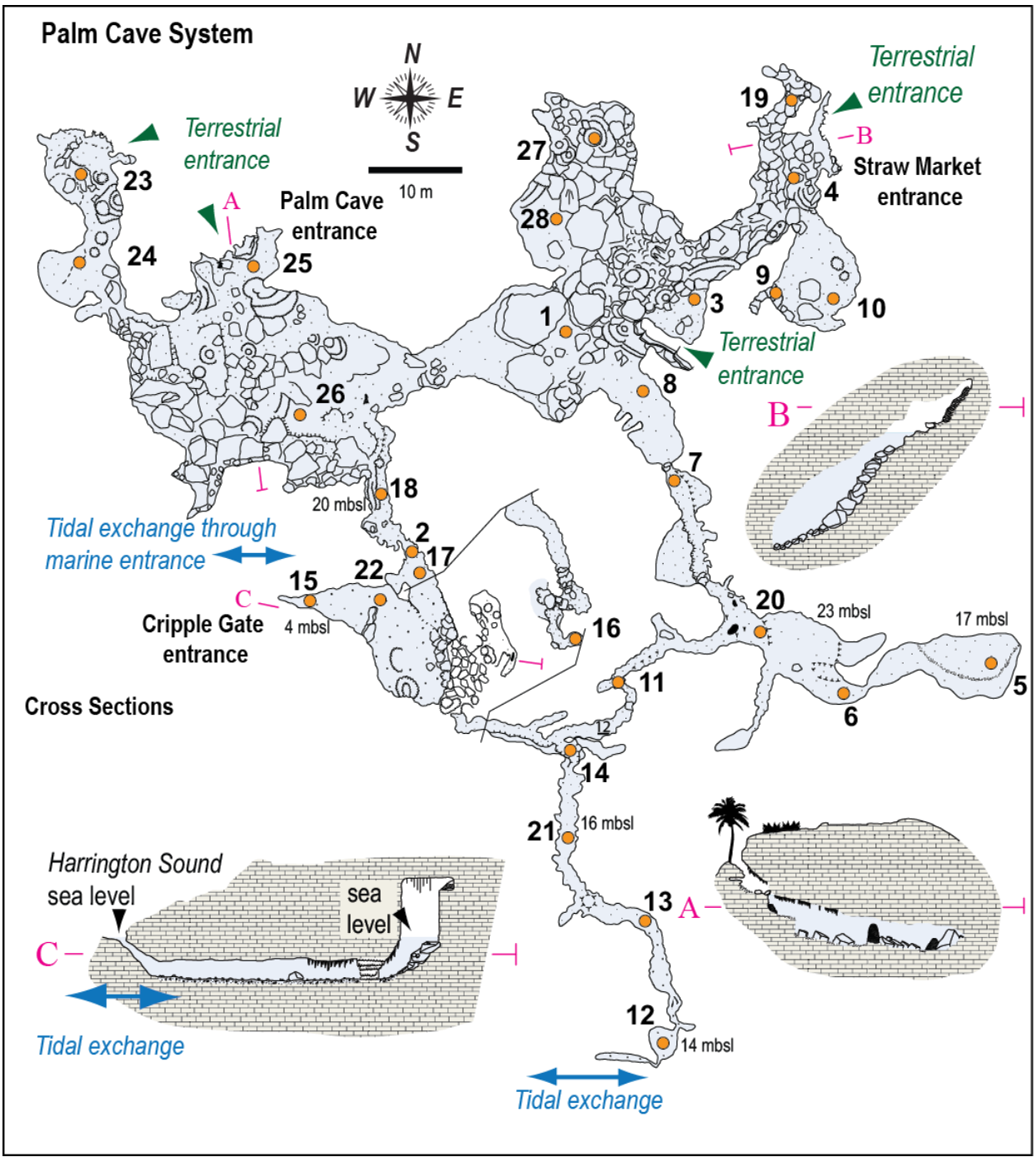

Figure 3. The Palm Cave System. Detailed survey map of Palm Cave System showing explored cave passages that provide direct access to the subterranean estuary, with locations of surface sediment samples (orange circles) and cave entrances (adapted from original survey of Jason Richards).

combined with the porosity of the carbonate means that no meteoric lens (freshwater or brackish) discharges through Palm Cave. During summer 2015, the saline groundwater flooding the Palm Cave had a pH of 7.8 ± 0.2, temperature of 28.5 ± 0.2°C, and salinity of 38.7 ± 0.4 psu, which are similar to the conditions previously observed (Stoffer, 2013). These hydrographic conditions indicate salinity and dissolved oxygen in the overlying water column are likely not driving benthic habitat variability at the sediment-water interface where epifaunal organisms reside.

Methods

Palm Cave surface samples collection and processing

Twenty-eight surface (<3 cm depth) sediment samples were collected from various depths and locations throughout Palm Cave in August 2015 using advanced technical cave diving procedures. Sediment sample processing generally follows van Hengstum and Scott (2011) and Little and van Hengstum (2019). Benthic foraminifera were concentrated by wet sieving sediment sub-samples (0.63 cm^3 to 5 cm^3) over a standard 63 μm screen mesh, with the remaining coarse sediment residues split using a wet splitter to enable representative census counts of ~300 individuals per sample (Scott & Hermelin, 1993). While van Hengstum and Scott (2011) used a 45 μm sieve to concentrate benthic foraminifera in their study of Green Bay Cave, Little and van Hengstum (2019) documented negligible difference between resultant foraminiferal assemblage from Bermudian caves using 45 versus 63 μm sieve sizes. Individual benthic foraminifera were wet picked onto micropaleontological slides and identified to generic level, with taxonomy confirmed by scanning electron microscopy of representative individuals and literature comparisons (Carman, 1993; Bermudez, 1949; Loeblich Jr & Tappan, 1987; Javaux & Scott, 2003; van Hengstum & Scott, 2011; Little and van Hengstum, 2019). A new

matrix was produced from Palm Cave comprising 28 samples by 114 foraminiferal species (observations), with a total of 43,087 benthic foraminifera taxonomically identified for this study.

Textural variability in sediment sub-samples from Palm Cave was examined using standard laser diffraction particle size analysis and loss on ignition (LOI) procedures. Organic matter was recorded as percent-lost relative to the original total sample weight after LOI at 550°C for 4.5 hours (Heiri et al., 2001). Mean particle size for sediment sub-samples was measured with a Malvern Mastersizer 2000S laser particle size analyzer (Sperezza et al., 2004), with individuals particles disaggregated in a sodium hexametaphosphate dispersant prior to analysis.

The relative contribution of terrestrial versus marine organic carbon deposited at each sample station was evaluated by measuring the stable carbon isotopic value ($\delta^{13}C_{org}$) and C:N ratio of bulk sediment in all samples ($n = 28$). In general, $\delta^{13}C_{org}$ values of bulk sedimentary organic matter reflects the relative contributions of marine, terrestrial versus algal carbon sources in coastal environments (Lamb et al., 2006) and this technique can also be applied to karst subterranean estuaries (van Hengstum et al., 2011). Terrestrial plants that preferentially use the C^3 photosynthetic pathway produce organic tissues that are ^{13}C-depleted and nitrogen-poor, with $\delta^{13}C_{org}$ values generally ranging between –32‰ and –21‰ (Lamb et al., 2006). In contrast, marine organic matter is relatively more ^{13}C-enriched and nitrogen-rich than terrestrial organic matter (Lamb et al., 2006). Carbonates were first digested with 1.0 M HCl for 12 hours, and the remaining sediment residue was rinsed, desiccated, powdered, and weighed into silver capsules. Stable carbon isotope ratios ($\delta^{13}C_{org}$) were measured against international standards at Baylor University Stable Isotope Laboratory on a Thermo- Electron Delta V Advantage Isotope Ratio

Mass Spectrometer. Final isotopic ratios are reported relative to the standard delta (δ) notation relative to Vienna Pee Dee Belemnite (VPDB) for carbon (expressed as parts per mil (‰)) with an uncertainty of ± 0.1‰.

Lastly, the relative proportion of terrestrial versus marine organic matter in the surface sediment samples were estimated by isotopic mass balance: $\delta X = F_m * \delta X_m + F_t * \delta X_t$; where $1 = F_t + F_m$ (Thornton & McManus, 1994). The terrestrial endmember (δX_t) was –27.7‰ as measured on a sample from Cow Cave in Bermuda (Little and van Hengstum, 2019), and the marine endmember (δX_m) was –15.2‰ as measured on a sample from Palm Cave (this work).

Statistical analysis

A final data matrix was compiled for further multivariate statistical analysis that contained 127 total samples: (a) the 28 new samples from Palm Cave (this study), 74 samples from Green Bay Cave (van Hengstum and Scott, 2011), 18 samples from Cow Cave (Little and van Hengstum, 2019), and 7 samples from Deep Blue (Little and van Hengstum, 2019). All these samples were integrated into a single data matrix to provide the broadest perspective yet of benthic habitat variability in Bermuda's anchialine caves. First, taxonomic observations were grouped to the generic level to omit any taxonomic biases related to individual researchers. The exception was the brackish water indicator *Trochammina inflata,* which was left identified to the specific level. Also, the final data matrix amalgamated the taxonomically similar genera *Pattelina*, *Heteropatellina*, and *Patellinoides* (all members of the family *Spirillind*) that were differentiated by Little and van Hengstum (2019, Deep Blue and Cow Cave), but lumped together by van Hengstum and Scott (2011, Green Bay Cave). Taxonomic units were considered insignificant and removed from further multivariate statistical processing if the proportional

abundance was less than the calculated standard error at a 95% confidence interval in all samples where it was observed (Patterson and Fishbein, 1989), or if the species was present in only one sample (9 genera omitted). Additionally, one sample from the Green Bay Cave dataset (ISC-72) was removed because benthic foraminiferal data differed from other samples collected nearby, which skewed the results enough to suspect the data quality of this sample. The final data matrix subjected to multivariate analysis was 127 samples by 71 foraminiferal taxonomic units (primarily genera).

Statistical analysis was completed using RStudio software (version 1.1.383; RStudio, 2016). The final data of raw count abundances was first converted to proportional abundances ('decostand' function in 'vegan' package; Oksanen et al., 2013) then used to calculate Shannon-Wiener Diversity Index. Unconstrained Q-mode cluster analysis was used to determine broader community assemblages that are ecologically meaningful by grouping statistically similar populations (Legendre and Legendre, 1998). Prior to cluster analysis, the proportional abundances were square root transformed to minimize the impact of dominant species and to better compare community structure (Legendre and Legendre, 1998). Samples were then subjected to hierarchical cluster analysis using an unweighted paired group averaging algorithm and the Bray-Curtis dissimilarity index ('simprof' function in the 'clustsig' package; Clarke et al., 2008; Whitaker and Christman, 2014; and the 'vegdist' function in the 'vegan' package; Oksanen et al., 2013). Similar dendrograms were produced regardless of the cluster analysis algorithm employed (i.e., Euclidean, Ward's, single-linkage), which introduces confidence that the groupings represent community assemblages. The proportion of dominant taxa in the dendrogram (5% proportional abundance in at least 1 sample) were illustrated between the

different samples by generating a vertical stratigraphic plot ('stratplot' function in the 'rioja' package; Juggins, 2015).

Several benthic environmental characteristics (explanatory variables, both categorical and quantitative) were statistically explored as potential drivers of the benthic foraminiferal assemblages (response variables). The quantitative variables measured were bulk organic matter content, $\delta^{13}C_{org}$, C:N, total organic carbon, terrestrial organic carbon, and mean particle size measured by the Malvern Mastersizer. The categorical variables included were tidal exposure, light, and water mass. For tidal exposure, we followed the approach of Little and van Hengstum (2019) and classified samples as tidally exposed (or not) if a sample station experienced exposure (or not) at any part of the tidal cycle. Photosynthetically available radiation at each station was not measured, but we categorized samples as either experiencing direct sunlight, indirect sunlight at some point during the day, or complete darkness. Finally, samples were categorized based on which water mass they were located: saline groundwater or meteoric lens. Note that a classic, 'Yucatan style mixing zone' between the meteoric lens and saline groundwater is not present in this area of Bermuda (van Hengstum and Scott, 2012), so the vast majority of samples were categorized as from the saline groundwater mass. The variance inflation factor (VIF) was calculated for each environmental variable to avoid collinearity issues between variables ('vif' function in 'car' package; Fox and Weisberg, 2011). In general, environmental variables with a VIF > 10 may influence multivariate models and therefore warrant exclusion from further analysis (Graham, 2003). By this logic, the variable terrestrial organic carbon was excluded from further analysis, since it is a linearly derived parameter from $\delta^{13}C_{org}$.

Multivariate regression trees (MRT) were generated in RStudio to explore relationships between the environmental characteristics (explanatory variables) and proportional abundances of benthic foraminifera (response variables). This exercise allows for an independent test of the *drivers* of the natural groupings, or foraminiferal assemblages that were identified through unconstrained Q-mode cluster analysis. The MRT analysis examines how environmental variables can explain species variation through numerous partitions and splitting of the data into subsets based on environmental thresholds or dissimilarities (De'Ath, 2002). MRT models were generated using absolute abundance data and the above mentioned environmental data ('mvpart' function in 'mvpart' package; De'Ath, 2007). Two separate MRT models were completed using all the surface samples and environmental variables previously discussed: (1) an MRT model was computed that used the same observations (taxonomic divisions) as the unconstrained hierarchical cluster analysis, and (2) an MRT model was computed that amalgamated all counts of any *Quinqueloculina* and *Triloculina* into a single pseudo-genera. The scientific reasoning for this second MRT model was to guard against any taxonomic bias imparted by individual researchers because of difficult-to-identify smaller miliolids. Smaller miliolid foraminifera are often juveniles, which do not have strong phenotypic expression of adults that is used for benthic foraminiferal taxonomy. Still further, Schnitker (1967) produced considerable morphologic variability in miliolid clone clusters, which considerable plasticity in the morphology of juvenile *Quinqueloculina* and *Triloculina*. Regardless, the two MRT models produced similar results in terms of nodding.

Results

Palm Cave sediment texture and organic matter

Palm Cave sediment is primarily coarse carbonate silt (mean 39.8 μm) with 8.6% bulk organic matter (range: 2.5% to 12.6%). Particle size increases from coarse silt to fine sand (mean 123 μm) with marine bioclasts (gastropod and bivalve shells, coral fragments) and some trash (e.g., aluminum cans, fishing line, etc.) from the interior of the cave to the marine entrance (exit) to Harrington Sound (Cripple Gate; Fig. 4).

Organic carbon delivered to the Palm Cave benthos is derived from both terrestrial and marine sources (Fig. 5). Samples with the most depleted carbonic isotope ratio and highest C:N values were collected near cave exits to the terrestrial surface above (i.e., PCS-25: –23.7‰ and C:N value 10.8; PCS-26: –23.7‰ and C:N value 14.2). Samples with the most enriched carbon-isotope values (i.e., –15.5 ‰ and –18.2‰) were collected from areas most distally positioned form these terrestrial exits (i.e., PCS-05: –15.2 ‰ and C:N value 10.5; PCS-06: –18.2‰ and C:N value 8.1). The remaining samples lay in between the marine and terrestrial dominated sections of the cave.

The $\delta^{13}C_{org}$ values of sediment from the Palm Cave System fall in between the previous results from Green Bay Cave (van Hengstum and Scott, 2011), Deep Blue, and Cow Cave (Little and van Hengstum, 2019). The samples with the most depleted carbon isotopes represent areas where the organic carbon is predominantly derived from terrestrial sources (i.e., shallow samples located in Cliff Pool in Green Bay Cave, Fig. 5). Alternatively, the enriched samples represent areas where the organic carbon is predominantly derived from marine sources and distal to any terrestrial or marine exits from the cave (Green Bay Cave Isolated). In some cases, however, the scattered $\delta^{13}C_{org}$ values alongside lower C:N values indicate the organic carbon source is likely a

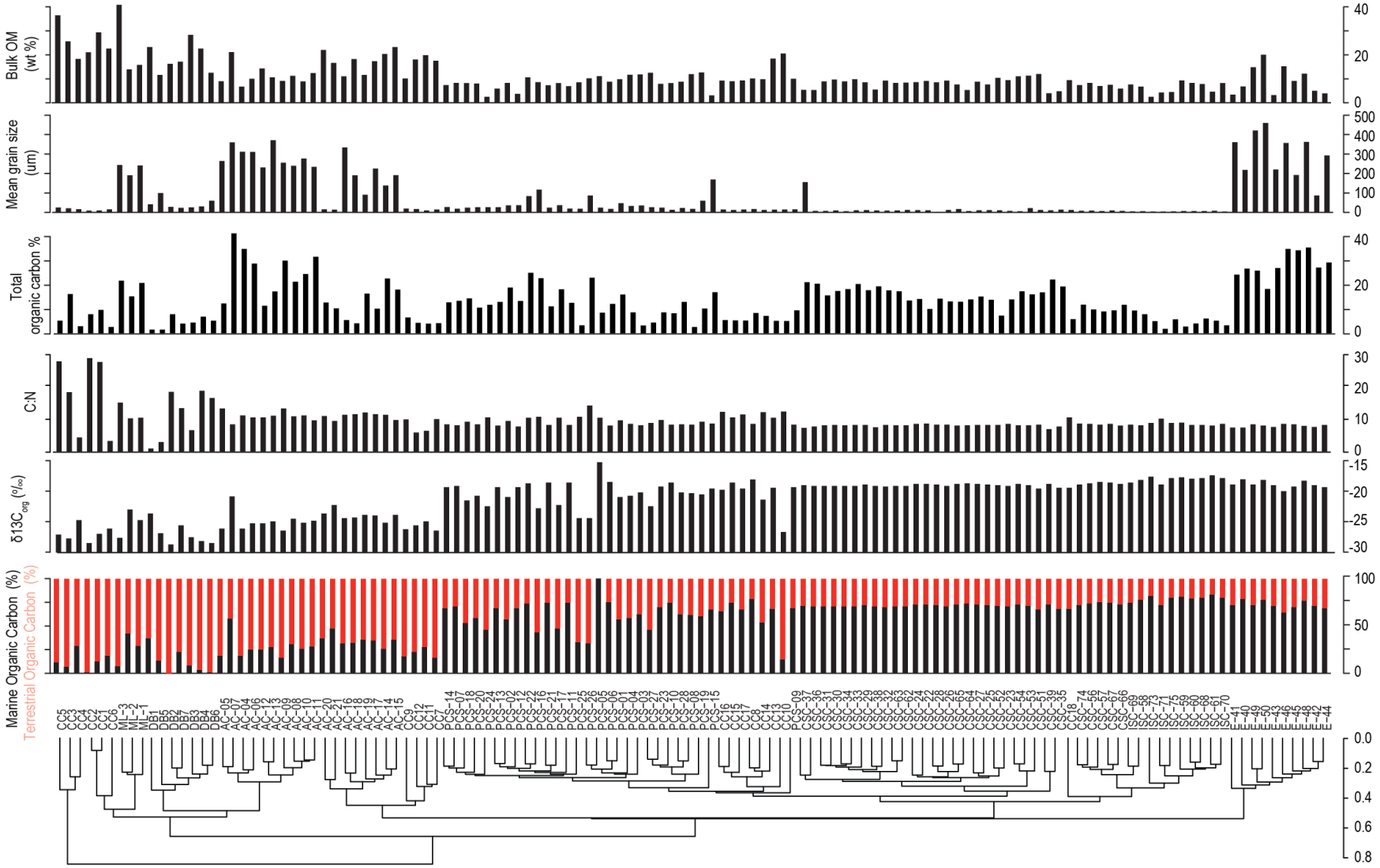

Figure 4. Measured environmental variables at each sample station in Palm Cave, Green Bay, Cow Cave and Deep Blue. Dendrogram produced by Q-mode cluster analysis using all faunal data.

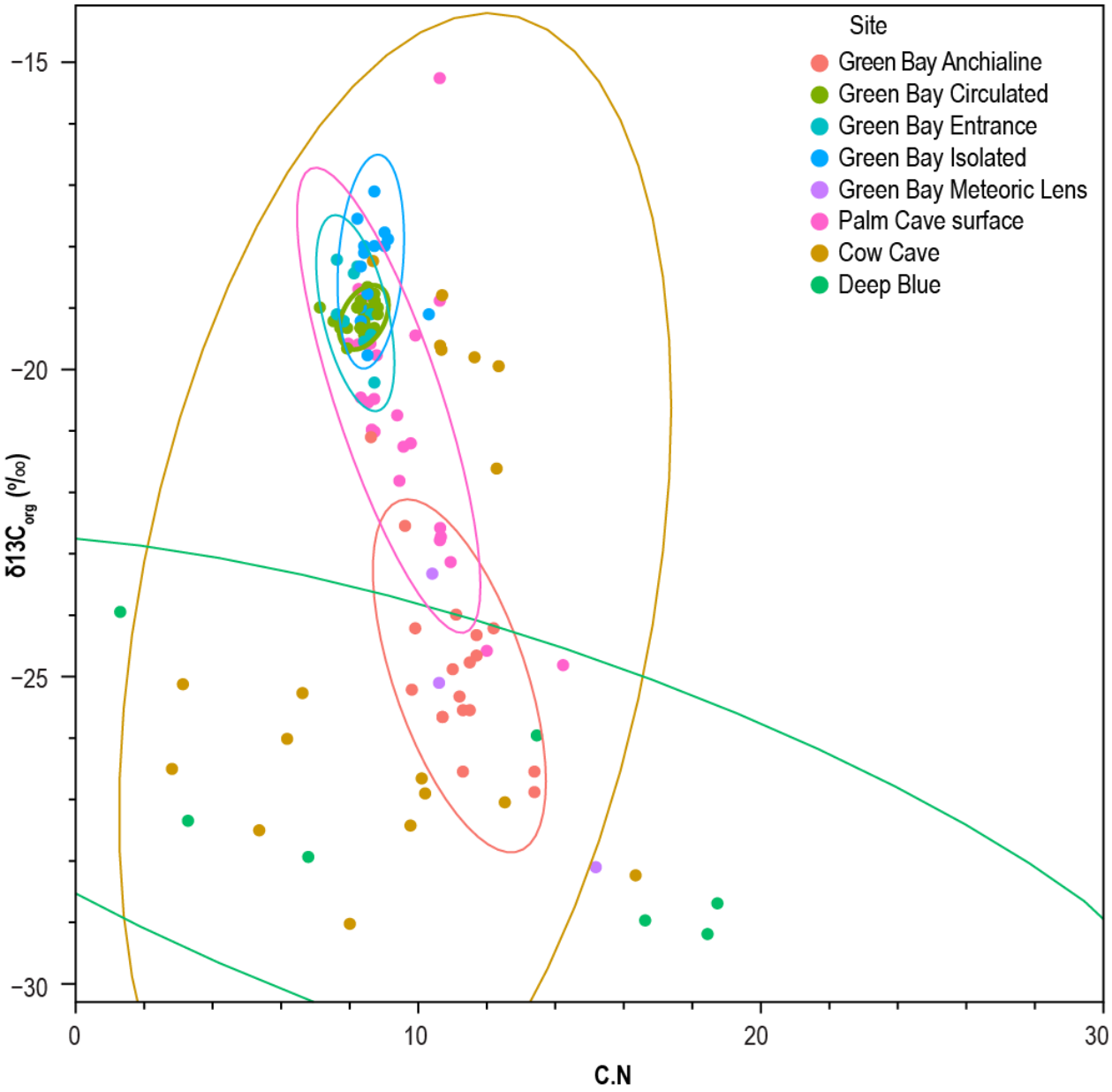

Figure 5. Cross plot measuring $\delta^{13}C_{org}$ and C:N values on bulk organic matter samples from the Palm Cave, Green Bay, Cow Cave, and Deep Blue. These results evaluate the relative contribution of terrestrial versus marine organic carbon to the KSE benthos, with 95% ellipse confidence intervals around the mean values for unique benthic anchialine habitats, identified using designated groups from the Q-mode cluster analysis results.

mix of terrestrial, marine, and algal sources (i.e., Deep Blue and Cow Cave). This corresponds to areas that are proximal to terrestrial entrances with light exposure, which likely have a higher proportion of nitrogen-rich algal-based carbon sources (Lamb et al., 2006). In comparison to Green Bay Cave and shallow areas (< 2.5 m) of Deep Blue and Cow Cave, the organic carbon in the Palm Cave is a more even mix of terrestrial and marine sources (average: –19.8 ‰, range: –15.2 to –23.7‰).

Benthic foraminiferal assemblages

Palm Cave has an abundance of benthic foraminifera, similarly to the previous caves examined from Bermuda (Green Bay Cave, Deep Blue and Cow Cave). In Palm Cave, there was a mean 3125 individuals per cm^3 (range: 40 to 13790). No new or cave endemic species of foraminifera were discovered, but foraminiferal assemblages can be identified in the caves that are distinct from those found in other Bermudian coastal environments (Carman, 1933; Javaux, 1999; van Hengstum and Scott, 2011). Unconstrained Q-mode cluster analysis can be used to identify seven foraminiferal assemblages at a dissimilarity index of ~0.55 (Fig. 6), which can be reconciled with the environmental variables evaluated with the MRT results (discussed further below).

Assemblage 1 is from the intertidal zone of Cow Cave (Assemblage 1A) and Cliff Pool Sinkhole in Green Bay Cave System (Assemblage 1B). These shallow areas experience at least periodic exposure related to tidal variability, and lower salinity in the case of Assemblage 1B. Assemblage 1 is characterized by the highest bulk organic matter (mean: 24.8%) which predominantly includes organic carbon derived from terrestrial sources, as indicated by the stable carbon isotopes and C:N ratio data (mean: –25.4‰, C:N ratio mean: 16.2; Table 1) and moderate

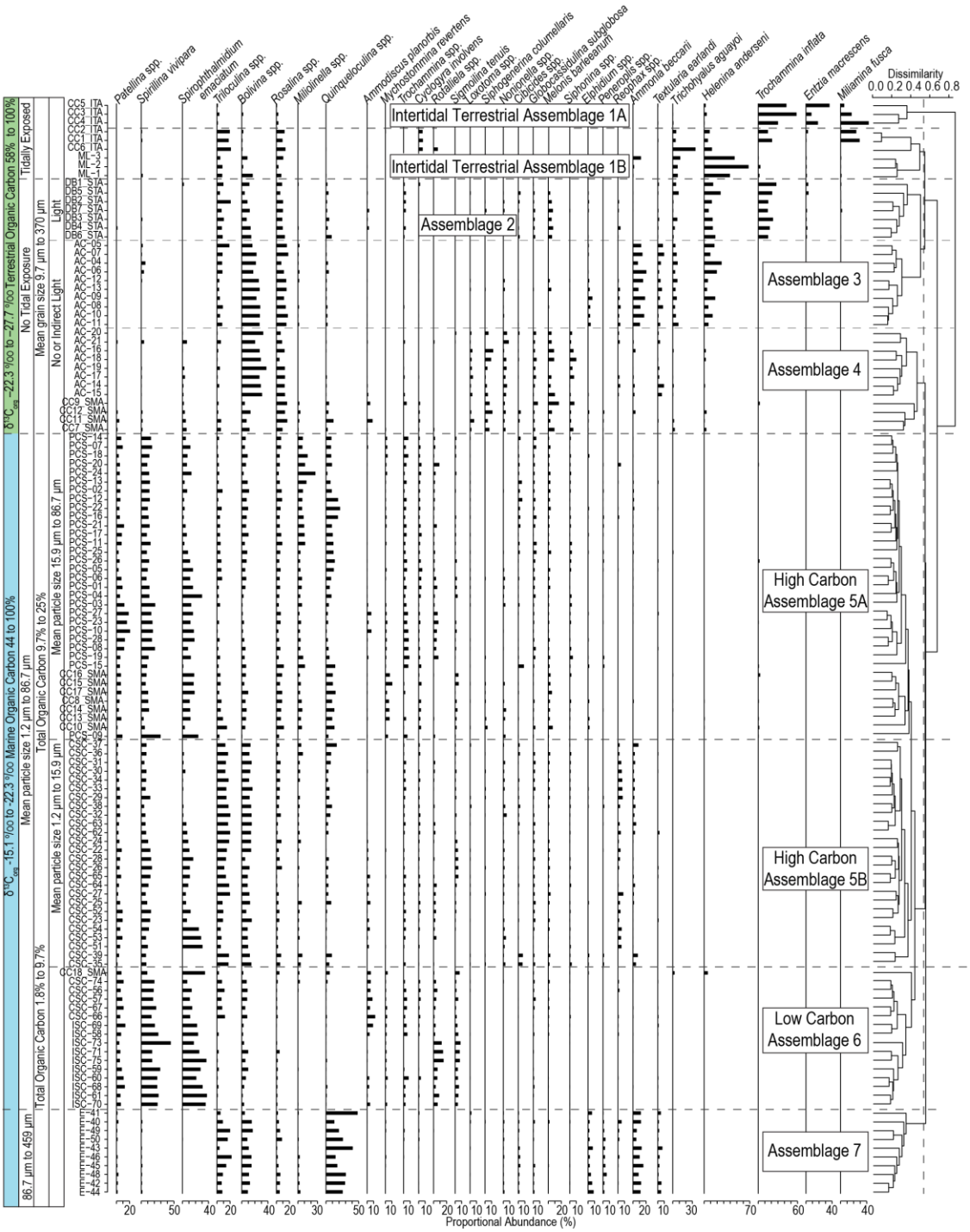

Figure 6. Detailed foraminiferal results from Palm Cave, Green Bay, Cow Cave, and Deep Blue illustrating the proportional abundance of statistically significant taxa in the surface sediment samples. Only taxa with >5% in at least one sample are shown to emphasize significant fauna. Dendrogram produced by Q-mode cluster analysis on all faunal data. A

seven- cluster interpretation (Bray- Curtis dissimilarity 0.55) of the dendrogram distinguishes the benthic anchialine habitats controlled by environmental variables.
total organic carbon (mean: 11.4%). This assemblage has the lowest diversity (*H* = 1.6) and species richness (R = 14.3) of all the identified assemblages. Foraminifera that are known to be tolerant of periodic tidal exposure, high organic matter, and lower salinities dominate the assemblage, and include *Trochammina inflata* (mean: 18%), *Miliammina fusca* (mean: 13%), and *Entzia macrescens* (mean: 7%; Table 1).

Assemblage 2 is located in subtidal areas of Deep Blue in the saline groundwater mass (van Hengstum and Little, 2019). These samples are exposed to normal diurnal sunlight variability, but are not subaerially exposed at any time during the tidal cycle (van Hengstum and Little, 2019). This assemblage is associated with decreased bulk organic matter (mean: 18.8%) and total organic carbon (mean: 4.5%), however, the organic matter present has the highest proportion of terrestrial organic carbon (mean: –26.1‰, C:N ratio mean: 11.1; Table 1). This assemblage has a species richness (R = 27) and a slight increase in diversity (*H* = 2.5). This assemblage is dominated by *T. inflata* (mean: 18%) *H. anderseni* (mean: 12.9 %), and the infaunal genera *Bolivina* spp. (mean: 10%).

Assemblage 3 occurs slightly deeper in the saline groundwater at Cliff Pool Sinkhole in Green Bay Cave that are neither tidally exposed nor exposed to brackish water (AC-04 to AC-11, van Hengstum and Scott, 2011). These samples are located in the saline groundwater mass, and experience attenuating sunlight through the water column. This assemblage is characterized by significant decrease in bulk organic matter (mean: 11.3%) yet increased total organic carbon (mean: 25.3%), which is predominantly derived from terrestrial sources (Fig. 5, mean: –24.2 ‰, C:N ratio mean: 11; Table 1). Mean species richness is 21.1, species diversity (*H*) of 2.3, and

samples are dominated by *Bolivina* spp. (mean: 26%), *Rosalina* spp. (mean: 11%), and *Ammonia beccarii* (mean: 13.5%).

Table 1. Diversity table for surface sediment samples. Arithmetic mean of the relative abundance of dominant taxa and textural characteristic for each assemblage. Species with a mean of <1% relative abundance in the biofacies were marked with a dash so dominant species could be emphasized.

	Terrestrial organic carbon				Marine organic carbon			
	Assemblage 1	Assemblage 2	Assemblage 3	Assemblage 4	Assemblage 5		Assemblage 6	Assemblage 7
					High Carbon 5A	High Carbon 5B	Low Carbon	
Sediment Characteristics	*n = 9*	*n = 7*	*n = 10*	*n = 12*	n = 36	n = 27	n = 16	*n = 10*
δ13Corg	-25.4 ± 1.7	-26.1 ± 1.7	-24.2 ± 1.5	-23.8 ± 1.1	-19.6 ± 1.2	-18.7 ± 0.2	-18.54 ± 1.3	-18.6 ± 0.5
Terrestrial organic carbon (%)	82.2 ± 13.2	87.5 ± 13.5	72.4 ± 11.6	69.5 ± 8.7	35.4 ± 9.6	28.6 ± 1.6	27.33 ± 10.6	27.7 ± 4.4
C:N	16.2 ± 9.9	11.1 ± 7.4	11 ± 1.4	10.1 ± 2	8.9 ± 0.9	8.2 ± 0.4	9.2 ± 1.3	8 ± 0.4
Total organic carbon (%)	11.4 ± 7.4	4.5 ± 2.4	25.35 ± 9.77	9.94 ± 6.4	13.7 ± 3.9	8.1 ± 1.9	6.7 ± 2.2	28.3 ± 5.4
Bulk organic matter (%)	24.8 ± 9.2	18.8 ± 6.1	11.3 ± 4	17.1 ± 4.2	8 ± 2.4	8.1 ± 2	8.9 ± 3.1	9.4 ± 5.9
Grain size (μm)	85.7 ± 105.4	43.9 ± 27.4	285.2 ± 50.9	104.9 ± 109.3	31.8 ± 17	9.4 ± 2.8	13.3 ± 8.7	296.7 ± 115.8
Foraminifera Diversity								
Total individuals (cm3)	601.8	206.6	379.3	1143.9	6669.7	4580.6	4208.4	3491.2
Species Richness (R)	14.3	27	21.1	31.1	34.4	36.4	29.7	31.9
Shannon-Wiener Diversity Index (H)	1.6	2.5	2.3	2.8	2.9	2.9	2.5	2.6
Relative Abundance								
Ammodiscus planorbis	–	1.4	–	–	**1.9**	–	2.7	–
Ammonia beccarii v. tepida	1.1	–	**13.5**	1.4	**2**	–	–	**10.9**
Bolivina spp.	2.9	**10**	**24.3**	**26**	**12.1**	7	4.6	**12**
Cibicides spp.	–	1.4	–	–	1.2	**1.9**	–	1.8
Cyclogyra involvens	3.3	–	–	–	1.7	**2.6**	1.8	–
Discorinopsis aguayoi	12	3.4	5.5	–	–	–	–	–
Elphidium spp.	–	–	2.7	–	–	–	–	4.4
Entzia macrescens	6.8	1.6	–	–	–	–	–	–
Globocassidulina subglobosa	–	2	–	3	2.1	**2.3**	1.4	1.1
Helenina anderseni	**16.6**	**12.9**	11.8	1.2	–	–	–	–
Loxotoma spp.	–	–	–	2.7	–	–	–	–
Melonis barleeanum	–	5.4	1.1	6.6	1.8	**2.2**	1.2	–
Miliolinella spp.	–	–	1.3	–	2.5	**8.8**	2.1	1.5
Miliamina fusca	12.9	1	–	–	–	–	–	–
Mychostommina revertens	–	–	–	–	–	**1.4**	2.5	–
Nonionella spp.	–	1	–	4.3	**1.6**	–	–	1.1
Patellina spp.	–	–	–	–	5.1	**7.3**	9.6	1.7
Peneroplis spp.	–	–	–	–	–	–	–	2.7
Quinqueloculina spp.	–	3.2	1.9	1.3	3.9	**7.6**	3.5	**26.6**
Reophax spp.	–	1.1	1.9	1.2	**3.3**	–	–	1.4
Rosalina spp.	8.3	9.5	**14.2**	**11**	4.3	**5.3**	3.8	4.2
Rotalliela spp.	1.7	–	–	–	1.6	**3.2**	4.8	–
Saccammina difflugiformis	–	–	–	–	**1.6**	–	–	–
Sigmoilina tenuis	–	–	–	–	**1.8**	1.4	3.6	–
Siphogenerina columellaris	–	–	–	5.3	–	–	–	–
Siphonina spp.	–	–	–	4.3	1.1	**1.3**	–	–
Spirillina vivipara	–	–	1.4	1.1	10.4	**11.8**	**19.6**	1.1
Spiroloculina spp.	–	–	–	–	–	–	–	1.3
Spirophthalmidium emaciatum	–	–	–	2.8	7.8	**10.3**	**20.4**	–
Textularia earlandi	–	1.2	5	3	–	–	–	3.5
Triloculina spp.	11.9	**10.9**	7	2.6	**14.2**	4.9	3.4	**11.4**
Trochammina spp.	–	2.5	–	–	2.1	**4.1**	3.7	–
Trochammina inflata	18.1	**18.2**	–	–	–	–	–	–
SUM	97.5	91	94.1	83.8	89.6	87.2	93.2	90.3

Assemblage 4 consists of samples primarily from two locations: (a) those located deeper in saline groundwater mass (depth: 13.7 to 18.6 mbsl), yet are still relatively proximal to Cliff Pool sinkhole in Green Bay Cave (AC-14 to AC-20; van Hengstum and Scott, 2011) and (b) subtidal areas of Cow Cave in the saline groundwater that experience more marine organic matter deposition than the shallow subtidal areas of Deep Blue (Little and van Hengstum, 2019). All these locations are located in the saline groundwater mass, are exposed to attenuating sunlight, and are not exposed during tidal cycle. There is an increase in bulk organic matter (mean: 17.1%) and a decrease in total organic carbon (mean: 9.9%), and the organic carbon is predominantly from terrestrial sources (mean: 69.5%, mean: –23.8‰, C:N ratio mean: 10.1; Table 1) relative to the entire database of samples investigated. This assemblage has an increased species richness (S = 31) and diversity (H = 2.8). *Bolivina* spp. dominates this assemblage (mean: 26%), followed by *Rosalina* spp. (mean: 11%) and *Melonis barleeanum* (mean: 6.6%). Other common species in this assemblage include *Siphogenerina columellaris* (mean: 5.3%), *Siphonina* spp. (mean: 4.3%), and *Nonionella* spp. (mean: 4.3%).

Assemblage 5 contains the majority of the samples that were collected from the Palm Cave, Cow Cave, and Green Bay Cave. Note that in the dendrogram Assemblage 5 can be further subdivided at a lower dissimilarity value (~0.38), which the MRT analysis further evaluated (discussed further below). Assemblage 5 samples were collected from the saline groundwater mass, are not subaerially exposed anytime during that tidal cycle, and are not exposed to any sunlight. Overall, this assemblage is characterized by the lowest bulk organic matter (mean: 8.5%), slight increase in total organic carbon (mean: 11.9%), and organic matter with a relatively more carbon isotopically enriched value and lower C:N ratio (mean: –19.1 ‰,

C:N ratio mean: 9; Table 1). Assemblage 5 has the highest species richness (R = 33.7) and diversity (*H* = 2.8) of all assemblages and is dominated by *Spirillina vivipara* (mean: 13.9%), *Spirophthalmidium emaciatum* (mean: 12.8%) and *Bolivina* spp. (mean: 8%). Other common species in this assemblage include *Patellina* spp. (mean: 7.1%), *Rosalina* spp. (mean: 4.5%), and *Sigmoilina tenuis* (mean: 2.3%).

Assemblage 6 contains samples that were collected from benthic areas most distal from any cave exit (either terrestrial or marine) in Green Bay Cave, and one sample from Cow Cave that is most distal from the entrance (CC-18). Assemblage 6 is characterized by sediments that are marine sourced (mean: –18.5 ‰, C:N ratio mean: 9.2), with low total organic carbon (mean: 6.7%) and bulk organic matter (mean: 8.9%). This diverse assemblage (R = 29.7, *H* = 2.5) is dominated by *Spirothalmidium emaciatum* (mean: 20.4%), *Spirillina vivipara* (mean: 19.6%) and *Patellina* spp. (mean: 9.6%).

Last, Assemblage 7 is located in samples collected from the marine cave entrance from Green Bay Cave into Harrington Sound. This assemblage is characterized by low bulk organic matter (mean: 9.4%), yet increased total organic carbon (mean: 28.3%), that is predominantly derived from a marine source, as indicated by the enriched carbon isotope value and C:N ratio (mean: –18.6 ‰, C:N ratio mean: 8; Table 1). This assemblage has the second highest diversity (*H* = 2.6) and species richness (R = 31.9). This assemblage is dominated by typical lagoonal foraminifera *Quinqueloculina* spp. (mean: 26%), *Bolivina* spp. (mean: 12 %), and *Triloculina* spp. (mean: 11.4%).

MRT analysis

The MRT analysis (MRT model 1 from Section 3.2) resulted in eight final nodes that explained 86% of the variance in the benthic foraminiferal data, and produce very similar groupings as the unconstrained Q-mode cluster analysis (Fig. 7). The MRT analysis indicates

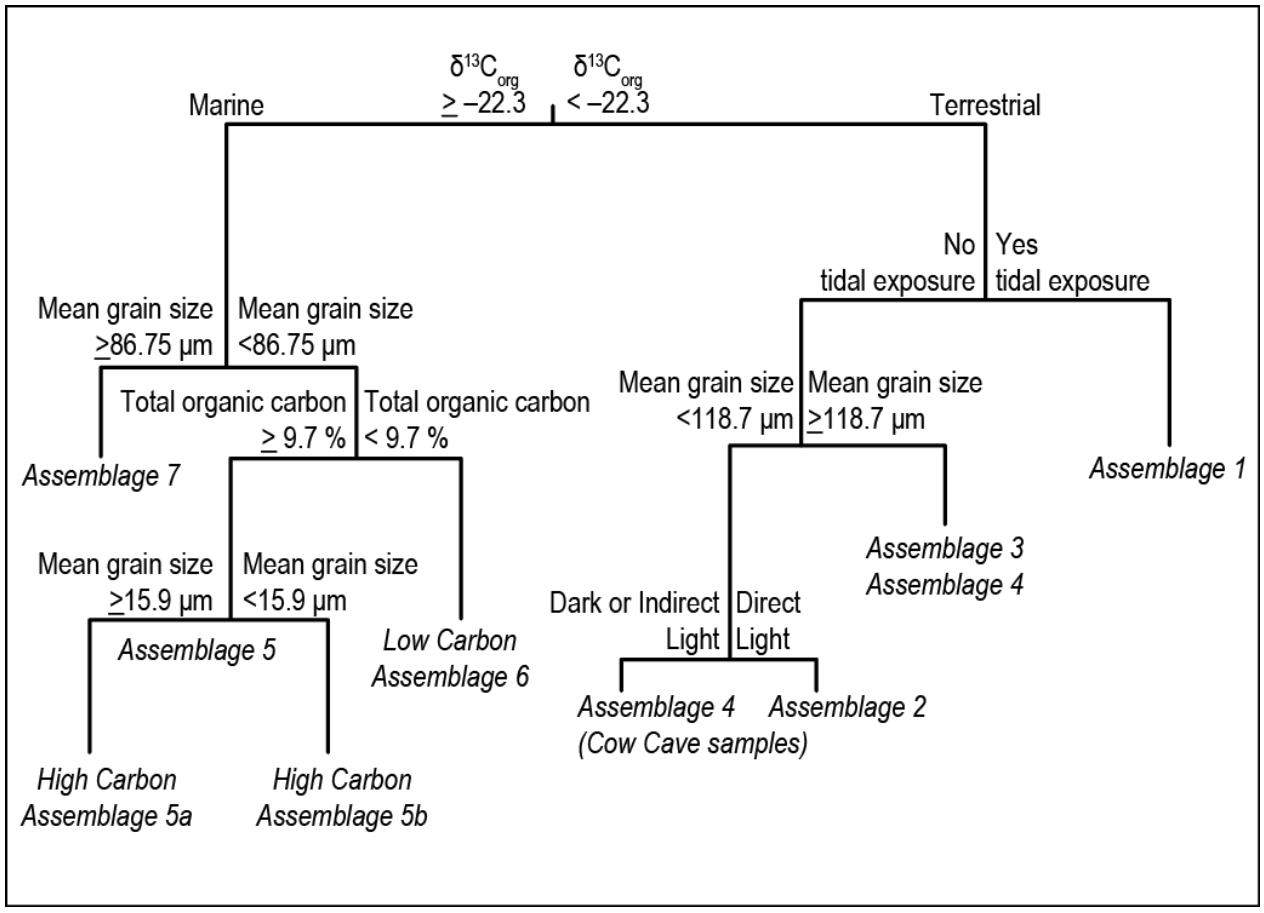

Figure 7. Multiple Regression Tree (MRT) model produced using the same database of taxonomic divisions as the unconstrained hierarchical cluster analysis (86% of variance explained).

that the origin of sedimentary organic carbon (terrestrial vs. marine) was the most important variable impacting the benthic foraminiferal assemblages. Samples with a more depleted carbon isotope value of bulk organic matter, which is indicative of proportionally more terrestrial

organic carbon (–22.3‰ to –27.7‰: Assemblages 1, 2, 3 and 4), were separated from those with a more enriched $\delta^{13}C_{org}$ value that indicates a dominance of marine organic carbon (–15.1‰ to –22.29‰: Assemblages 5, 6, and 7).

Benthic anchialine habitats that are dominated by the flux of terrestrial organic carbon were secondarily divided by tidal exposure (Assemblage 1) versus subtidal areas (Assemblage 2, 3 and 4). Mean particle size then further divided subtidal assemblages. Those with coarser substrates (particle size >118.7 μm) included Assemblage 3 from the cluster analysis dendrogram, and some of Assemblage 4 that were associated with the Cliff Pool sinkhole in Green Bay Cave. In contrast, finer substrates (particle size <118.7 μm) were dominated by Assemblage 2, and the samples from Cow Cave that formed part of Assemblage 4 in the dendrogram (Fig. 6). Light exposure determines the final split assemblages dominated by the flux of terrestrial organic carbon, with samples exposed to direct light (Assemblage 2) differentiating from those exposed to indirect light or darkness (some of Assemblage 4).

The MRT model indicates that cave areas receiving primarily marine organic carbon are colonized by Assemblage 5, 6 and 7, as identified through cluster analysis (Figs. 7, 4). The MRT analysis further separated Assemblage 7 from Assemblages 5 and 6 based on mean particle size. Assemblage 7 is from the marine entrance into Green Bay Cave from Harrington Sound, which had a substrate with coarser particle sizes (exceeding mean 86.75 μm, very fine sand) relative to Assemblages 5 and 6 (less than 86.75 μm). Assemblage 7 is dominated by *Quinqueloculina, Ammonia, Elphidium*, and *Peneroplis* (Fig. 6), which are all taxa that dominate the shallow carbonate lagoons in Bermuda and elsewhere in the tropical North Atlantic Ocean (Javaux and Scott, 2003).

Further into the caves where variations in light, salinity and tidal exposure are not relevant at our field sites, these benthic anchialine habitats that primarily receive marine organic carbon are generally dominated by *Spirillina*, *Patellina*, and *Spirophthalmidium* (Assemblage 5 and 6). In the MRT model (Fig. 7), however, total organic carbon emerges as segregating Assemblage 5 (High Carbon Marine Assemblage: >9.7% Total Organic Carbon) versus Assemblage 6 (Low carbon Marine Assemblage: <9.7 Total Organic Carbon). Assemblage 6 has proportionally more *Spirophthalmidium* and *Spirillina* than Assemblage 5, and has ancillary dominant taxa that include *Rotaliella*, *Sigmoilina*, and lower diversity (*H* index 2.5). This suggests these taxa are relatively more adapted to benthic areas with less sedimentary organic carbon. In contrast, the High Carbon Marine Assemblage 5 has similar dominant species present, but the High Carbon Marine Assemblage 5 has higher species richness (R = 36) and increased abundance of *Bolivina* spp. (mean: 10%), *Triloculina* spp. (mean: 10.5%), and *Rosalina* spp. (mean: 4.7%), while the Low Carbon Marine Assemblage 6 has a lower species richness (R = 29.4) with higher abundance of *S. emaciatum* (mean: 20.4%), *Patellina* spp. (mean: 9.6%), and *Rotaliella* spp. (mean: 4.8%).

While Assemblage 5 (High Carbon Marine Assemblage) was not divided into groups at a Bray-Curtis dissimilarity distance of 0.55 (Fig. 6), it should be noted that distinct sub-groups emerge at a Bray-Curtis dissimilarity index of 0.38 on the dendrogram. Based on the MRT model, sediment grain size determines a final split of Assemblage 5 (High Carbon Marine Assemblage) into samples with a mean particle size of 15.9 to 86.7 μm (fine sand to medium silt, Assemblage 5A) versus samples with a mean particle size <15.9 μm (medium and clay, Assemblage 5B). The slightly coarser substrate (>15.9 μm) characterize Palm Cave and Cow Cave samples (Assemblage 5A) from samples with the finest textured substrates (< 15.9 μm) in

circulated regions of Green Bay Cave (Assemblage 5B). Both Assemblage 5A and 5B have similar species richness, but substrates with finer particle sizes (Assemblage 5B) have a greater abundance of *Reophax* spp. (mean: 3.3%) and *Bolivina* spp. (mean: 12%), while larger particle sizes (Assemblage 5A) are associated with increased abundance of *Spirillina vivipara* (mean: 11.8%) and *Patellina* spp. (mean: 7.6%).

Discussion

Benthic anchialine habitats dominated by terrestrial organic carbon

In general, benthic foraminiferal assemblages distinguish between benthic anchialine habitats with different source (terrestrial vs. marine) and amount of organic carbon (Fig. 8). Given the lack of photosynthetic primary productivity in the dark cave, this organic carbon was most likely delivered to the cave benthos as particulate organic carbon from outside the cave. Benthic habitats that receive proportionally greater inputs of terrestrial organic carbon are colonized by groups of benthic foraminifera that are well-defined in the dendrogram (Assemblage 1 to 4), and they have a range of $\delta^{13}C_{org}$ values of –22.3‰ to –27.7‰. The proximity of the samples to cave openings to the forest landscape above is the obvious control on these benthic differences. Cave exits (entrances) provide a direct conduit for a flux of terrestrial sedimentation. Assemblage 1 is a mix of samples from Cow Cave and Green Bay Cave near Cliff Pool Sinkhole. The Cow Cave is a shallow, roofed cave with one entrance surrounded by the forest landscape. Cliff Pool Sinkhole is the only subaerial entrance into the Green Bay Cave System that likely contributes to the high quantities of terrestrial organic carbon. Assemblage 3 and 4 are also located within Cliff Pool Sinkhole. Lastly, Assemblage 2 is made of samples from

Deep Blue's exposed entrance at the base of a limestone cliff that is directly exposed to terrestrial sedimentation.

Dominant benthic foraminifera in areas dominated by a terrestrial organic carbon flux are well known from other coastal environments influenced by terrestrial organic carbon (e.g.,

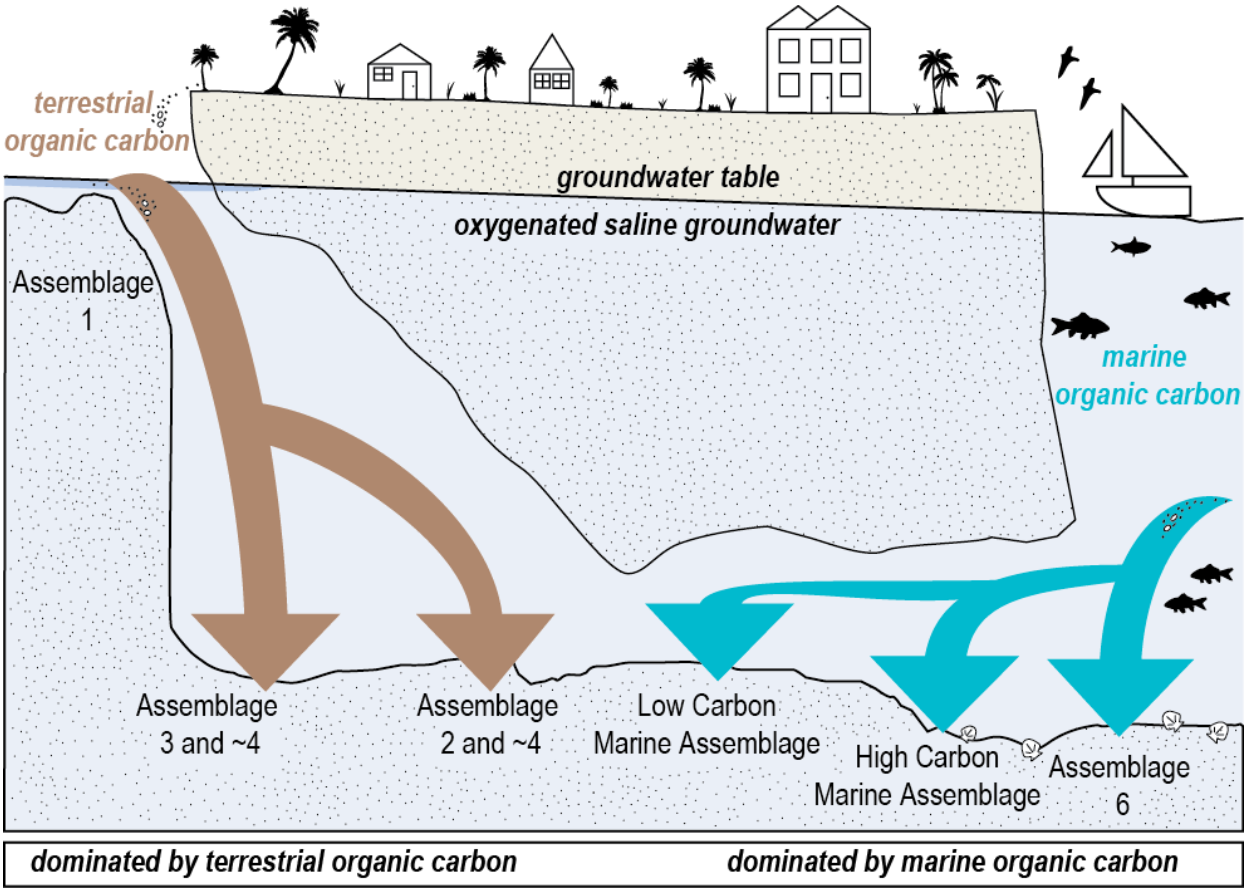

Figure 8. Conceptual model reflecting source of sedimentary organic carbon controls on benthic anchialine habitat variability in karst subterranean estuary. This is evidenced by changing foraminiferal, geochemical, and sedimentological proxies.

Trochammina inflata, Entzia macrescens, and Miliammina fusca). For example, Armynot du Chatelet et al. (2009) document increased abundances of *E. macrescens* and *T. inflata* in mixed

siliciclastic-carbonate tidal flat sediments with high C:N ratios, indicating dominant contributions from vascular (terrestrial) plants along the Canche estuary, France. *M. fusca* is known from sediments dominated by terrestrial leaf-litter in the mangrove swamps of French Guiana (Debenay et al., 2002) and in land-locked Bermuda ponds (Javaux and Scott, 2003), that are primarily influenced by terrestrial organic carbon. Additionally, the abundance of *Ammonia* spp. and *Triloculina* spp. in some of the terrestrial dominated habitats are comparable to those from terrestrially influenced carbonate lagoons in Brazil (Debenay et al., 2001). The foraminiferal distributions in Bermuda's caves are consistent with previous research documenting distinct foraminiferal assemblages in areas receiving a higher flux of terrestrial versus marine organic carbon (Mojtahid et al., 2009; Armynot du Châtelet et al., 2016).

Tidal exposure is the second most influential variable on benthic foraminifera in the benthic habitats dominated by terrestrial organic carbon. Samples that experience tidal exposure were collected from shallow areas (-0.3 to 0.6 mbsl) in Cow Cave and the Cliff Pool Sinkhole in Green Bay Cave (i.e., Assemblage 1). The micro-tidal changes in Green Bay and Cow Cave are sufficient enough to expose these sample stations during low tides. Assemblage 1 is notably less diverse with reduced species richness compared to all other subtidal assemblages. Reduced diversity and richness are common in other tidally exposed habitats (Diz et al., 2004). The dominant taxa present in the tidally exposed assemblages include the agglutinated brackish-tolerant species *Trochammina inflata*, *Miliammina fusca*, and *Entzia macrescens*, which are common in salt marsh habitats that are also vulnerable to tidal exposure (Hayward et al., 1999; Camacho et al., 2015). For example, Ruiz et al. (2005) documented *T. inflata* and *E. macrescens* dominating (exceeding 90% in most samples) mixed siliciclastic-carbonate sediments in salt marshes that are characterized by tidal exposure. Furthermore, *E. macrescens* is a useful sea-

level indicator due to its significant correlation with tidal elevation (Guilbault et al., 1995; Gehrels and van de Plassche, 1999). These results demonstrate that tidal exposure creates a distinction between assemblages vulnerable to tidal exposure at low tides and those that are consistently submerged. However, a limitation in our total understanding of how benthic foraminifera in different cave benthic habitats is that we currently do not have a modern analogue from a tidally exposed habitat that is dominated by marine organic carbon.

Particle size is the third most important variable influencing benthic foraminiferal distributions in areas dominated by terrestrial organic carbon in subtidal locations in the saline groundwater. Our results show that coarser particle sizes (very coarse sand; mean: 195.1 μm) is associated with assemblages from Cliff Pool Sinkhole in Green Bay Cave (Assemblage 3 and ~4) and dominated by *Bolivina* spp., *Ammonia beccarii*, and *Rosalina* spp. The abundance of *Rosalina* is consistent with previous research that correlates this taxon with coarser sediments, as they are often epibenthic on large particles, shells and rocks (Hayward, 1990). Additionally, Diz et al. (2004) observe abundant infaunal (e.g., *Bolivina* spp. and *Ammonia beccarii*) and epifaunal (*Rosalina* spp.) taxa in coarse sediments, suggesting that coarser particle size is better suited for benthic foraminiferal settlement. However, our results show no significant difference i*n diversity or abundance between habitats characterized by coarse and fine particle size.* The habitats characterized by fine particle size (coarse silt; mean: 33.5 μm) are associated with Deep Blue and distal regions of Cow Cave (Assemblage 2 and ~4), and characterized by a notable increase of *Trochammina inflata*. Armynot du Chatelet et al. (2009) observed dominant *T. inflata* within marsh environments, characterized by similar particle size to those of Deep Blue. Additionally, similar distinctions in benthic foraminiferal assemblages based on coarse versus fine particle size is observed along the Guadiana River Basin (Mendes et al., 2004). While the importance of mean

particle size is a disputed issue (Diz et al., 2004; Debenay et al., 2001; Armynot du Châtelet et al., 2009), our results suggest that textural variability in the substrate creates benthic anchialine habitat variability in karst subterranean estuaries that influence foraminifera.

In anchialine benthic habitats dominated by terrestrial organic carbon, the MRT model determined the categorical variable of 'light' to be the final driver of benthic foraminiferal distributions. None of the benthic foraminifera observed are those that employ photosymbionts (e.g., *Amphistegina*), therefore, foraminifera are all feeding on materials available in the substrate (e.g., algae, bacteria, detritus, or dissolved organic carbon). The results show that samples experiencing no restriction in diurnal light variability were collected from the large entrance of Deep Blue Cave (Assemblage 2), while samples that experienced attenuating light or complete darkness were collected from the sheltered Cow Cave (~Assemblage 4). The most dominant taxa present in Assemblage 2 was, *Trochammina inflata*, which is known to feed on algae (Armynot du Chatelet et al., 2009), bacteria, and terrestrial detritus (Frail-Gauthier et al., 2019). Additionally, the abundance of epiphytic species, *Rosalina* spp. (Langer, 1993), further suggests light is likely influencing the growth of algae and plants, therefore impacting benthic foraminiferal distributions. Importantly, the results from this study indicate benthic foraminiferal assemblages can define discrete habitats based on light.

Benthic anchialine habitats dominated by marine organic carbon

Assemblage 5 and 6 are found in benthic habitats that have organic matter with a more enriched $\delta^{13}C_{org}$value (range: –15.1‰ to –22.3‰) value, which is indicative of proportionally more marine organic carbon in the benthos. A more marine organic carbon signature is likely a result of the distance of sampling areas from cave exits that supply terrestrial organic matter

from the land surface (Assemblage 5), or areas with enough marine organic carbon production and accumulation to diminish the final proportion of terrestrial organic carbon (Assemblage 6). Assemblage 5 is within the deeper, dark, well-oxygenated regions of the Palm Cave, Green Bay Cave and Cow Cave, where KSE conduit morphology likely isolates this assemblage from terrestrial organic carbon influences. Assemblage 6 is located in the marine entrance of Green Bay Cave which opens into Harrington Sound. This marine entrance is a large cave passage that allows unrestricted tidal currents to deposit marine-derived organic carbon.

Habitats influenced by marine organic carbon are dominated by benthic foraminifera (e.g., *Quinqueloculina* spp., *Spirophthalmidium emaciatum*, *Spirillina vivipara*, and *Patellina* spp.) that are well-known from other coastal environments influenced by marine organic carbon. Specifically, *Quinqueloculina* spp. and other miliolids dominating the entrance of Green Bay Cave are similar to lagoonal assemblages worldwide. For example, in New Caledonia and Australia, miliolids dominate the external part of mangrove swamps open to the sea and marine influences (Debenay and Guillou, 2002), while Javaux and Scott (2003) document abundant *Quinqueloculina* in the marine dominated carbonate lagoons around Bermuda. Therefore, marine organic carbon impacting the Green Bay Cave entrance likely supports the miliolid's high relative abundances. Additionally, epifaunal suspension feeders (e.g., *Spirillina* and *Patellina*) that dominate distal areas of the KSE marine habitats are also documented from carbonate reefs and lagoons around Bermuda (Javaux and Scott, 2003). This suggests these taxa are well suited to take advantage of the marine organic carbon present deep within the KSE. The dominant taxa in marine influenced habitats further emphasize provenance of organic carbon flux to the benthos is a primary control on benthic anchialine habitat variability.

Particle size is the second driver of benthic foraminiferal distributions within marine dominated habitats. Coarse particle size (very coarse sand; mean grain size 296.7 μm) is associated with the marine entrance in Green Bay Cave (Assemblage 6), where prevalent hydrodynamic conditions likely favour the deposition of coarse sedimentary particles. The dominant epifaunal taxa (e.i., *Quinqueloculina* spp. and *Triloculina* spp.) are comparable to those found in large particles characterized by shelly sands, which provide both shelter and stable substrate for epifaunal feeding (Murray, 1988; Corliss, 1991; Schönfeld, 2002). Alternatively, fine particle size (medium silt; mean 21.6 μm) is associated with the distal sections of Green Bay Cave, Palm Cave, and Cow Cave (Assemblage 5). This habitat favours a diverse assemblage dominated by *Spirophthalmidium emaciatum*, *Sprillina vivipara*, *Bolivina* spp., and *Patellina* spp. Outside of Bermuda's caves, the response of benthic foraminifera to sediment texture is variable, potentially dependant upon different environments. For example, it has been previously observed that benthic foraminifera standing crops are higher in finer substrates in carbonate lagoons, compared to coarser sediments (Debenay et al., 2001; Armynot du Châtelet et al., 2009). However, our results show habitats defined by both fine and coarse particle size have similar benthic foraminiferal diversity and richness. Therefore, particle size is likely significant to specific taxa and remains an important variable for benthic foraminiferal distributions in this study (Boltovkoy et al., 1991; Frontalini et al., 2013; Armynot du Châtelet et al., 2016; Little and van Hengstum, 2019).

The amount of total organic carbon delivered to the benthos is the third and final driver of benthic foraminiferal distributions in habitats dominated by marine organic carbon, which divides remaining samples into two groups: Low Carbon Marine Assemblage 6 and High Carbon Marine Assemblage 5. The Low Carbon Marine Assemblages (<9.7% total organic carbon) are

located in the most distal locations, away from any karst windows (entrances), in Green Bay Cave and the Palm Cave, while the High Carbon Marine Assemblage (>9.7% total organic carbon) is found in the well-circulated Green Bay and Palm Cave passages. Additionally, the High Carbon Marine Assemblage can be divided into two sub-groups based on particle size. Samples with larger particle size (mean: >15.9 μm) are located in the passages of the Palm Cave, while samples characterized by smaller particle size (mean: <15.9 μm) are located in the passages of Green Bay Cave. The particle size differences define habitats dominated by medium versus fine silt and likely are cave-specific. Both High Carbon and Low Carbon Marine assemblages are dominated by *Spirophthalmidium emaciatum, Spirillina vivipara, Patellina* spp., and *Bolivina* spp., however, the High Carbon Marine Assemblage has a higher diversity and species richness while the Low Carbon Marine Assemblage has higher abundances of *S. emaciatum* and members of the order Sprillinida (e.g., *Mychostommina, Patellina, Spirillina*). The abundance of benthic foraminifera within the deep, dark passages of Green Bay Cave and the Palm Cave suggest dominant taxa are taking advantage of marine organic carbon, however the increased abundance of *S. emaciatum* and other spirillinids in the Low Carbon Marine assemblage further indicates these taxa are likely indicators of anchialine habitats flooded by an oxygenated saline groundwater mass under oligotrophic conditions. Therefore, the results from this study indicate that benthic foraminifera can discriminate between benthic anchialine habitats, that are no longer exposed to other abiotic variables (e.g., tidal exposure, light, salinity), based on the source of total organic carbon.

Conclusions

The following conclusions were drawn from this study:

- Bermuda's caves that are primarily flooded by oxygenated saline groundwater are populated by foraminifera that identify benthic anchialine habitats that are controlled by organic matter source (terrestrial vs. marine), total organic carbon, different groundwater masses in the karst subterranean estuary (i.e., salinity), benthic substrate texture, general light availability, and tidal exposure.
- The flux of terrestrial organic carbon (i.e., organic matter source) to the benthos is the most significant environmental variable distinguishing benthic anchialine habitat variability in the saline groundwater mass, according to the benthic foraminifera.
- Benthic areas with increased terrestrial organic carbonate (>58% terrestrial organic carbon) are dominated by *Rosalina*, *Triloculina*, and *Bolivina*, versus benthic areas with more marine organic carbon dominated by *Pattellina*, *Sprillina*, *Spiropthalmidium*. Additional foraminiferal taxa, community diversity, and species richness can evaluate the impact of tidal exposure, ground water mass salinity, light, and substrate texture.
- Reduced total organic carbon (TOC) accumulation in the dark inner cave (i.e., organic matter quantity) further divides anchialine benthic habitats. These areas are dominated by *Spirophthalmidium*, *Spirillina*, *Patellina*, and *Rotaliella*.

CHAPTER III

DEVELOPMENT OF ANCHIALINE CAVE HABITATS AND KARST SUBTERRANEAN ESTUARIES SINCE THE LAST ICE AGE*

Introduction

Sea-level oscillations during the last 500 million years (Phanerozic Eon) have impacted marine and terrestrial island biogeography and evolution by modifying habitat availability and opportunities for organismal gene flow (Hallam & Wignall, 1999; Peters, 2008; Pimiento et al., 2017). It is generally thought that sea-level regressions can reduce the areal extent of coastal and neritic habitats and can cause bottlenecks in the marine realm (Valentine & Jablonski, 1991; Klaus et al., 2011; Ludt & Rocha, 2015), whereas terrestrial island fauna and flora benefit from habitat expansion during regressions (Weigelt et al., 2016; Ali & Aitchison, 2014; Fernández et al., 2015; Papadopoulou & Knowles, 2017). The defaunation risk in the coastal zone is elevated during the Anthropocene from several human-caused factors like habitat degradation and urbanization (McCauly et al., 2012), but disentangling how modest rates of current sea-level rise threaten aquatic island fauna remains difficult to assess (Holland, 2012; Harnik et al., 2012).

Worldwide on carbonate islands and platforms, subsurface mixing of rain and marine water creates karst subterranean estuaries (KSEs, Fig. 1). Hydrographically, KSEs are analogous to subaerial estuaries by having an upper meteoric water mass of varying salinity buoyed on a saline groundwater mass below (Moore, 1999; Gonneea et al., 2014). These two groundwater bodies often destabilize in the subsurface to create mixing zones (Menning et al., 2015;

* Reprinted with permission from "Development of anchialine cave habitats and karst subterranean estuaries since the last ice age" by van Hengstum *et al., accepted* (expected to be published in 2019) *Scientific Reports*, DOI: 10.1038/s41598-019-48058-8. Copyright 2019 by Springer Nature.

Brankovits et al., 2017; Beddows et al., 2005; Whitaker & Smart, 1990), and their oceanic discharge impacts global biogeochemical cycles (Gonneea et al., 2014; Trezzi, et al., 2016). Only in the late 20th century did technical SCUBA diving procedures allow human exploration of KSEs through flooded caves, which lead to the discovery of their unique ecosystems, fauna, and habitats that are now prefaced with the adjective 'anchialine' (Stock et al., 1986). The fossil record (Steinthorsdottir & Håkansson, 2017; van Hengstum et al., 2009; Rosso et al., 2014) and molecular phylogenetics (Jurado-Rivera et al., 2017; Legg et al., 2013; Gonzales et al., 2017) suggests that anchialine fauna and ecosystems persisted through the Phanerozoic and predated angiosperms, whose evolutionary history and biogeochemical functioning inform early Paleozoic marine ecosystems and invertebrate evolution (Regier et al., 2010; Schwentner et al., 2017). Steep environmental gradients create diverse benthic and pelagic sub-habitats in the subsurface from the ocean transecting inland (Fig. 1), such that aquatic coastal caves are often categorized as freshwater caves (meteoric water mass), anchialine caves (both water masses), or marine caves (saline water mass). Despite this segregation, some taxa have a modern distribution and evolutionary history in both water masses (e.g., atyid shrimps; Moritsch et al., 2014). If these habitats are also linked through allogenic succession, then it is perhaps more appropriate to consider these sub-habitats as part of an anchialine habitat continuum so evolutionary adaptions to environmental change can be more easily assessed (Fig. 1).

Pioneering cave ecologist Riedl first hypothesized that coastal cave habitats experienced allogenic succession from sea-level forced vertical migration of KSEs, which isolated subterranean aquatic fauna and promoted speciation through vicariance (Riedl & Ozretić, 1969). This process was subsequently termed the 'regression model' (Holsinger, 1994; Stock, 1980), which could be caused by either tectonic uplift or relative sea-level fall, and used to evaluate the

disjunct biogeography of subterranean fauna. However, significant barriers exist for developing physical data on developmental succession in anchialine habitats, during either regressions or transgressions. Instrumental records (e.g., decadal scale) of hydrographic change in KSEs are unavailable, and speleothems (e.g., stalagmites) cannot be used to document millennial-scale environmental change when caves are flooded (Richards et al., 1994; Dutton et al., 2009). Soft-bodied endemic cave fauna have a poor fossil preservation, and picturesque clean cave galleries are created by either poor sedimentation in caves (Collins et al., 2015), or subsurface currents blowing-out cave sediment. Thus far, available sediment records of environmental change in KSEs are either temporally-fragmented (Fornós et al., 2009; van Hengstum et al., 2011), or only document the hydrographic history of an individual groundwater mass (Collins et al., 2015; Collins et al., 2015; van Hengstum et al., 2010). These knowledge gaps mean that 21st century marine ecosystem risk assessments have little evidence to support forecasting how sea-level rise will impact global *subsurface* aquatic island fauna.

Here we present the most complete record yet known of developmental succession in anchialine habitats in response to concomitant relative sea-level rise and vertical migration of a KSE since the last ice age. The highest quality sediment record yet found in an underwater cave in Bermuda documents the turnover of anchialine habitats, and their sub-habitats, in response to vertical migration of the KSE. Sea-level rise during the early Holocene first flooded cave passages with a meteoric lens, followed by a paleo mixing zone, and finally saline groundwater to create modern marine cave habitats in western Bermuda. Developmental succession of anchialine habitats during a transgression is now resolved, and more significantly, the results illuminate how sea-level rise can force subsurface aquatic island fauna to experience a previously unknown bottleneck event. It is highly likely that this process impacted the

evolutionary history of global subsurface aquatic island fauna during the Phanerozoic. More problematically, 21st century island-based marine ecosystem risk assessments are incomplete if the impact of sea-level rise on anchialine ecosystems is not regionally evaluated.

Study site

Bermuda is a ~35 million year old volcanic seamount in the North Atlantic Ocean capped by Quaternary-aged carbonates (limestone) that were deposited during sea-level highstands, interspaced by paleosols that accumulated during the ice ages (Vacher et al., 1995). The limestone units are lithified wind-blown dunes of shallow marine carbonate particles (Rouse et al., 2018), which subsequently weathered into a mature karst landscape. Large caves in Bermuda were first dissolved by both rain and groundwater, which then subsequently experienced repetitive collapse events (Vacher & Rowe, 1997; Land et al., 1967; Palmer et al., 1977).

Bermuda is an ideal location for this study for several reasons. The local flooded caves are an established biodiversity hot spot of endemic anchialine fauna, and the region has served as an important island model for understanding the evolutionary history of anchialine fauna (Iliffe et al., 1983). The ~30-80 m thick carbonate cap and its caves (Pirsson, 1914; Mylroie et al., 1995) would have been dry during the last glacial maximum (~20,00 years ago) when local relative sea level and groundwater was ~120 m lower (Miller et al., 2005). Since then, deglacial sea-level and groundwater-level rise first flooded topographic depressions to create freshwater lakes in the Bermuda banktop, followed by their conversion to shallow lagoons with complete platform flooding (Vollbrecht, 1996; Ashmore & Leatherman, 1984). Modern Bermudian flooded caves must have similarly developed by the upward displacement of the KSE, with endemic anchialine fauna migrating into newly created ecospace either from the volcanic lithology below or oceanic dispersal (Iliffe et al., 1983). Low groundwater current velocities

allow sediment to accumulate on cave floors, and most caves in western Bermuda are at the final stage of oceanic flooding with active seawater circulation.

On the northeastern margin of Harrington Sound in Bermuda, the Palm Cave System occurs to a maximum depth in the subsurface of 23 m below modern sea level (mbsl). There is no halocline in Palm Cave because a meteoric lens does not develop on the narrow isthmus between Harrington Sound and Castle Harbour, so the passages are all flooded by oxygenated saline groundwater (Fig. 9). Despite the absence of a local meteoric lens, Palm Cave is part of the anchialine habitat continuum, and can be colloquially referred to as a marine cave (Fig. 1). In summer 2015, the conditions of the saline groundwater mirrored the impact of strong summertime evaporative and radiative forcing on the adjacent Harrington Sound source water (pH of 7.8 ± 0.2, 28.5 ± 0.2°C, 38.7 ± 0.4 psu, Fig. 9). Multiple physical openings from the coastal lagoon (i.e., Harrington Sound) and subaerial forest landscape (e.g., 32.34°, −64.71) allow terrestrial and marine organic matter to erode into the cave. Sediment push cores (n = 13) were collected using technical cave diving procedures (Fig. 9, Supplementary Table S1) from the deepest parts of the cave that preserve sediment accumulations, and areas with representative sedimentary units. Multiple cores sampled the stratigraphy to limestone bedrock.

Methods

After collection, cores were transported back to the laboratory to be split lengthwise for x-radiography, photography, textural and micropaleontological analysis (Table 2). Cores were sub-sampled at 1-cm intervals downcore for analysis of sedimentary bulk organic matter content using a standard Loss-on-Ignition procedure, whereby the mass lost during combustion at 550°C for 4.5 hrs is expressed as a weight percent (Heiri et al., 2001). The textural variability in the

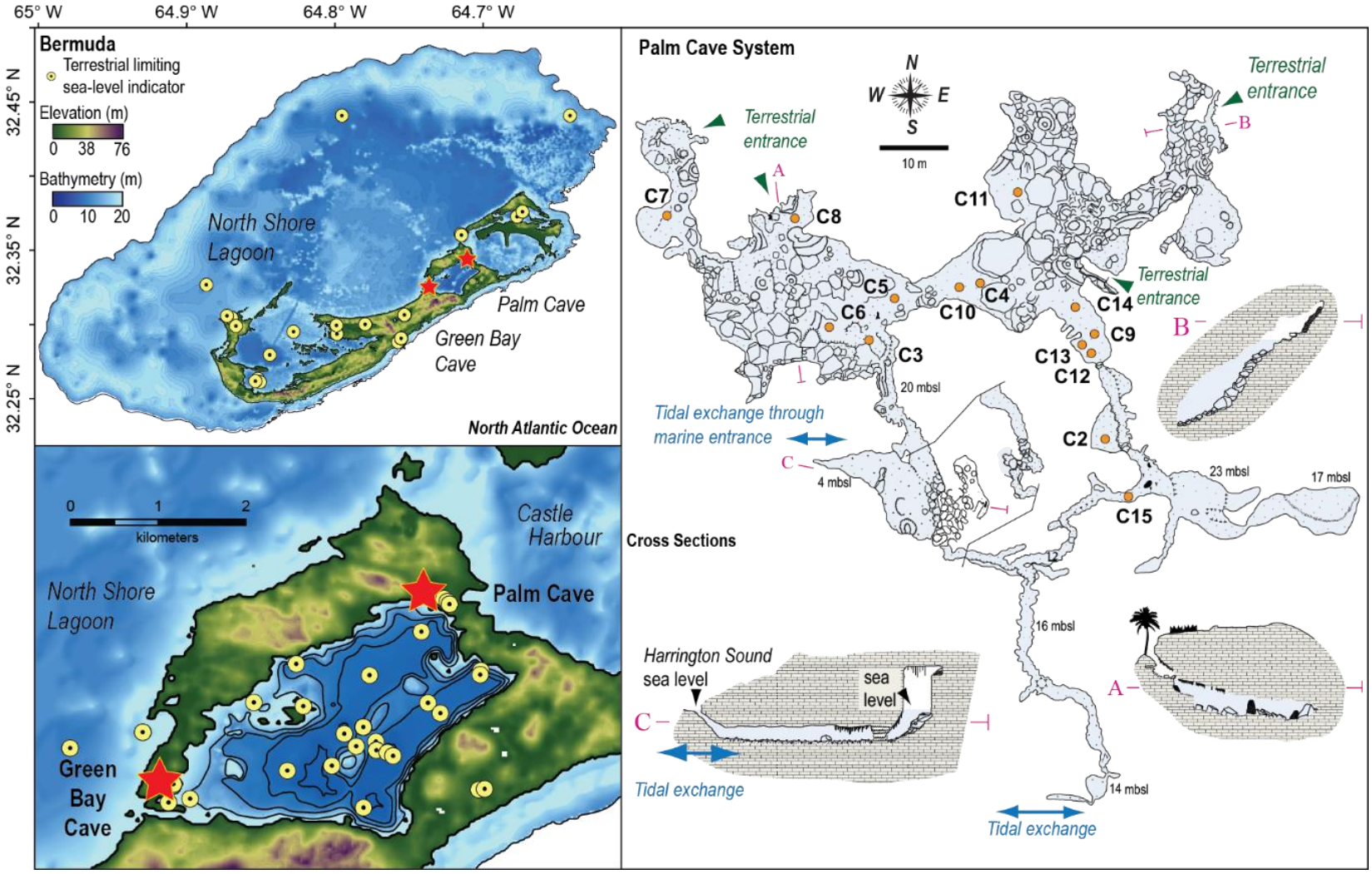

Figure 9. Bermuda and detailed survey Palm Cave System. Digital elevation model of Bermuda in the North Atlantic Ocean. (Bottom) Detailed map of Harrington Sound plotted in ArcGIS. Yellow markers identify locations of geological sea-level indicators from Bermuda (peat, *n* = 113, Appendix A). Detailed survey of Palm Cave (adapted after original survey of Jason Richards, with locations of sediment cores and cave entrances.

Table 2. Detailed information on core locations in Palm Cave relative to the Earth's surface. GPS co-ordinates were estimated from overlaying cave survey (≤ 3 m horizontal uncertainty) in Google Earth (± 3 m horizontal uncertainty).

Core Label	Water Depth (m)	Water Depth Uncertainty	Latitude	Longitude	Core termination	Final core length (cm)
SM-C2	20.1	0.3	32.345072°	-64.711072°	sediment	0.78
SM-C3	20.3	0.3	32.345411°	-64.711962°	hardground	0.8
SM-C4	20.7	0.3	32.345627°	-64.711658°	sediment	0.79
SM-C6	20.3	0.3	32.345466°	-64.712108°	sediment	0.78
SM-C7	9.7	0.3	32.345822°	-64.712690°	hardground	0.66
SM-C8	5.3	0.3	32.345869°	-64.712214°	hardground	0.25
SM-C9	20.3	0.3	32.345438°	-64.711141°	hardground	0.57
SM-C10	20.7	0.3	32.344779	-64.711037	hardground	1.75
SM-C11	18	0.3	32.346000°	-64.711450°	sediment	0.46
SM-C12	20.4	0.3	32.345367°	-64.711143°	hardground	0.38
SM-C13	20.4	0.3	32.345417°	-64.711189°	sediment	0.43
SM-C14	20.7	0.3	32.345039°	-64.711257°	hardground	0.88
SM-C15	21.9	0.3	32.345361°	-64.711628°	hardground	0.83

coarse sedimentation deposition (e.g., coarse fraction) was quantified in contiguous 1-cm intervals downcore on separate sediment sub-samples using a Sieve-first Loss-on-Ignition procedure (van Hengstum et al., 2016). Contiguous 1-cm sediment sub-samples, with a standardized initial volume of 2.5 cm^3, were first wet sieved over a 63-μm mesh, dried for 12 hours in an oven at 80 °C and weighed to determine the original sediment mass. Samples were the ignited for 4.5 hours at 550 °C in a muffle furnace to remove organic matter from the sediment samples to concentrate the remaining mineral residue, and re-weighed to determine remaining mineral mass after combustion. The variability in coarse sediment was then expressed as mass per unit volume ($D_{>63\ um}$ mg cm^{-3}). Core 4 (n = 26) and core 10 (n = 23) were quantitatively analyzed for preserved subfossil benthic foraminiferal assemblages. Downcore sediment subsamples (2.5 cm^3, 0.5 cm core width) were sieved over a 63 μm mesh, and wet-picked onto micropaleontological slides for taxonomic identification and assemblage analysis

Figure 10. Downcore proportional abundance of dominant benthic foraminifera in cores 4 and 10. Assemblages of foraminifera were identified with dendrograms produced from Q-mode constrained cluster analysis on statistically significant taxa. Benthic foraminifera were rare in core 4 from 15.5 to 32.5 cm, and core 10 from 12.5 to 25.5 cm, but *Bolivina* sp. was observed.

with Q-mode cluster analysis (Fig. 10). The qualitative (presence vs. absence) preservation of meiofauna (e.g., ostracodes, foraminifera) and macrofauna (e.g., bivalves, gastropods) in all cores was assessed by wet sieving bulk sediment over a 63 μm mesh at 3 to 5 cm downcore, with representative individuals imaged with a Hitachi desktop scanning electron microscope. To further understand the provenance of accumulating bulk organic matter, sediment samples (n = 215) from selected cores (3, 6, 10, 14, 15) were analyzed for the stable carbon isotopic value ($\delta^{13}C_{org}$) and C:N ratio of bulk organic matter. Samples were first treated with a 10% HCl digestion to remove carbonates, followed by geochemical measurements in a Costech 200 Elemental Analyzer connected to Thermo-Electron Delta V Advantage Isotope Ratio Mass Spectrometer. Final $\delta^{13}C_{org}$ values are reported in per mil notation (‰) relative to the standard Vienna Pee Dee Belemnite (VPDB) for carbon (expressed as parts per mil, ‰), with analytical precision on $\delta^{13}C_{org}$ better than ±0.2‰ (1σ) and ±0.1 on C:N. Age control is provided by radiocarbon dating (n = 51) on a combination of bulk organic matter from the organic-dominated facies, terrestrial plant macrofossils (when available), and marine bivalves. Twenty-seven samples were processed by accelerator mass spectrometry radiocarbon, with twenty-six dated using the Continuous Flow AMS (CFAMS) method. All radiocarbon dates were calibrated to sidereal years before 1950 AD (Cal Yrs BP_{1950}) using IntCAL13[86] (Table 3). Samples from notably iron-rich carbonate and paleosols (cores 10 and 4) were subject to X-ray diffraction to determine dominant minerals (Table S4). Selected samples were analyzed on a Bruker-AXS D8 Advanced Bragg-Brentano X-ray powder diffractometer employing the standard XRD laboratory protocols. Final mineral determination was made by comparing the resultant diffractograms with the 2005 International Center for Diffraction Data material identification database to determine final mineralogy.

Table 3. Radiocarbon data (*n* = 51) generated by the National Ocean Sciences Accelerator Mass Spectrometry (NOSAMS) facility at Woods Hole Oceanographic Institution, and all were calibrated to sidereal years before present (BP_{1950}) using IntCal 13[5], with the highest probability 2σ result used to frame the results. Other lower probability calibration results do not change the interpretations of the data. Raw calibration data from this table is then rounded to the nearest decade for presentation in Figure 3 in the text, as per radiocarbon convention. The NOSAMS process abbreviations include: (a) gas bench (GB) is the continuous-flow accelerator mass spectrometry technique[6] (CF-AMS), (b) OC is for the standard alkali-acid-alkali organic carbon pretreatment for Standard AMS dating, and (c) HY is for hydrolysis of biogenic carbonate.

Sample Identifier	Core	Depth Mid-Point	Material dated	NOSAMS Process Abbreviation	Sample Processing Type	Accession Number	F Modern	Fm Err	Age	Age Err	δ13C	D13C Source	Highest Probability 2σ Midpoint	Highest Probability 2σ Uncertainty	Probability
SM-C2-14.5 cm	C02	14.5	mollusc	GB	CF-AMS	NA	0.5372	0.0077	4991	115	NA	Not Measured	5650	375	0.949
SM-C2-31.5 cm	C02	31.5	mollusc	GB	CF-AMS	NA	0.4824	0.0071	5855	118	NA	Not Measured	6679	278	1
SM-C2-32.5-33	C02	32.75	mollusc	HY	Standard AMS	OS-112233	0.4861	0.0016	5790	25	1	Measured	6596	66	0.949
SM-C2-47-47.5	C02	47.25	organic carbon	OC	Standard AMS	OS-112146	0.368	0.0014	8030	30	-25.01	Measured	8934.5	79.5	0.719
SM-C2-49.5-50 cm	C02	49.75	organic carbon	OC	Standard AMS	OS-109436	0.3569	0.0014	8280	30	-24.3	Measured	9263	71	0.576
SM-C2-73-74	C02	73.5	Plant/Wood	OC	Standard AMS	OS-112147	0.3448	0.0017	8550	40	-26.48	Measured	9519	34	1
SM-C3_5-6 cm	C03	5.5	mollusc	GB	CF-AMS	OS-129491	0.7645	0.0182	2160	190	NA	Not Measured	2137	411	0.935
SM-C3-15.5 cm	C03	15.5	mollusc	GB	CF-AMS	NA	0.6721	0.0093	3192	112	NA	Not Measured	3395	254	0.987
SM-C3_23-24 cm	C03	23.5	organic carbon	OC	Standard AMS	OS-119838	0.3902	0.0017	7560	35	-22.32	Measured	8374	42	1
SM-C3_59-60 cm	C03	59.5	organic carbon	OC	Standard AMS	OS-119837	0.3816	0.0015	7740	30	-22.44	Measured	8516.5	72.5	1
SM-C3_66-67 cm	C03	66.5	organic carbon	OC	Standard AMS	OS-119837	0.3589	0.0015	8230	35	-24.21	Measured	9189.5	116.5	0.959
SM-C4_24-25 cm	C04	24.5	organic carbon	OC	Standard AMS	OS-119843	0.3836	0.0015	7700	30	-22.53	Measured	8481.5	62.5	1
SM-C4_59-60 cm	C04	59.5	organic carbon	OC	Standard AMS	OS-119844	0.3677	0.0014	8040	30	-25	Measured	8975	46	0.547
SM-C4_72-73 cm	C04	72.5	organic carbon	OC	Standard AMS	OS-119840	0.3596	0.0015	8220	35	-23.97	Measured	9183	111	0.948
SM-C6_10-11 cm	C06	10.5	mollusc	GB	CF-AMS	OS-129493	0.6846	0.0165	3040	190	NA	Not Measured	3205	433	1
SM-C6_19-20 cm	C06	19.5	mollusc	GB	CF-AMS	OS-129494	0.6067	0.0151	4010	200	NA	Not Measured	4436.5	539.5	0.996
SM-C6_20-21 cm	C06	20.5	mollusc	GB	CF-AMS	OS-129495	0.6501	0.016	3460	200	NA	Not Measured	3764.5	526.5	1
SM-C6_70-71 cm	C06	70.5	organic carbon	OC	Standard AMS	OS-119839	0.3576	0.0014	8260	30	-24.11	Measured	9225	97	0.892
SM-C7_10-11 cm	C07	11.5	mollusc	GB	CF-AMS	OS-129497	0.9136	0.0213	725	190	NA	Not Measured	717.5	292.5	0.96
SM-C7_58-60 cm	C07	58.5	mollusc	GB	CF-AMS	OS-129497	0.8621	0.0203	1190	190	NA	Not Measured	1072.5	344.5	0.987
SM-C9_7-8 cm	C09	8.5	mollusc	GB	CF-AMS	OS-129499	0.8809	0.0206	1020	190	NA	Not Measured	976	323	0.99
SM-C9_19-20 cm	C09	19.2	mollusc	GB	CF-AMS	OS-129499	0.6332	0.0156	3670	200	NA	Not Measured	4003	527	0.999
SM-C9_47-48 cm	C09	47.5	organic carbon	OC	Standard AMS	OS-122741	0.3384	0.0016	8700	35	-24.42	Measured	9646.5	99.5	0.993
SM-C10-D1_15.5-16 cm	C10	15.75	organic carbon	OC	Standard AMS	OS-124667	0.3842	0.0014	7690	30	-23.17	Measured	8479	62	1
SM-C10-D2_39-40 cm	C10	109.5	organic carbon	OC	Standard AMS	OS-122742	0.3577	0.0017	8260	35	-23.37	Measured	9228	103	0.86
SM-C10-D2_66-67 cm	C10	136	organic carbon	OC	Standard AMS	OS-122743	0.3493	0.0014	8450	35	-23.62	Measured	9480	47	1
SM-C10-D3_45-46 cm	C10	157	organic carbon	OC	Standard AMS	OS-122744	0.3445	0.0019	8560	45	-24.29	Measured	9535.5	61.5	1
SM-C10-D3_62-63 cm	C10	174.5	organic carbon	OC	Standard AMS	OS-122745	0.3395	0.0015	8680	35	-23.7	Measured	9624	80	0.998
SM-C11_8.5-9 cm	C11	8.75	organic carbon	OC	Standard AMS	OS-122737	0.3567	0.0016	8280	35	-24.37	Measured	9271	135	1
SM-C11_30-31 cm	C11	30.5	organic carbon	OC	Standard AMS	OS-122738	0.3534	0.0016	8360	35	-24.11	Measured	9382	87	1
SM-C12_3-4 cm	C12	4.5	mollusc	GB	CF-AMS	OS-129501	0.7263	0.0174	2570	190	NA	Not Measured	2688	393	0.948
SM-C12_11-12 cm	C12	11.5	mollusc	GB	CF-AMS	OS-129501	0.676	0.0163	3140	190	NA	Not Measured	3298.5	433.5	0.977
SM-C14_31-32 cm	C14	31.5	organic carbon	OC	Standard AMS	OS-135567	0.3383	0.0013	8710	30	-25.88	Measured	9648.5	97.5	0.992
SM-C14_86-87 cm	C14	86.5	organic carbon	OC	Standard AMS	OS-135568	0.3369	0.0013	8740	30	-24.71	Measured	9747.5	207.5	0.881
SM-C15_6-7 cm	C15	6.5	mollusc	GB	CF-AMS	OS-129502	0.8951	0.021	890	190	NA	Not Measured	859	324	0.993
SM-C15_9-10 cm	C15	10.5	mollusc	GB	CF-AMS	OS-129504	0.8478	0.0214	1330	200	NA	Not Measured	1261	365	0.97
SM-C15_10-11 cm	C15	10.5	mollusc	GB	CF-AMS	OS-129504	0.714	0.0173	2710	190	NA	Not Measured	2802.5	452.5	0.987
SM-C15_15-16 cm	C15	15.5	mollusc	GB	CF-AMS	OS-129505	0.7355	0.0175	2470	190	NA	Not Measured	2502.5	458.5	1
SM-C15_19-20 cm	C15	20.5	mollusc	GB	CF-AMS	OS-129507	0.7255	0.0174	2580	190	NA	Not Measured	2691	392	0.951
SM-C15_39-40 cm	C15	39.5	mollusc	GB	CF-AMS	OS-129507	0.6931	0.0167	2940	190	NA	Not Measured	3148.5	426.5	1
SM-C15_40-41 cm	C15	40.5	mollusc	GB	CF-AMS	OS-129508	0.6595	0.016	3340	190	NA	Not Measured	3613.5	475.5	0.991
SM-C15_43-44 cm	C15	43.5	mollusc	GB	CF-AMS	OS-129509	0.633	0.0163	3670	210	NA	Not Measured	4014	556	1
SM-C15_48-49 cm	C15	49.5	mollusc	GB	CF-AMS	OS-129511	0.6481	0.0159	3480	200	NA	Not Measured	3812.5	485.5	0.982
SM-C15_54-55 cm	C15	54.5	mollusc	GB	CF-AMS	OS-129478	0.6264	0.0153	3760	200	NA	Not Measured	4130	517	0.981
SM-C15_63-64 cm	C15	64.5	mollusc	GB	CF-AMS	OS-129480	0.5941	0.015	4180	200	NA	Not Measured	4761.5	538.5	0.986
SM-C15_64-65 cm	C15	64.5	mollusc	GB	CF-AMS	OS-129480	0.6087	0.0151	3990	200	NA	Not Measured	4427.5	541.5	1
SM-C15_65-66 cm	C15	66.5	mollusc	GB	CF-AMS	OS-129482	0.5243	0.0136	5190	210	NA	Not Measured	5991.5	412.5	0.987
SM-C15_66.5 cm	C15	67.5	mollusc	HY	Standard AMS	OS-129619	0.5938	0.0015	4190	20	1.23	Measured	4726	36	0.595
SM-C15_71 cm	C15	71	Plant/Wood	OC	Standard AMS	OS-129934	0.3616	0.0014	8170	30	NA	Not Measured	9081.5	63.5	0.793
SM-C15_79-80 cm	C15	79.5	organic carbon	OC	Standard AMS	OS-122740	0.339	0.0019	8690	45	-27.51	Measured	9661.5	121.5	0.995
SM-C15_79-80 cm	C15	79.5	organic carbon	OC	Standard AMS	OS-129829	0.3383	0.0015	8710	35	-26.81	Measured	9665	117	0.996

A new database of sea-level indicators from Bermuda was compiled from earlier work (Vollbrecht, 1996; Ashmore & Leatherman, 1984; Ellison, 1993; Redfield, 1967; Neumann, 1971; Kuhn, 1984) that is mostly derived from basal peat in contact with limestone (Appendix A). This database is currently unavailable in other databases of global sea-level indicators (Hibbert et al., 2018). The radiocarbon-dated sedimentary deposit is these earlier works is often designated simply peat, without any differentiation between brackish and freshwater peat using preserved microfossils (i.e., defined indicative meaning). Nevertheless, much of the new database compiled here is derived from peat collected at the limestone contact (Vollbrecht, 1996; Kuhn, 1984), and thus can still be conservatively used as maximum sea-level indicators (terrestrial limiting)(Hibbert et al., 2018).

The model results were determined using the same glacial isostatic adjustment model as described elsewhere (Milne & Peros, 2013), but using different inputs. These inputs are: (1) a reconstruction of changes in grounded ice distribution and (2) solid Earth viscosity structure. In one case, the ice model used was ICE-5G (Peltier, 2004) and the viscosity model one that provides good fits to a global distribution of various data types for this ice model (VM2, with a 90 km thick lithosphere; Peltier, 2004). The other model estimate is also based on the ICE-5G ice history but with North American component replaced with output from a calibrated glaciological model (L2016, model #9894; Tarasov et al., 2012). The Earth viscosity model was one found to produce an optimal fit to a regional Holocene sea-level data base that includes the Atlantic and Gulf coasts of the US (Love et al., 2016). The main cause of the difference between the two curves are the higher Earth viscosity values found in L2016, which provides a modeled sea level curve that is most compatible with the Bermuda observations.

Sedimentary deposits and habitats

The deposits from Palm Cave can be organized into four groups (paleosols, organic-rich deposits, iron-rich deposits, and carbonate deposits), and further subdivided into seven units (Fig.11). These units correspond to hydrographic and environmental change in the cave from internal and external flooding of the Bermuda carbonate platform by concomitant groundwater and relative sea-level rise (Fig. 9). Limitations of the record include decreased sedimentation rates from ~8500 to ~7000 calibrated years before present (Cal yrs BP), and no one single location in the cave preserves a complete Holocene environmental history. However, the recovered deposits collectively provide the most detailed physical and biological picture yet known of Holocene environmental change in a KSE, and are described below from oldest to youngest.

Pre-Holocene vadose deposits

The oldest deposits are pre-Holocene (>11,600 years ago) terra rosa paleosols, which occur at the base of cores (core 13), in areas with negligible Holocene sedimentation (core 8), and near terrestrial openings. These coarser-grained sediments have a deep red color (Fig. 12; Table 4), and they contain no fossil material (Fig. 11). Mineralogically, they are primarily crandallite (mean 52.6%), kaolinite (mean 16.5%), quartz (22.8%) and goethite (8.1%, Table 5), which is similar to Bermudian Pleistocene-aged terra rosa paleosols (Muhs et al., 2013). African dust is an important contributor to Bermudian soils during Quaternary Ice Ages (Muhs et al., 2013), which helps create diagnostic terra rosa soils that are known to erode into Bermudian caves (Hearty et al., 2004). Similarly, paleosol eroded into Palm Cave prior to Holocene flooding.

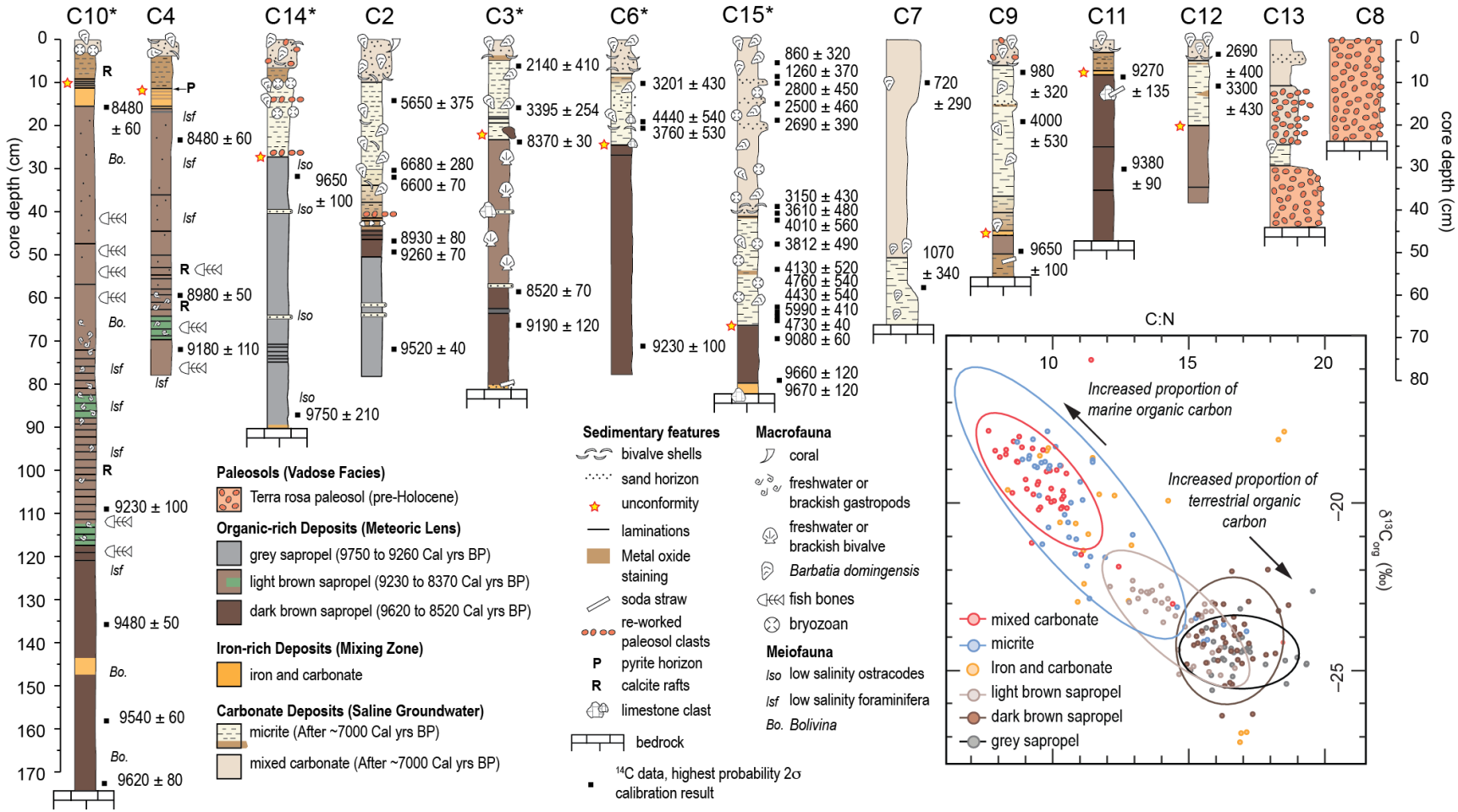

Figure 11. Preserved sedimentary and biological archives. The sediment and biological remains deposited into Palm Cave, Bermuda, over the last 10,000 years. Inset is crossplot of $\delta^{13}C_{org}$ and C:N values on sub-samples from cores marked with an asterisk to evaluate the relative contribution of terrestrial versus marine organic carbon to the sedimentary record, with 95% ellipse confidence intervals around the mean values for individual sedimentary units (except iron-rich deposits).

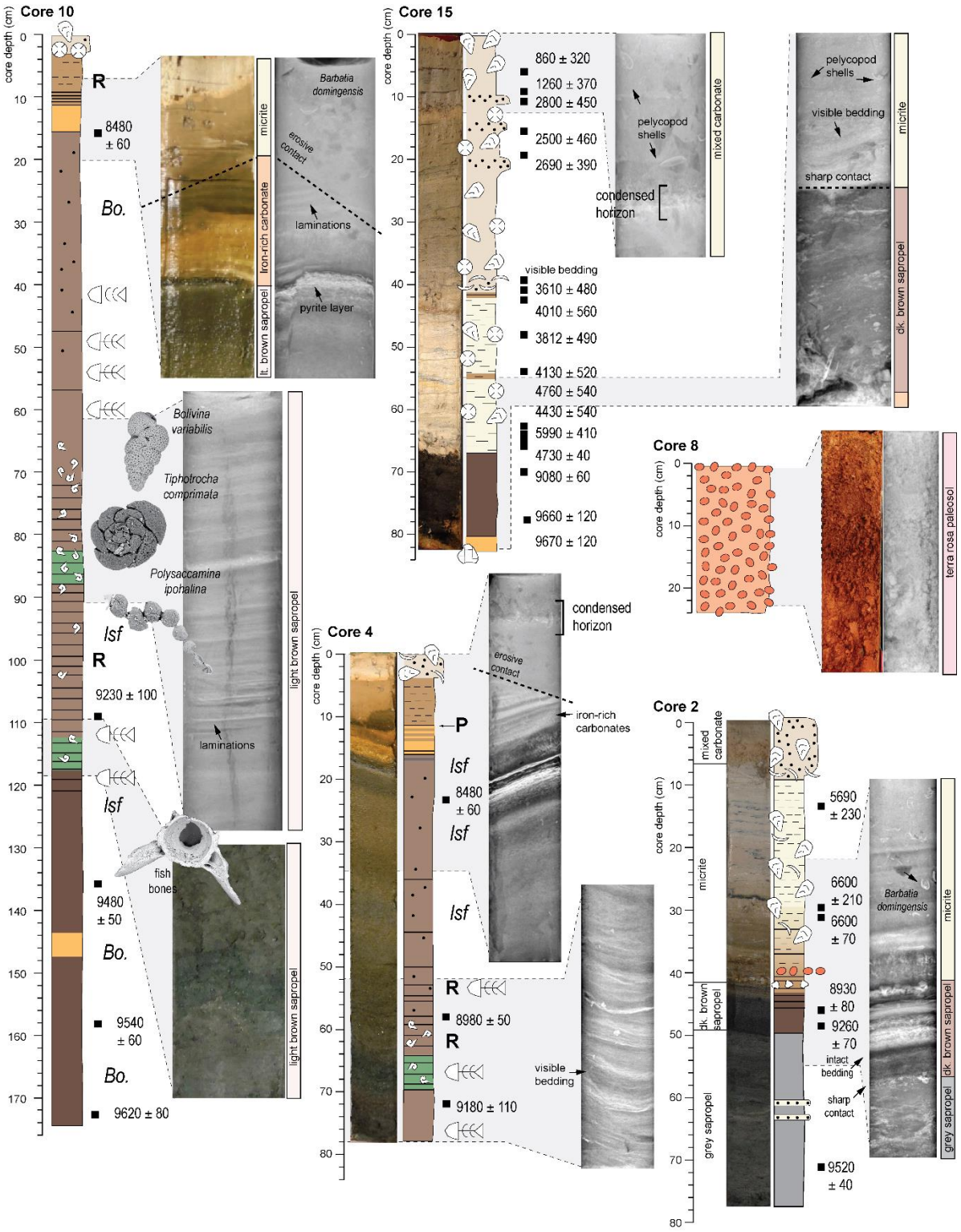

Figure 12. Representative photographs and radiographs for key sedimentary units and transitions, along with the core logs (and symbols) from the core logs (and symbols) from Figure 11.

Table 4. Arithmetic averages for measured sedimentary characteristics in the recovered seven different sedimentary units and preserved biological remains. Note that the stable carbon isotopic ratio ($\delta^{13}C_{org}$ ‰ VPBD, analytical uncertainty ±0.2‰) and C:N (analytical uncertainty ±0.1‰) were only determined on cores 3, 6, 10, 14, and 9 (n = 215). Symbols for biological remains: ostracods (o) and foraminifera (f).

Sediment Group	Sedimentary Unit	Timing of Deposition (Calibrated years before present)	Maximum estimated sedimentation rate	Area of Deposition	Sediment Texture (mg/cc)	Organic Matter Geochemistry			Preserved Biological Remains	Environmental Setting
						Bulk Organic Content (%)	δ13Corg (‰ VPDB)	C:N		
Paleosol	Terra Rosa Paleosol	>11,600		Base of deposists (core 13), expsed in areas with non-deposition (core 8)	66 ± 49 (n = 38)	14 ± 1 (n = 38)	Not analyzed	Not analyzed	none	Vadose Cave
Organic Deposit	Grey Sapropel	9750 ± 210 to ~9400 (cores 14 and 2)	6 mm/yr (core 2)	Eastern passages only (core 14, core 2)	7 ± 11 (n = 89)	16 ± 4 (n = 89)	−24.4 ± 0.6‰ (n = 33)	17.2 ± 1.0 (n = 33)	Darwinula stevensoni (o), Cypridopsis vidua (o)	Oligohaline Meteoric Lens
Organic Deposit	Dark Brown Sapropel	9620 ± 80 (core 10, 15) to 8520 ± 70 (core 3)	1.6 mm/yr (core 10)	Deepest areas of Palm Cave	4 ± 4 (n = 177)	31 ± 8 (n = 180)	−24.1 ± 0.9‰ (n = 43)	16.8 ± 0.8 (n = 43)	Polysaccamina ipohalina (f), Trochammina spp. (f)	
Organic Deposit	Light Brown Sapropel	~9180 ± 110 (core 4) to 8370 ± 30 (core 3)	1.25 mm/yr (core 10)	Proximal to Sailors Choice Entrance	9 ± 11 (n = 201)	24 ± 4 (n = 198)	−23.5 ± 0.8‰ (n = 39)	14.9 ± 1.1 (n = 39)	Trochammina spp (f)., fish vertebrea	
Iron-rich	Iron and Carbonate	After 8480 ± 60 (core 10)	inadequately constrained	Above limestone, or in deep areas of cave	9 ± 11 (n = 21)	15 ± 5 (n = 21)	−21.2 ± 2.9‰ (n = 22)	13.3 ± 2.9 (n = 22)	Bolivina spp. (f),	Mixing Zone
Carbonate	Micrite	By 6600 ± 210, 6600 ± 70 (core 2) to generally ~3000 to 4000 years ago	0.2 mm/yr (c 15)	Widspread throughout Palm Cave	19 ± 33 (n = 188)	9 ± 4 (n = 188)	−20.4 ± 1.9‰ (n = 40)	11.7 ± 2.0 (n = 40)	*Spirophthalmidium emaciatum* (f), *Sigmoilina tenuis* (f), *Spirillina vivipara*, *Barbatia domingensis* (b), bryozoans, sponge spicules, brachiopods, serpulid worms	Oxygenated Saline Groundwater Mass
Carbonate	Mixed Carbonate	~3610 ± 480 (core 15)	0.5 mm/yr C7	Widspread throughout Palm Cave	71 ± 117 (n = 178)	14 ± 1 (n = 178)	−19.4 ± 1.2‰ (n = 38)	10.3 ± 1.2 (n = 38)	*Spirophthalmidium emaciatum* (f), *Sigmoilina tenuis* (f), *Spirillina vivipara*, *Barbatia domingensis* (b), bryozoans, sponge spicules, brachiopods, serpulid worms	

Table 5. Difference in mineralogy between the terra rosa paleosols and iron-rich sedimentary units. Some samples were re-analyzed after treatment with 10% HCl to observe remaining minerals after removal of carbonates (aragonite and calcite), and amplify the XRD-signal of the non-acidified mineral residue.

Core	Depth Interval	Sedimentary unit	Pretreatment	Minerals (Relative Abundance %)											
				Crandallite	Kaolinite	Quartz	Goethite	Pyrite	Aragonite	Calcite	Woodhouseite	Maghemite	Lepidocrocite	Rectorite	Montroseite
8	5-6	terra rosa paleosol	none	43.5	12.2	39.1	5.2	0	0	0	0	0	0	0	0
8	10-11		none	50.3	14.7	28.8	6.3	0	0	0	0	0	0	0	0
8	15-16		none	58	17.7	16.6	7.7	0	0	0	0	0	0	0	0
13	35-36		none	50	17.4	20.5	12.1	0	0	0	0	0	0	0	0
13	40-41		none	61	20.6	9.3	9	0	0	0	0	0	0	0	0
		Arithmetic averages		*52.6*	*16.5*	*22.9*	*8.1*	0	0	0	0	0	0	0	0
14	14	iron and carbonate	none	0	0	0	0	0	53.3	36.4	9.4	0	0.9	0	0
14	14		10% HCl	0	0	87.5	2.8	0	0	0	6.2	0	0	2.4	1.1
15	15		none	25.8	17.3	8.2	30.3	18.4	0	0	0	0	0	0	0
4	7		none	0	0	0	0	0	68.4	31.6	0	0	0	0	0
4	7		10% HCl	0	17.2	22.3	0	0	8.1	1.2	39.9	9.2	2.1	0	0
4	16		none	0	16.7	28.4	20.7	0	0	26.8	7.4	0	0	0	0
4	16		10% HCl	0	23.1	10.8	37.2	0	0	2	26.9	0	0	0	0
10	13		none	0	0	67.8	3.7	0	0	27.8	0	0	0.7	0	0
10	13		10% HCl	0	4.4	82.6	6.9	0	0	0	5	0	1	0	0
10	145		none	0	0	61.6	2.9	0	0	27.9	4.4	0	3.2	0	0
10	145		10% HCl	0	0	87.7	3.9	0	0	0.4	4.8	0	3.2	0	0
		Arithmetic averages		5.16	5.666667	27.6667	9.6	3.0667	20.2833	25.0833	3.533333333	0	0.8	0	0

Freshwater habitats in a meteoric lens

The preserved sedimentary and biological remains (e.g., fish bones, foraminifera, ostracodes) indicate that freshwater aquatic habitats were created in the Palm Cave from 9750 ± 210 (core 14) to 8370 ± 30 (core 3) Cal yrs BP when a fresh to oligohaline meteoric lens first flooded the cave. The modern marine anchialine ecosystem in Palm Cave could not have colonized these conditions. In contrast, these early Holocene freshwater conditions would have been suitable to Bermuda's olighaline-adapted anchialine amphipods like *Pseudoniphargus carpalis* and *P. grandimanus* (Stock et al., 1986). In eastern passages, grey sapropel (mean 16% organic matter) with calcium-rich layers was accumulating by ~9750 Cal yrs BP (cores 14 and 2, Table 3). The organic carbon was primarily terrestrial in origin, based on the stable carbon isotopic content of the bulk organic matter ($\delta^{13}C_{org}$: −24.1 ± 0.6‰) and relative amounts of organic carbon and nitrogen (C:N ratios: 17.2 ± 1.1). The only meiofauna preserved in the grey sapropel were the benthic ostracodes *Darwinula stevensoni* and *Cypridopsis vidua*, which occur in global freshwater habitats and Yucatan freshwater caves. At ~9620 Cal yrs BP, the deepest cave areas (e.g., cores 4, 10) began accumulating dark brown sapropel (mean 31% organic matter, −24.1 ± 0.9‰, 16.8 ± 1.1, n = 43), which pass into a lighter-hued light brown sapropel upcore (mean: 24% organic matter, $\delta^{13}C_{org}$: −23.5 ± 0.9‰, C:N: 14.9 ± 1.1, n = 39). Biologically, the sapropel primarily contains benthic foraminiferal assemblages that are dominated by *Polyscammina iophalina*, *Entzia macrescens*, *Tiphotrocha comprimata* (Fig. 10, 13). At the base of some cores (core 10), *Bolivina* sp. was dominant at first, but the high sedimentation rate at this site indicates these assemblages rapidly transitioned to *Entzia*-dominated assemblages. In modern settings, these benthic foraminifera dominate subtidal anchialine habitats that are flooded by a low salinity (oligohaline) meteoric lens on the Yucatan

Figure 13. Representative scanning electron micrographs of significant biological and sedimentary remains preserved in the different sedimentary units from core 4 and 10 (1-48, benthic foraminifera; 49- 65, other). Benthic foraminiferal taxonomy followed published regional[2,3] and international literature[4]. 1-3, Dorsal and ventral views of *Tiphotrocha comprimata* (Cushman & Brönnimann, 1948). 4-7, *Polysaccammina ipohalina* (Scott, 1976). 8, *Eggerella scabra* (Williamson, 1858). 9, *Labrospira evoluta* (Natland, 1938). 10-12, Dorsal and ventral views of *Trochammina quadriloba* (Höglund, 1948). 13, *Entzia macrescens* (Brady, 1870).14, *Bolivina pseudopunctata* Höglund (1947). 15, *Bolivina paula* (Cushman and Ponton, 1932). 16, *Bolivina striatula* (Cushman, 1922). 17-18, *Bolivina variablis* (Williamson, 1858). 19-22, *Miliolinella circularis* (Bornemann, 1855). 23, *Quinqueloculina bosciana* d,Orbigny (1846). 24, *Spirophthalmidium emaciatum* (Haynes, 1973). 25 *Sigmoilina tenuis* (Czjzek, 1848). 26-27, *Patellina corrugata* Williamson (1858). 28, *Mychostommina revertens* (Rhumbler, 1906). 29- 30, *Spirillina vivipara* (Ehrenberg, 1843). 31, *Cyclogyra involvens* (Reuss, 1850). 32-33, *Melonis barleeanum* (Williamson, 1858). 34, *Nonion pauperatum* (Balkwill & Wright, 1885). 35, *Globocassidulina subglobosa* (Brady, 1881). 36, Dorsal view of *Svratkina australiensis* (Chapman, Parr, & Collins, 1934). 37- 40, Dorsal and ventral views of *Rosalina* spp. 41-43, *Siphonina temblorensis* (Garrison, 1959). 43-45, Dorsal and ventral views of *Rotaliella arctica* (Scott & Vilks, 1991). 46-47, Dorsal and ventral views of *Heronallenita* spp. 48, *Trifarina occidentalis* (Cushman, 1922). 49 dorsal view of ostracode *Cypridopsis vidua* (Müller, 1776) 50-51, ventral view of ostracode *Cypridopsis vidua* (Müller, 1776), 52, dorsal view of *Paranesidea sterreri* Maddocks (1986). 53. Sponge spicules. 54- 55, Branching bryozoans. 56, Cheilostome bryozoan. 57, Bivalve. 58, Brachiopod. 59, Mollusk. 60, Encrusting tube-worm. 61- 63, Teleost (Fish) vertebrae. 64-65, Calcite rafts. All scale bars represent 100 µm.


1
2
3
4
5
6
7
8
9
10
11
12
13
14
15
16
17
18
19
20
21
22
23
24
25
26
27
28
29
30
31
32
33
34
35
36
37
38
39
40
41
42
43
44
45
46
47
48
49
50
51
52
53
54
55
56
57
58
59
60
61
62
63
64
65

Peninsula (*Tiphotrocha, Entzia*)(van Hengstum et al., 2010; van Hengstum et al., 2008), and subtidal marine settings in Bermuda dominated by terrestrial organic carbon (*Bolivina*)(Little & van Hengstum, 2019). Calcite rafts occurred intermittently in the organic-rich deposits, which only form near freshwater-air interfaces in caves (van Hengstum et al., 2011; Kovaks et al., 2017), and their occurrence indicates the continual cave passage flooding. Previous work indicates that the shoreline of an early Holocene inland brackish pond in Harrington Sound was very close to Palm Cave by ~9500 years ago (Vollbrecht, 1996), which likely provided a source of organic-rich sediment that was transported into the cave through a southern tunnel connecting Palm Cave to Harrington Sound (Fig. 9). Continual water-level rise in the cave or conduit collapse events likely decreased organic matter sedimentation at the core sites, as has been observed in Yucatan flooded caves (Collins et al., 2015).

Mixing zone iron curtain deposits

The Iron-rich carbonate deposits provide evidence for benthic habitats becoming flooded with saline groundwater, whereby upwelling anoxic saline groundwater was mixing with the overlying freshwater in a paleo mixing zone [base of cores 3, 15 and 9, and intercalated within cores 4,10, 11 and 9 (Fig. 11)]. These deposits were not recovered from shallower sampling locales (Table 2). Unlike the terra rosa paleosols, these iron-rich carbonate sediments have a distinctive orange-hue (Fig. 12), have a fine texture, and they contain rare marine benthic foraminifera adapted to low-oxic environments (i.e., *Bolivina* spp.). The dominant minerals present were carbonates (mean 45% calcite and aragonite), quartz (mean 27.6%), Fe-based minerals (mean 13.4% goethite, woodhouseite, and lepidocrocite), and less crandallite and kaolinite than the paleosol deposits (Table 5). Organic carbon was dominated by marine sources

($\delta^{13}C_{org}$: −21.2 ± 2.9‰, CN: 13.3 ± 2.9, *n* = 22, Fig. 11). The meiofuna and minerology differentiates these sediments from known Fe-oxide deposits produced by microbialites in anoxic saline groundwater[59]. A Saharan dust origin is also not likely, given the contemporaneously flooded cave would have hampered wind-borne dust accumulation, and African dust export to the western tropical North Atlantic was diminished from ~11,000 to 5,000 years ago (McGee et al., 2013).

Alternatively, these iron-rich deposits developed at the deepest elevations from the oxidative precipitation of Fe(II) in an 'iron curtain' at the sediment-water interface. On siliciclastic coastlines, the oxidative precipitation of dissolved Fe(II) from the mixing of seawater and groundwater generates a distinctive increase in iron oxide deposits in a subsurface zone (Charette & Sholkovitz, 2002). This process is driven by pH gradients between the anoxic saline versus oxygenated freshwater above (Spiteri et al., 2006), and the iron curtain can spatially migrate in response to sea-level (Roy et al., 2010) or rainfall (Roy et al., 2013) changes. It is likely that anoxic saline groundwater was displaced upwards under sea-level forcing, and iron oxide precipitated when anoxic water upwelled and mixed with an overlaying oxygenated water mass. The previously observed iron-oxide coatings on early Holocene calcite rafts in another Bermudian flooded cave likely formed through the same process (van Hengstum et al., 2011).

Oxygenated marine habitats in saline groundwater

By a maximum of 6600 ± 70 Cal yrs BP (core 2), the entirety of Palm Cave became a fully-oxygenated marine aquatic habitat. This is demarcated by widespread carbonate deposition (fine-grained micrite and mixed carbonate), and the appearance of marine bivalves (e.g., *Barbatia domingensis*), bryozoans (*Cheilostomata*), coral (*Coenocyathus goreaui*), brachiopods

and marine ostracodes. The marine foraminifer *Spirophthalmidium emaciatum* also colonizes Palm Cave, which lives in marine caves in Bermuda and Cozumel with oxygenated saline groundwater[65] (Fig. 12, 13). White- to brownish-hued micrite deposits often transition into mixed carbonate facies (e.g., cores 14, 2, 15) towards the top of cores, but the timing is site specific (e.g., core 12: ~2690 Cal yrs BP vs. core 15: ~3610 Cal yrs BP). The spatial and temporal variability of carbonate sedimentary units is perhaps related to conduit-specific physical or hydrodynamic processes (e.g., diffuse- vs. conduit-driven saline groundwater circulation). The carbonate deposits contained the highest proportion of marine organic matter based on the C:N and $\delta^{13}C_{org}$ values (micrite: $\delta^{13}C_{org}$ −20.4 ± 1.9‰; C:N 11.7 ± 2.0‰, n = 40, mixed carbonate facies: $\delta^{13}C_{org}$ −19.4 ± 1.2‰; C:N 10.3 ± 1.2, n = 38). Occasionally, clasts of the terra rosa paleosol become eroded and re-worked into the carbonate deposits (cores 13 and 14). These deposits indicate that conditions in Palm Cave were finally suitable for colonization by the soft-bodied marine anchialine fauna, such as *Parhippolyte sterreri* and *Procaris chacei* sp.

Sea-level forcing of successional development

There is striking congruency between when aquatic ecosystems were emplaced in Palm Cave, subaerial indicators of sea-level change from the Bermuda carbonate platform, and numerical models of relative sea-level rise (Fig. 14). Terrestrial and freshwater peat deposits recovered in contact with the carbonate platform from Bermuda provide *maximum* sea-level indicators (Fig. 14), meaning sea level was no higher in elevation at this time. This constrains glacioisotatic processes and past sea levels (Hibbert et al., 2018). In contrast, cave sedimentary deposits are *minimum* sea-level indicators because groundwater must have achieved this elevation for aquatic habitats develop (Little & van Hengstum, 2019). The sedimentary and

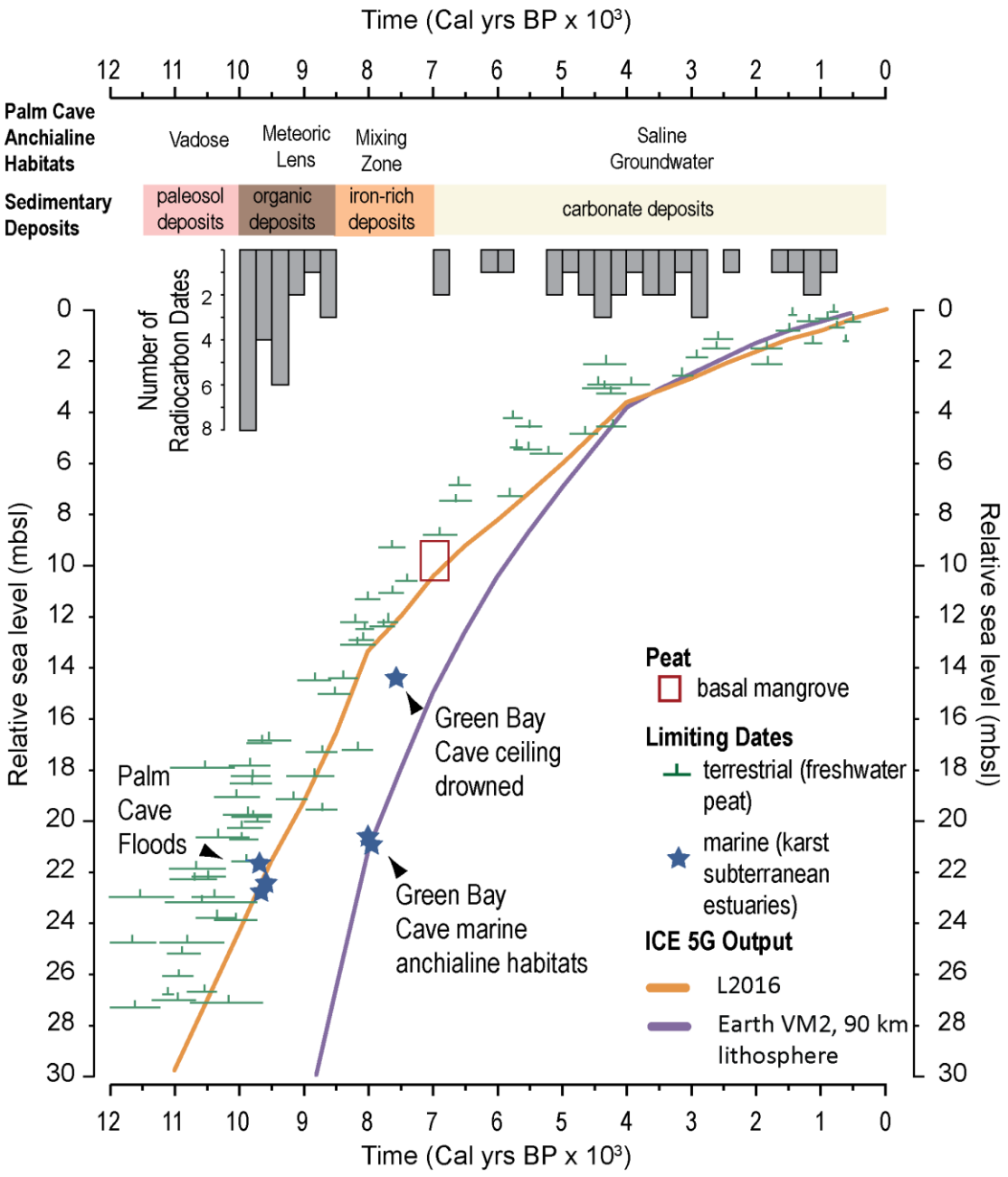

Figure 14. Evidence for Holocene sea-level rise in Bermuda and the allogenic succession of anchialine habitats in Palm Cave, which is caused by the upward migration of the local karst subterranean estuary. Marine limiting sea level indicators from Palm Cave (this study) and Green Bay Cave (van Hengstum et al., 2011; symbol size exceeds age and depth uncertainties), along with a new regional database of terrestrial limiting sea level indicators (freshwater peat, see methods) are compared to the output from two glacial isostatic adjustment models (purple: Peltier, 2004 and orange: Love et al., 2016). The L2016 model allows for marine limiting sea level indicators from Palm Cave and Green Bay to be flooded, whole coeval terrestrial limiting dates remain exposed.

meiofaunal remains in contact with the limestone indicates a meteoric lens flooded Palm Cave by 9750 ± 210 Cal yrs BP at core 14 (21.6 ± 0.3 mbsl), 9620 ± 80 Cal yrs BP at core 10 (22.5 ± 0.3 mbsl), and 9670 ± 120 Cal yrs BP at core 15 (22.7 ± 0.3 mbsl). A comparison with output from the ICE-5G model is within uncertainties of early Holocene minimum (cave-based) and maximum (terrestrial peat) sea-level indicators (Fig. 14, L2016 Model). From previous work in Green Bay Cave in Bermuda, there was a delayed onset in sedimentation to first documented aquatic conditions at ~7,900 Cal yrs BP (van Hengstum et al., 2011). However, the estimated time for drowning of the ceiling in Green Bay Cave is very close to the anticipated position of relative sea level (Fig. 14, L2017 Model). By 7,000 years ago, both Harrington Sound (Vollbrecht, 1996) and North Lagoon (Gischler & Kuhn, 2018) were transitioned into marine lagoons from continual inundation of the Bermuda banktop by Holocene sea-level rise. This allowed tidal exchange of seawater between the saline groundwater and adjacent marine carbonate lagoons, which initiated oxygenated saline groundwater habitats in Palm Cave. Collectively, these results indicate that relative sea-level change is a principle driver of successional development of anchialine habitats. This primarily occurs from sea-level forced vertical migration of groundwater, and secondarily by sea-level forced changes to banktop oceanographic-groundwater circulation regimes.

Global implications

The successional development of anchialine habitats caused by sea-level rise has multiple implications for the biogeography, evolutionary history, and ecosystem functioning across the anchialine habitat continuum. Today, anchialine fauna include taxa that are adapted to habitats and environmental conditions created by specific groundwater masses in the KSE, in addition to

taxa that have an evolutionary history in both water masses. For example, Bahamian remipedes remain in their ancestral marine-based habitat, whereas others like the Yucatan decapod *Creaseria morleyi* have become adapted to the low salinity habitat created by the meteoric lens. On geologic timescales, anchialine fauna and ecosystems must vertically migrate upwards (or downwards) with sea-level rise (or fall) with groundwater masses in the KSE to remain within their suitable ecological tolerance ranges. The sedimentary record from Palm Cave indicates that the available anchialine habitat in western Bermuda associated with a meteoric lens (freshwater to brackish salinity) *decreased* with Holocene sea-level rise. This is likely coincident with regional reduction in the Holocene aerial extent of Bermuda, and ultimate potential for a meteoric lens to form in the antecedent limestone. The possibility of suitable aquatic habitat is first established by the sea level boundary condition, and thereafter, the subsurface hydrography is modified by other known secondary factors, such as changes in coastal circulation (van Hengstum & Scott, 2012), conduit morphology and connectivity to adjacent marine and terrestrial environments (Collins et al., 2015; van Hengstum et al., 2011), or changing rainfall (Cant & Weech, 1986; Vacher & Wallis, 1992; Brankovits et al., 2018).

On Phanerozoic timescales, transgressions cause bottlenecks to anchialine habitats and fauna dependent upon a meteoric lens, if carbonate platform areal extent and island relief are considered (Fig. 15). The earlier regression model first proposed by Riedl (Riedl & Ozretić, 1969; Stock, 1980) hypothesized how the draining of epicontinental seas on geologic timescales first promoted subsurface habitat colonization. However, the regression model did not evaluate or describe how sea-level oscillations can continuously drive adaptation, community evolution, and potential for regional extinctions. During the Quaternary alone, smaller carbonate platforms and islands were repetitively and completely flooded by sea level during interstadials from the

~100,000-year climate cycle (Lisiecki, 2010). As such, meteoric lenses contracted, fragmented, and potentially disappeared (e.g., Bermuda, or Cay Sal Bank in The Bahamas). The sediment and preserved meiofauna in Palm Cave effectively documents habitat reduction associated with a contracting meteoric lens in northwestern Bermuda from sea-level rise during the most recent deglaciation. There is little evidence to suggest that this process has not persisted through geologic time. By extension, this means that fauna and ecosystems in the anchialine habitat continuum that depend upon a meteoric lens must have faced recurrent habitat fragmentation and bottleneck events coincident with sea-level rise linked to the ~100,000-year climate cycle during the Quaternary (Lisiecki, 2004). Indeed, recently discovered anchialine food web dynamics and habitats that depend on terrestrial organic carbon and meteoric lenses could not exist on low-relief carbonate islands and platforms during transgressions (Brankovits et al., 2017). The mechanism for carbon and energy transfer between anchialine fauna and ecosystems in saline groundwater devoid of meteoric lenses remains currently unknown. It is likely that global anchialine fauna in the meteoric lens of KSEs experienced increased extinction rates during Pliocene (+6 above present) or late Paleocene (+75 m above present) transgressions (Miller et al., 2005; Rohling et al., 2014). More broadly, subsurface defaunation on different types of carbonate platforms from transgression-related extinction events requires evaluation.

In contrast, carbonate platforms with higher elevation may have insulated the anchialine habitat continuum from transgression related bottlenecks during global ice volume, tectonic changes or isostatic changes (e.g., Yucatan Peninsula, Fig. 15). For example, the post-Pliocene migration and diversification history of Yucatan freshwater copepods *Microcyclops* and *Diacyclops Diacyclops* have benefited from the continuous presence of a meteoric lens on the

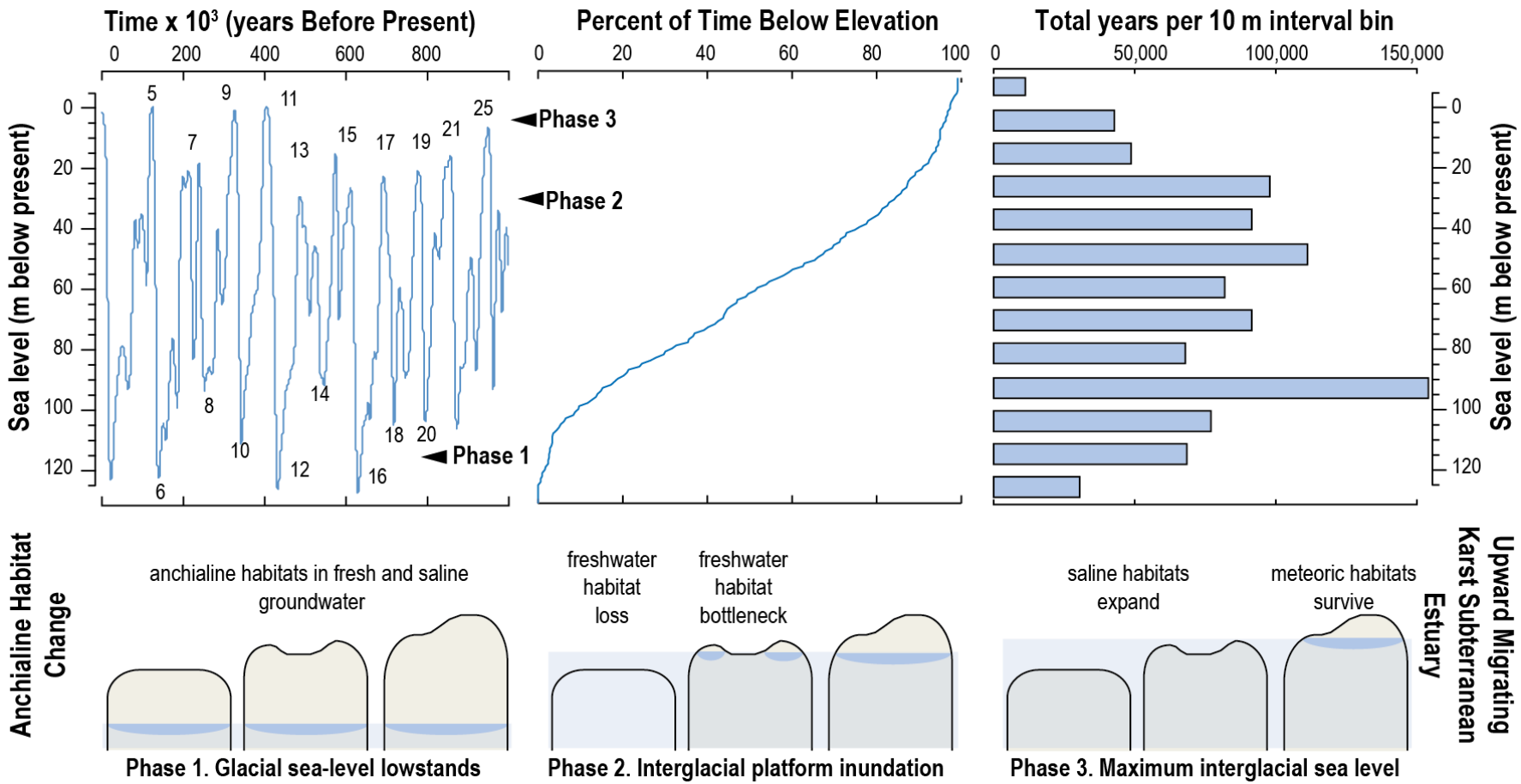

Figure 15. Sea-level change over the last million years impacts anchialine habitat availability. Eustatic sea-level change based on global ice-volume changes (Bintanja & van de Wal, 2008), the relative time spent below the modern sea level position, and the time spent at different eustatic sea level elevations spanning the last million years. This is compared to a single transgression event on three idealized carbonate platforms with different topographic relief and internal migration of their karst subterranean estuaries, which in turn causes bottlenecking (expansion) of the freshwater (saline) anchialine habtitats.

Yucatan Peninsula during the Quaternary, and associated lack of regional bottlenecking during sea-level highstands (Suárez et al., 2014). Anchialine fauna in the saline groundwater mass of a KSE may actually benefit from habitat expansion during banktop inundation coincident with Quaternary interstadials, potentially favoring increased genetic exchange or speciation through the mixing-isolation-mixing mechanism (He et al., 2018).

Looking forward, worldwide fauna in the anchialine habitat continuum remain omitted from 21st century marine ecosystem risk assessments (Mammola et al., 2019). The threat of habitat loss related to subsurface contaminants is now apparent (Metcalfe et al., 2011), along with potential impacts from increasing coastal sea surface temperatures (Chevaldonné & Lejeusne, 2003). However, recent groundwater modeling work indicates that <1 m of sea-level rise can reduce meteoric lens volumes by over 50%, and thus available area of brackish and freshwater ecological niches in the anchialine habitat continuum, when inherited topography and platform flooding are collectively considered (Gulley et al., 2016). The results presented here indicate that the effects of sea-level rise on the anchialine habitat continuum must also be regionally evaluated. It is likely that anchialine fauna on low-lying carbonate platforms and islands are most vulnerable to potential bottlenecking during 21st century sea-level rise.

CHAPTER IV

10,000 YEARS OF BENTHIC HABITAT CHANGE IN A KARST SUBTERRANEAN ESTUARY: IMPACTS OF SEA-LEVEL FORCING ON THE LOCAL GROUNDWATER, ORGANIC CARBON FLUX, AND CARBONATE PLATFORM FLOODING

Introduction

In the subsurface coastal zone, the mixing of continental derived groundwater with the ocean creates subterranean estuaries, which impacts the biogeochemical cycles of coastal oceans (Moore et al., 1999). In general, an upper meteoric lens is stratified from the lower saline groundwater, which circulates with the ocean (Garman and Garey, 2005; Santos et al., 2018; Menning et al., 2015; Moore, 1999). Subterranean estuaries can occur on either carbonate (Goneaa et al., 2014) or volcanic landscapes, which are often perforated by cave networks that allow for human exploration and scientific observation in the subterranean estuary (Bowman and Iliffe, 1985; Iliffe et al., 2011; Kornicker and Iliffe, 2009). The groundwater and biology of caves in subtropical and tropical carbonate islands have received considerable scientific attention, giving rise to their environmental designation as karst subterranean estuaries (Goneaa et al., 2014; Fig. 1). Traditionally, the unique fauna and ecosystems that live in volcanic and karst subterranean estuaries have been classified with the adjective ‘anchialine’ (Stock et al., 1986). Our understanding of how anchialine habitats change as a result of sea-level-forced vertical migration of karst subterranean estuaries on geologic timescales remain poorly understood.

Many authors have published conceptual models for the vertical migration of groundwater masses belong to subterranean estuaries in response to rising global sea levels since the last ice age (Shinn et al., 1996; Suric et al., 2005; van Hengstum et al., 2011; Gregory et al.,

2017). This framework is well-supported by speleothem data from the tropical North Atlantic and Mediterranean indicating that groundwater levels concomitantly rise with sea-level (Li et al., 1989; Lundberg et al., 1994; Richards et al., 1999; Dutton et al., 2009). However, detailed knowledge on how habitats in the subsurface change in response to the vertically migrating subterranean estuary remain less well understood because speleothems cannot record how cave environments change when they become flooded. Like their subaerial counterparts, however, the geochemical and biological processes that depend upon specific groundwater masses in the subterranean estuary must vertically migrate with the coastal aquifer. Change in the vertical position of the subterranean estuary results in shifts to environmental gradients, including salinity (van Hengstum et al., 2010), dissolved oxygen, nutrients (van Hengstum and Scott, 2012), which in turn impacts benthic and pelagic fauna and anchialine habitats within KSEs**.**

Sediment that accumulates in cave networks can be used to investigate cave environmental change on millenial and human timescales (White, 2007; Fornos et al., 2009; van Hengstum et al., 2010; van Hengstum et al., 2011; Collins et al., 2015). Sediment particles can be derived from the terrestrial landscape above (e.g., Schmitter-Soto et al., 2002; van Hengstum et al., 2010; Collins et al., 2015a), adjacent marine environments (e.g., carbonate bioclasts), or produced within the cave itself (e.g., calcite rafts and micrite mud). Cave sediments can even preserve the remains of meiofanua (e.g., benthic foraminifera, ostracode valves, testate amoeba) that live in the cave and provide diagnostic information of paleo groundwater conditions like salinity and dissolved oxygen (van Hengstum et al., 2011; van Hengstum and Scott, 2012; Maddocks and Iliffe, 1991; Gabriel et al., 2009; Collins et al., 2015). Problematically, cave sediment records are often limited through intervals of hiatus or negligible sedimentation rates, so available records often document only when the cave was flooded by meteoric water (Collins

et al., 2015; van Hengstum et al., 2011; Kovaks et al., 2017) or saline groundwater (Fornos et al., 2009).

Recent results indicate that the Palm Cave in Bermuda has accumulated sediment spanning at least the last 10,000 years, with clear evidence documenting how the cave was first flooded by a meteoric lens with deglacial sea-level rise ~9500 years ago, followed by multiple environmental changes driven by Holocene regional oceanographic and groundwater development. Here we use subfossil benthic foraminifera preserved in sediment records from Palm Cave to better understand the development of benthic anchialine habitats in response to groundwater changes in northwestern Bermuda during Holocene sea-level rise. Benthic foraminifera are unicellular protists that are highly sensitive to environmental gradients (Gooday et al., 1992; Gupta and Machain- Castillo, 1993; Murray, 2001). Given the preservation potential of their simple tests and their statistically significant and diverse populations, benthic foraminifera are particularly suitable to characterize the environmental drivers of benthic anchialine habitat development associated with sea-level rise (van Hengstum and Scott, 2012). The results indicate that changing groundwater conditions, feedbacks between inundation of carbonate platform and groundwater, and particulate organic carbon flux to the benthos are important drivers of long-term benthic habitat change.

Study site

The North Atlantic archipelago of Bermuda is ~35 million year old volcanic seamount capped by Quaternary-aged carbonates that have weathered into a mature karst landscape (32.31°, -64.75°; Land et al., 1967; Palmer et al., 1977; Vacher and Rowe, 1997)(Fig. 9). Caves on Bermuda are characterized by large chambers that formed in both phreatic and vadose settings

that are presently interconnected by collapse zones (Palmer and Quenn, 1977; Mylroie et al., 1995). The ~30 to 80 m thick carbonate cap was in the unsaturated (vadose) zone during the last glacial maximum when relative sea-level was ~120 meters lower (Miller et al., 2005). Now, majority of the limestone platform is submerged due to deglacial sea-level and groundwater-level rise.

The caves of Bermuda are ideal to study how a karst subterranean estuary changes on Holocene timescales as the caves are now in a mature environmental state (flooded by marine groundwater). Previous research in Green Bay Cave in Bermuda documents change in environmental conditions in response to sea-level rise over the Holocene (van Hengstum and Scott, 2012). In response to rising sea and groundwater, modern cave environments developed by the upward displacement of the KSE, transitioning from vadose through freshwater in the upper KSE to completely marine in the lower KSE when the platform flooded. However, Holocene sedimentation in Green Bay Cave was episodic, leading to many millennial-scale intervals of interrupted environmental history.

The Palm Cave System (32.34º, –64.71º) is located on the isthmus between Harrington Sound and Castle Harbour (Fig. 9). The Palm Cave System has been extensively explored and mapped, with at least seven karst windows (entrances) that are interconnected by ~1,500 m long network of underwater conduits. The cave geometry extends to a maximum depth of 23 m below modern sea level. Karst windows provide physical openings to the subterranean habitats, which allow for the influx of terrestrial nutrient sediments from the surrounding forest landscape. There is currently a direct, but narrow, connection between Harrington Sound and Palm Cave through subterranean conduits that provides a source for direct tidal exchange of seawater and marine nutrients.

The Palm Cave is entirely flooded by well-oxygenated saline groundwater (>3 mg/L) that tidally circulates with seawater from the adjacent coastal lagoons. The narrow island width combined with porosity of the carbonate lithology means that no meteoric lens (freshwater, brackish) discharges through, or is formed in the area of, the Palm Cave. The groundwater conditions (i.e., pH, temperature, salinity) are hydrographically similar to those measured in van Hengstum et al. (2019, *submitted*) and remain consistent with conditions previously observed (Stoffer, 2013).

Methods

Sediment core collection and analysis

Fourteen push cores were collected from throughout the Palm Cave using advanced technical cave diving procedures in August 2015, with multiple cores reaching refusal on limestone below. Cores were transported back to the laboratory, split lengthwise for x-radiography and photography, and perpetually stored at 4°C until further analysis.

Textural variability of all cores was examined at 1-cm intervals downcore through loss on ignition (LOI, Heiri et al., 2001) and sieve-first LOI (van Hensgtum et al., 2016). Bulk organic matter was quantified by mass lost through combustion at 550°C for 4.5 hours (Heiri et al., 2001), with organic matter content recorded as weight percent. Sieve-first LOI procedure was used to quantify the variability in coarse sediment particle deposition (>63 μm, fine sand and coarser). Separate sediment sub-samples (2.5 cm^3) were *first* wet-sieved over a 63 μm mesh, then dried in an oven (80°C for 14 hours), and remaining organic matter in the sample was ignited in a muffle furnace (at 550°C for 4.5 hours). Remaining coarse sedimentary particles were recorded as milligrams per cm^3 (van Hengstum et al., 2016).

Chronological constraint for the cores was established using accelerator mass spectrometry (AMS) and Continuous Flow AMS (CF-AMS; McIntyre et al., 2011). Bulk organic matter from the organic-dominated facies, and marine bivalves were used for radiocarbon dating (*n* = 51; Table 1). Radiocarbon data was generated by the National Ocean Sciences Accelerator Mass Spectrometry (NOSAMS) facility at Woods Hole Oceanographic Institution, and all were calibrated to sidereal years before 1950 AD (Cal yrs BP_{1950}) using IntCal 13 (Reimer et al., 2013), with the highest probability 2 result used to frame the results. Other lower probability calibration results do not change the interpretation of the data. Raw calibration data is then rounded to the nearest decade for presentation in Figure 4 (strat plot) in the text, as per radiocarbon convention.

The stable carbon isotopic value ($\delta^{13}C_{org}$) and C:N ratio of bulk sedimentary organic matter was measured to estimate the provenance of organic matter accumulating through time. In general, $\delta^{13}C_{org}$ values of bulk sedimentary organic matter reflects the relative contributions of marine, terrestrial versus algal carbon sources in coastal sediment records (France 1995; Lamb et al., 2006), and has also been demonstrated as also useful indicator in coastal underwater caves (van Hengstum et al., 2011; Little and van Hengstum, 2019). In dark underwater caves, however, photosynthetic primary productivity can potentially be negligible, so the flux of organic matter in flooded caves can be proportionally estimated between terrestrial (and freshwater phytoplankton) organic carbon with a more depleted $\delta^{13}C_{org}$ value, versus marine organic carbon that has a more enriched $\delta^{13}C_{org}$ value. Separate sediment sub-samples were obtained from the core for geochemical analysis from core levels also targeted for benthic foraminiferal analysis (core 3, *n* = 33; core 6, *n* = 27; core 10, *n* = 55; core 14, *n* = 48; core 15, *n* = 52). For processing, carbonates were first digested with 1.0 M HCl for at least 12 hours, while the remaining

sediment residue was rinsed, desiccated, powdered, and weighed into silver capsules. Stable carbon isotope ratios ($\delta^{13}C_{org}$) were measured against international standards at Baylor University Stable Isotope Laboratory on a Thermo- Electron Delta V Advantage Isotope Ratio Mass Spectrometer. Final isotopic ratios are reported relative to the standard delta (δ) notation relative to Vienna Pee Dee Belemnite (VPDB) for carbon (expressed as parts per mil (‰)) with an uncertainty of ± 0.1‰. Lastly, the relative proportion of terrestrial versus marine organic matter in the surface sediment samples were estimated by isotopic mass balance: $\delta X = F_m * \delta X_m + F_t * \delta X_t$; where $1 = F_t + F_m$ (Thornton & McManus, 1994). The terrestrial endmember (δX_t) was –27.7‰ as measured on a sample from Deep Blue Cave in Bermuda (Little and van Hengstum, 2019), and the marine endmember (δX_m) was –15.2‰ as measured on a sample from Palm Cave (*this dissertation, Chapter 2).*

Benthic foraminiferal analysis

The most expanded sedimentary records were selected for detailed benthic foraminiferal analysis (sampled in cores 2, 4, 7, 10, 14, and 15). Benthic foraminifera were first concentrated by wet sieving 0.63 cm^3 to 1.25 cm^3 of bulk sediment sub-samples over standard 63 μm screen meshes, with the remaining coarse sediment residues split using a wet splitter (Scott & Hermelin, 1993) to enable representative census counts of ~300 individuals per sample. Individual benthic foraminifera were wet picked onto micropaleontological slides and identified to generic level, with taxonomy confirmed by scanning electron microscopy of representative individuals and literature comparisons (Carman, 1993; Bermudez, 1949; Loeblich Jr & Tappan, 1987; Javaux & Scott, 2003; van Hengstum & Scott, 2012; Little and van Hengstum, 2019).

An original data matrix from containing 110 samples and 64 taxonomic observations was produced from the Palm Cave sediment cores, with a total 38,618 individual foraminifera tests counted as part of this study. However, taxa were considered insignificant and removed from further multivariate cluster analysis if the proportional abundance was less than the calculated standard error at a 95% confidence interval in all samples (Patterson and Fishbein, 1989), or if the species was present in only one sample. A final data matrix contained 110 samples with 49 taxonomic observations after insignificant taxa were removed. The final data of raw count abundances was first converted to proportional abundances ('decostand' function in 'vegan' package; Oksanen et al., 2013), and was also used to calculate Shannon-Wiener Diversity Index (*H*) (using 'vegan' package; Oksanen et al., 2013). Statistical analysis was completed using RStudio software (version 1.1.383; RStudio, 2016).

Unconstrained Q-mode cluster analysis was used to emphasize community-level patterns (Legendre and Legendre, 1998) and identify assemblages that are ecologically meaningful. Prior to cluster analysis, the proportional abundances were square root transformed to minimize the impact of dominant species and to better compare community structure (Legendre and Legendre, 1998). Samples were then clustered using an unweighted paired group averaging algorithm and the Bray-Curtis dissimilarity index ('simprof' function in 'clustsig' package; Clarke et al., 2008; Whitaker and Christman, 2014; and 'vegdist' function in 'vegan' package; Oksanen et al., 2013). Lastly, a stratigraphic plot was created in RStudio to compare membershop of dominant benthic foraminifera in relation to the previously generated assemblages identified in the dendrogram from cluster analysis. The stratigraphic plot only shows taxa with 5% proportional abundance in at least 1 sample ('stratplot' function using 'rioja' package; Juggins, 2017).

Cave stratigraphy and age

Four sediment deposits that are further subdivided into seven units were identified within the cores (Fig. 10; Chapter 3, this study). The oldest deposits are pre-Holocene (>11,600 years ago) terra rosa paleosols, that contain coarse-grained sediments with a deep red color, and no fossil material. Mineralogically, they are similar to Bermudian Pleistocene-aged terra rosa paleosols (i.e., crandallite, kaolinite, quartz, and goethite; Muhs et al., 2012).

The organic rich deposits along the north and eastern passages (cores 2, 3, 4, 6, 10, 11, 14, 15), preserved sedimentary and biological remains (e.g., fish bones, foraminifera, ostracodes) that indicate freshwater aquatic habitats developed in the Palm Cave from 9750 ± 210 to 8370 ± 30 Cal yrs BP, when a fresh to oligohaline meteoric lens first flooded the cave. The organic-rich deposits can be subdivided into three units. Grey sapropel (9750 ± 210 to 9650 ± 100 Cal yrs BP), dominated by the freshwater ostracodes *Darwinula stevensoni* and *Cypridopsis vidua*, passed into the second unit of organic rich deposits, the dark brown sapropel. The dark brown sapropel (9650 to 9000 Cal yrs BP) passes into the third unit, the light brown sapropel was deposited approximately 9000 to 8370 Cal yrs BP. Biologically, the dark to light brown sapropel contains benthic foraminiferal assemblages that are dominated by *Polysaccammina ipohalina, Entzia macrescens*, and *Tiphotrocha comprimata*. At the base of some cores, *Bolivina* sp. initially dominated, but the high sedimentation rate at this site indicates these assemblages rapidly transitioned to *Entzia*-dominated assemblages. Additionally, calcite rafts occurred intermittently throughout the organic- rich sediments, which form at a near freshwater air-water interface in caves.

The iron-rich carbonate deposits formed in the deepest areas of the Palm Cave (base of core 3, 15, and 9, and intercalated within cores 4,10,11 and 9), which indicated that the KSE

benthic habitats was flooding with anoxic saline groundwater that displaced the overlaying oxygenated water mass through the vertical migration of the mixing zone. Mixing of the anoxic saline groundwater and oxygenated water mass created an 'iron curtain' at the sediment-water interface with a distinctive orange-hue, a fine texture, marine-sourced organic carbon, and rare marine benthic foraminifera that are knowth to be adapted to low-oxic environments (i.e., *Bolivina*, Gupta & Macahin-Castillo, 1993; Chapter 3, this dissertation).

The complete onset of carbonate deposits by a maximum age of 6600 ± 70 Cal yrs BP across the entirety of the Palm Cave suggests that the benthos became an oxygenated marine aquatic habitat. The carbonate deposits are subdivided into two units. The micrite unit passes upcore into the carbonate mud unit and both sediment units are characterized by marine bivalves (e.g., *Barbatia domingensis*), bryozoans (*Cheilostomata*), coral (*Coenocyathus goreaui*), brachiopods and marine ostracodes. The marine foraminifera *Spirophthalmidium emciatum*, known from modern Bermudian KSEs with oxygenated saline groundwater (van Hengstum and Scott, 2011), also colonize these deposits.

Benthic foraminiferal results

Seven assemblages of benthic foraminifera can be identified on the dendrogram produced through unconstrained Q-mode cluster analysis, and are so-named in relation to water mass variability and organic carbon content: (i) terrestrial organic matter dominated subtidal assemblage (ii) low-brackish, (iii) mid-brackish, (iv) high-brackish, (v) marine low-organic carbon assemblage, (vi) marine mid-organic carbon assemblage, and (vii) marine high-organic carbon assemblage (Fig. 16). Faunal differences and their inferred environmental conditions during deposition are described in further detail below, generally from oldest to youngest.

Figure 16. Detailed foraminiferal results from sediments cores in the Palm Cave System illustrating proportional abundance of statistically significant taxa in the surface sediment samples. Only taxa with >5% in at least one sample are shown to emphasize significant fauna. Dendrogram produced by Q-mode cluster analysis on all faunal data. A seven-cluster interpretation (Bray- Curtis dissimilarity 0.55) of the dendrogram distinguishes the benthic anchialine habitats controlled by environmental variables.

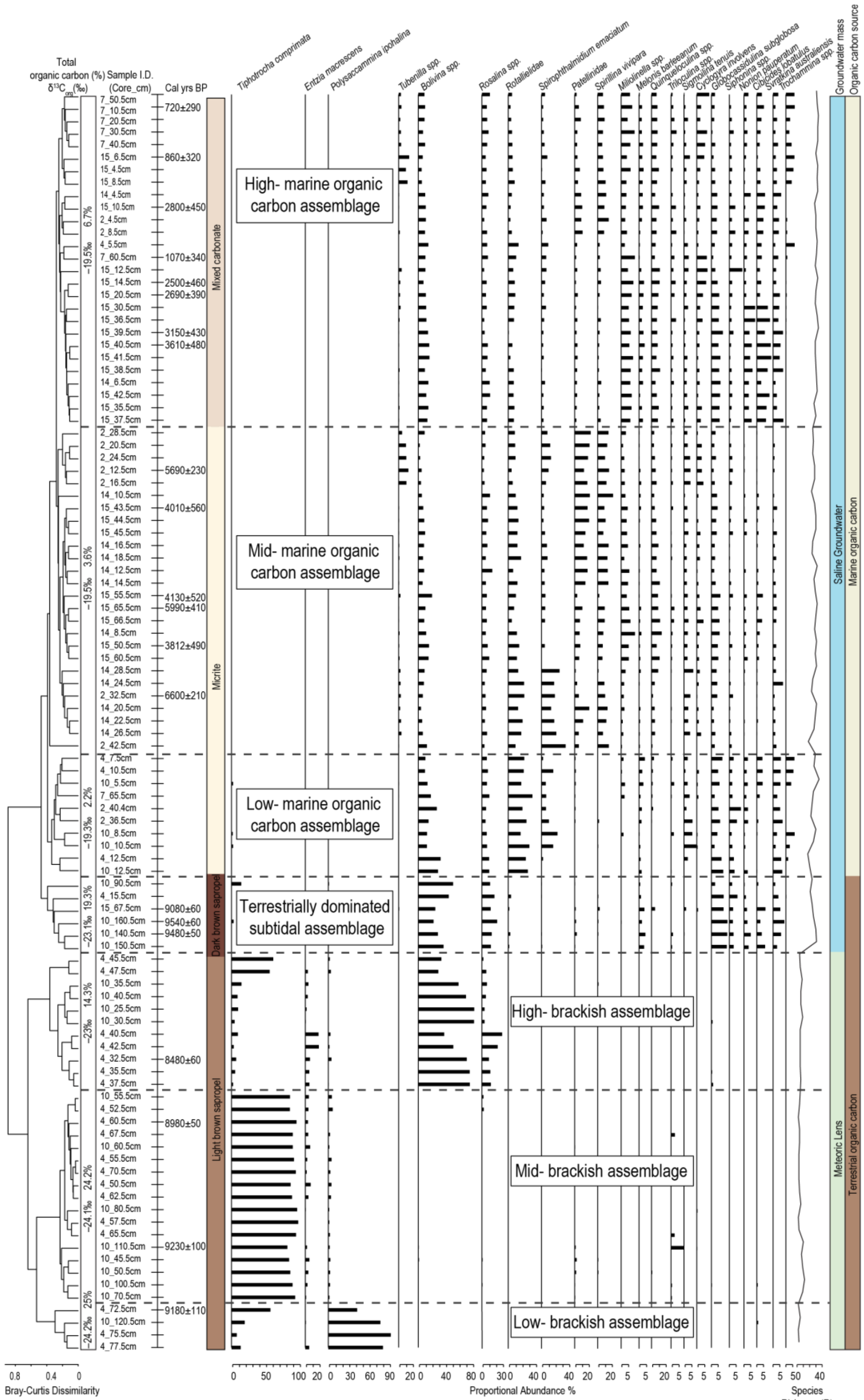

Total organic carbon (%)
δ13C org (‰)
Sample I.D. (Core_cm)
Cal yrs BP
High- marine organic carbon assemblage
Mid- marine organic carbon assemblage
Low- marine organic carbon assemblage
Terrestrially dominated subtidal assemblage
High- brackish assemblage
Mid- brackish assemblage
Low- brackish assemblage
Mixed carbonate
Micrite
Dark brown sapropel
Light brown sapropel
Saline Groundwater
Meteoric Lens
Marine organic carbon
Terrestrial organic carbon
Groundwater mass
Organic carbon source
Bray-Curtis Dissimilarity
Proportional Abundance %
Species Richness (R)

Terrestrially- dominated subtidal assemblage (9540 ± 60 to 9480 ± 50 Cal yrs BP)

The oldest sediments sampled from the deepest cave areas are dark brown sapropel, which contains the Terrestrially- dominated subtidal assemblage. This assemblage is located in core 4 (15 cm), core 10 (140 to 160 cm) and core 15 (67 cm), characterized by terrestrially-sourced organic carbon ($\delta^{13}C_{org}$ mean: –23.1 ‰; terrestrial organic carbon mean: 62.8%), abundant total organic carbon (mean: 19.3%), and very fine silt (mean: 4.3μm). Radiocarbon ages collected at 67 cm in core 15, and 140 cm and 160 cm in core 10 were 9080 ± 60, 9480 ± 50, and 9540 ± 60 Cal yrs BP, respectively. The Terrestrially- dominated subtidal assemblage is diverse (*H*' = 2.3; R = 26) and dominated by *Bolivina* spp. (mean: 36.4%), and epifaunal rotaliids such as *Rosalina* spp. (mean: 15.1%), *Globocassidulina subglobosa* (mean 10.8%), and *Svratkina australiensis* (mean: 3.5%; Table 6).

Low- brackish assemblage (9180 ± 110 Cal yrs BP)

The Low-brackish assemblage is located at the base of the light brown sapropel sediments in core 4 (72 to 78 cm) and in core 10 (120 cm). The silty sediments (medium silt mean: 27.7 μm) are primarily terrestrial in origin (terrestrial organic carbon mean: 72.2%; total organic carbon mean: 25%), based on the stable carbon isotopic content of the bulk organic matter ($\delta^{13}C_{org}$ mean: –24.2 ‰) and C:N ratio (mean: 15.8). The radiocarbon age at 72 cm in core 4 is 9180 ± 110 Cal yrs BP. The benthic foraminiferal community has a low diversity (*H*' = 0.6) and species richness (R= 3), and is dominated by *Polysaccammina ipohalina* (mean: 69.6%), *Tiphotrocha comprimata* (mean: 28.1%), and *Entzia macrescens* (mean: 1.3%). These are well known taxa that colonize low salinity water in coastal environments elsewhere (Scott, 1976; Scott et al., 1990; Scott et al., 1996), likely less than 5 psu. Additional meiofaunal remains

Table 6. Diversity table for sediment cores. Arithmetic mean of the relative abundance of dominant taxa and textural characteristic for each assemblage. Species with a mean of <1% relative abundance in the biofacies were marked with a dash so dominant species could be emphasized.

	Saline groundwater	Meteoric Lens			Saline groundwater		
	Terrestrial Organic Carbon				Marine Organic Carbon		
Assemblages	**Terrestrial-organic carbon dominated subtidal assemblage**	**Low brackish**	**Mid brackish**	**High brackish**	**Low- marine organic carbon**	**Mid- marine organic carbon**	**High- marine organic carbon**
	n = 6	*n* = 4	*n* = 17	*n* = 11	*n* = 10	*n* = 25	*n* = 27
Approximate Timeframe	9540- 9080	9180 ± 110	8980- 9230	8480 ± 60		6600- 3812	3610- 720
Sediment Properties							
Coarse sediment (mg/cc)	4.3 ± 4.1	27.7 ± 26.4	15.4 ± 14.4	8.6 ± 6.6	18.2 ± 20.5	9.7 ± 14.3	52.7 ± 129.4
δ13Corg	−23.1 ± 1.6	−24.2 ± 0.4	−24.1 ± 0.8	−23 ± 0.3	−19.3 ± 2	−19.5 ± 1.3	−19.5 ± 1.1
C:N	15.7 ± 2.6	15.8 ± 0.6	15.6 ± 0.7	14.3 ± 0.7	11.6 ± 1.7	11.4 ± 1.6	10.3 ± 1
Terrestrial organic carbon (%)	62.8 ± 13.1	72.2 ± 3.5	71.3 ± 6.3	62.7 ± 2.6	32.5 ± 16.3	34.1 ± 10.6	33.8 ± 8.5
Total organic carbon (%)	19.3 ± 11	25 ± 5.9	24.2 ± 4.5	14.3 ± 3.6	2.2 ± 1.5	3.6 ± 1.6	6.7 ± 3
Foraminifera							
Total Individuals (cm-3)	355	85.8	197	168.4	5743.5	14021	9855
Shannon-Wiener Diversity (H)	2.3	0.6	0.4	1	2.4	2.6	3
Species Richness (R)	26	3	5.3	5.8	25.6	27.8	31
Relative Abundance							
Bolivina spp.	**36.4**	–	–	**71.8**	17.1	8.2	7.8
Cibicides lobatulus	3.6	–	–	–	1.4	–	2.8
Cyclogyra involvens	–	–	–	–	–	1.7	4
Entzia macrescens	–	1.3	3.2	4.3	–	–	–
Globocassidulina subglobosa	10.8	–	–	–	5.6	3.8	2.5
Melonis barleeanum	3.4	–	–	–	1.9	–	2.6
Miliolinella spp.	–	–	–	–	1.2	4.3	7.3
Patellina spp.	1.2	–	–	–	1.1	13.5	5.5
Polysaccammina ipohalina	–	**69.6**	2.5	1	–	–	–
Quinqueloculina spp.	–	–	–	–	1.1	7.3	8.6
Rosalina spp.	15.1	–	–	8.1	7.9	7	7.7
Rotalliella spp.	1.6	–	–	–	**24.2**	**13.8**	5.8
Sigmoilina tenuis	–	–	–	–	3.7	3	1.7
Siphonina spp.	2.7	–	–	–	2.5	–	1.3
Spirillina vivipara	–	–	–	–	1.4	11.1	**8.9**
Spirophthalmidium emaciatum	–	–	–	–	12.4	10.7	4.1
Svratkina australiensis	3.5	–	–	–	3.8	1.5	2.3
Tiphotrocha comprimata	2.4	28.1	**90.6**	9.8	–	–	–
Triloculina spp.	–	–	1.4	–	–	–	1.5
Trochammina spp.	–	–	–	–	2.8	–	5
Tubenilla spp.	–	–	–	–	–	2.8	6.8
Sum	**99.4**	**100**	**99.9**	**99.9**	**99.3**	**99.6**	**98.9**

include the freshwater ostracodes *D. stevensoni* and *C. vidua* (Gandolfi et al., 2001; Külköylüoğlu & Vinyard, 2000; Külköylüoğlu, 2004; Yilmaz & Külköylüoğlu, 2006) and multiple fish vertebrae (Table 6).

Mid- brackish assemblage (9230 ± 100 to 8980 ± 50 Cal yrs BP)

The light brown sapropel sediments also contain the Mid-brackish assemblage. The Mid-brackish assemblage is located in core 4 (52 to 71 cm) and core 10 (55 to 111 cm). The fine silt sediments (mean: 15.4 μm) are characterized by terrestrially sourced organic carbon ($\delta^{13}C_{org}$ mean: –24.1 ‰; terrestrial organic carbon mean: 71.3%; total organic carbon mean: 24.2%). The age in core 4 at 60 cm is 8980 ± 50 Cal yrs BP and in core 10 at 110 cm is 9230 ± 100 Cal yrs BP. The Mid-brackish assemblage has a low diversity (*H*' = 0.4) and species richness (R = 5.3) and is characterized by *T. comprimata* (mean: 90.6%), with low abundance of *P. ipohalina* (mean: 2.5%) and *Entzia macrescens* (mean: 3.2%)(Table 6).

High- brackish assemblage (8580 ± 60 Cal yrs BP)

The High-brackish assemblage is present in core 4 (35 to 47 cm) and in core 10 (25 to 35 cm). The High-brackish assemblage is present at the top of the light brown sapropel sediments that are characterized by fine silt (mean: 8.6 μm) and terrestrial organic carbon ($\delta^{13}C_{org}$ mean: –23 ‰; total organic carbon mean 14.3%). This radiocarbon date collected from core 4 at 32 cm was aged at 8480 ± 60 Cal yrs BP. This assemblage is characterized by increased diversity and species richness (*H*' = 1; R = 5.8). There is also increased abundance of the infaunal biserial taxa *Bolivina* spp. (mean: 71.8 %) and the epifaunal rotaliid *Rosalina* spp. (mean: 8.1%), while *T. comprimata* decreased (mean: 9.8%; Table 6).

Low-marine organic carbon assemblage

Micrite sediments in cores 4 (7 to 12 cm), 10 (5 to 12 cm), 2 (36 to 40 cm), and 7 (65 cm) contain the Low-marine organic carbon assemblage. The sediments are characterized by medium silt (mean: 18.2 μm) and an enriched carbon isotope value ($\delta^{13}C_{org}$ mean: –19.3 ‰; C:N ratio mean: 11.6; total organic carbon mean: 2.2%). An enriched carbon isotope value suggests that the organic carbon at this time is likely sourced from the marine environment, entering from adjacent lagoons. The Low-marine organic carbon assemblage is notably diversified from previous assemblages (*H'* = 2.4; R = 25.6). There were no radiocarbon ages collected within these samples however, based on the deposition of these sediments and known dates above and below these samples, it can be assumed that the age is between 8480 ± 60 and 6600 ± 210 Cal yrs BP. The Low-marine organic carbon assemblage is dominated by *Rotaliella* spp. (mean: 24.2%), *Bolivina* spp. (mean: 17.1%), *Spriophthalmidium emaciatum* (mean: 12.4%) and other rotaliid taxa (e.g., *Svratkina, Globocassidulina, Rosalina*, and *Cibicides*) are present in smaller abundances. The common marine taxa present within this assemblage suggests marine conditions were established at this time (Table 6).

Mid- marine organic carbon assemblage (6600 ± 210 to 3812 ± 490 Cal yrs BP)

The Mid- marine organic carbon assemblage is present in core 2 (12 to 32 cm), core 14 (8 to 28 cm), and core 15 (43 to 66 cm). The carbonate mud sediments (terrestrial organic carbon mean: 32.5%) are characterized by fine silt (mean: 9.7 μm) and marine organic carbon ($\delta^{13}C_{org}$ mean: –19.5 ‰; C:N ratio mean: 11.4) with low total organic carbon (mean: 2.2%). The ages collected from core 2 (32 and 12 cm) and core 15 (43, 50, 55, and 65 cm) indicates these sediments were deposited 6600 ± 70 to 3812 ± 490 Cal yrs BP. The Mid- marine organic carbon

assemblage is diverse (*H'*= 2.6; R= 27.8) and characterized by *Rotalliella* spp. (mean: 13.8%), *Patellina* spp. (mean: 13.5%), and *Spirillina vivipara* (mean: 11.1%). *S. emaciatum*, *Bolivina* spp., *Quinqueloculina* spp, and *Rosalina* spp. were also present in smaller abundances (Table 6).

High- marine organic carbon assemblage (3610 ± 480 to 720 ± 290 Cal yrs BP)

Mixed carbonate sediments in core 2 (4 to 8 cm), core 14 (4 to 6 cm), core 15 (4 to 42 cm), and core 7 (10 to 60 cm) contain the High- marine organic carbon assemblage. The sediments are characterized by marine organic carbon ($\delta^{13}C_{org}$ mean: –19.5 ‰; C:N ratio mean: 10.3) and increased total organic carbon (6.7%) with coarse silt (mean: 52.7 μm). The ages collected from core 7 (10 cm & 60 cm) and core 15 (6, 10, 14, 20, 39, and 40 cm) indicate these sediments were deposited 3610 ± 480 to 720 ± 290 Cal yrs BP. The High- marine organic carbon assemblage is a diverse assemblage (*H'* = 3; R = 31) that is dominated by *Spirillina vivipara* (mean: 8.9%), *Quinqueloculina* spp. (mean: 8.6%), *Bolivina* spp. (mean: 7.8%), and *Rosalina* spp. (mean: 7.7%; Table 6).

Discussion

Findings of this study demonstrate that benthic habitats within the Palm Cave System have changed over the last 9,500 years in response to Holocene sea-level rise. Habitat shifts inferred from changes in core assemblages were influenced primarily by groundwater mass (meteoric lens vs. saline groundwater) and secondarily by organic carbon flux (terrestrial vs. marine) to the sediment. The recovered cores collectively provide the most detailed physical and biological picture yet known of Holocene environmental change in a karst subterranean estuary.

Initial flooding: ~9600 Cal yrs BP

Based on relative sea-level in Bermuda and the depth of the cave (~23 mbsl), the floor of the Palm Cave System was initially flooded by the vertically rising saline groundwater in response to sea-level rise approximately 9,500 Cal yrs BP. While the dominant dark-brown sapropel sediments suggest the organic matter is largely sourced from the forest landscape entering through subaerial karst windows, the benthic foraminiferal community indicates marine conditions were present. The Terrestrial-organic matter dominated subtidal assemblage within the dark-brown sapropel sediments is characterized by high species richness (R=26) and benthic foraminifera that are known from other marine environments (e.g., lagoons, reefs; Javaux and Scott, 2003). After initial flooding of saline groundwater, the benthic habitat was dominated by *Bolivina* spp, *Rosalina* spp., and *Globocassidulina subglobosa*, which suggests low-oxic, marine conditions were likely present in the benthos. *Bolivina* are common low-oxic indicators (Sen Gupta & Machain- Castillo, 1993), while Bernhard (1989) found *Globocassidulina* to be tolerant of oxygen deprivation in deep- Antarctic sediments. Additionally, according to Kaiho's (1994) benthic foraminiferal dissolved-oxygen index, *Rosalina* spp. is a suboxic (0.3-1.5 mL/L) indicator taxa. This suggests that in the case of Palm Cave, it is likely that, contrary to other literature, saline groundwater was the initial water mass to flood the cave floor, and only after saline inundation did that meteoric lens develop. Flooding created permanent standing water in the cave, resulting in new physical processes, aquatic ecosystems, and diverse deposition of terrestrial organic matter, fish bones, benthic foraminifera, and calcite rafts.

Meteoric lens and associated benthic habitats: 9200 to 8400 Cal yrs BP

Groundwater flooding the Palm Cave rapidly shifted from saline groundwater at 9500 Cal yrs BP to either a mixing zone or brackish meteoric lens at ~9100 Cal yrs BP, as noted by a significant decrease in species richness (R=3) and benthic foraminiferal community switch to brackish taxa. Overall, the benthic foraminifera within the light-brown sapropel deposits (e.g., *Polysaccammina ipohalina*, *Tiphotrocha comprimata*, and *Entzia macrecens*) suggests low-saline, brackish conditions (discussed below). A decrease in salinity is likely in response to increased rainfall events (Odum, 1988), which resulted in development of the meteoric lens (Mylroie and Carew, 1995). The meteoric lens would have been suitable to brackish-adapted cave crustaceans, like *Typhlatya*, that is known from current subterranean habitats flooded by the meteoric lens (Sanz and Platvoet, 1995; Alvarez et al., 2005). However, these fauna are not preserved in the sediment record, and must have emigrated from the Palm Cave in response to continued habitat change during the Holocene. Alternatively, benthic habitat change in response to the development of the meteoric lens is evidenced by three benthic foraminiferal assemblages throughout the light-brown sapropel deposits.

In general, the light-brown sapropel sediments are dominated by taxa that closely resemble those from brackish environments (i.e., marshes). Marsh habitats are characterized by salinity gradients which are strongly impacted by precipitation and tidal flooding (Odum, 1988) and distribution patterns of benthic foraminifera are generally related to this salinity gradient (Hayward and Hollis, 1994). The dominant benthic foraminifera (i.e., *P. ipohalina*- 69.6% and *T. comprimata*- 28.1%) in the Low-brackish assemblage (~ 9100 Cal yrs BP) are known from high marsh environments, that receive less tidal inundation compared to mid- and low- marsh environments (Scott, 1976; Scott et al., 1990; Scott et al., 1996), suggesting these taxa are

tolerant to low- salinity conditions. A significant increase of *T. comprimata* (90.6%) and decrease of *P. ipohalina* (2.5%) in the Mid-brackish assemblage (~8980 Cal yrs BP) suggests increased salinity in the meteoric lens, as *T. comprimata* is a dominant taxa in mid- to low-marsh environments (Scott, 1976; Scott et al., 1990; Scott et al., 1996) and has been closely associated with paleo-tidal levels (Gehrels, 1994). Therefore, the dominance of *P. ipohalina* (Low-brackish assemblage) followed by *T. comprimata* (Mid-brackish assemblage) suggests increasing salinity in the meteoric lens as it was vertically shifting at this time as saline groundwater continued to rise with sea-level.

The High-brackish assemblage (~8480 Cal yrs BP) dominates the light-brown sapropel sediments, upcore from the Low- and Mid- brackish assemblages. This assemblage is characterized by a significant increase of *Bolivina* spp. (71.8%), *Rosalina* spp. (8.1%), *Entzia macrescens* (4.3%), and a decrease of *T. comprimata* (9.8%) and *P. ipohalina* (1%). Abundance of calcareous taxa (e.g., *Bolivina*, *Rosalina*) suggests increasing saline conditions (Sen Gupta, 1999), while *E. macrescens* has been documented in higher-saline areas along salinity gradients in marsh environments (Scott et al., 1996). Alternatively, the dominance of *Bolivina* and *Rosalina* suggests low-oxic conditions are present (Seiglie, 1968; Kaiho, 1994), likely in response to the abundant organic matter deposited in the sediments at this time. Additionally, *Entzia macrscens* has been shown to flourish in organic rich environments, due to its epiphytic and infaunal life modes (Matera & Lee, 1972; Alve and Murray, 1999; Ozarko et al., 1997). These results suggest increasing salinity in a low-oxic meteoric lens habitat, in response to the vertically rising saline groundwater.

Overall, Brackish assemblages develop in the karst subterranean estuary when it became flooded by the meteoric lens and dominated by terrestrial processes. Historically, anchialine has

been characterized based on the distribution of characteristic stygobitic fauna and having marine and terrestrial influences, subterranean connections to the sea, and restricted exposure to open air (Holthuis, 1973; Stock et al., 1986). Therefore, salinity and organic matter likely controlled the benthic anchialine environment 9100 to 7000 Cal yrs BP. Importantly, cave sediments deposited during periods of brackish conditions are useful sea-level indicators because the terrestrially dominated organic matter and brackish benthic foraminiferal taxa indicate general position of the meteoric lens/mixing zone (Gehrels, 1994). Anchialine sedimentation patterns are observed elsewhere and are useful sea-level indicators. For example, Steadman et al. (2007) used mid- to late- Holocene anchialine entrance diamicts from Sawmill Sink, Bahamas to reconstruct local paleoecology. Based on the available evidence, similar sedimentary processes operate globally in anchialine environments.

Deposition of iron-rich carbonates: ~8400 to 7000 Cal yrs BP

The Iron-rich carbonates deposits were largely void of meiofaunal remains. Negligible foraminifera were noted, only the rare low-oxic tolerant *Bolivina* spp. were observed. Previous research has shown oxidative precipitation of dissolved Fe (II) from the mixing of seawater and groundwater generates a distinctive increase in iron oxide deposits in the subsurface zone (Charette & Sholkovitz, 2002). This process is driven by pH gradients between the anoxic saline versus oxygenated freshwater above (Spiteri, et al., 2006), and the iron curtain can spatially migrate in response to sea-level (Roy et al., 2010). Therefore, the Iron-rich carbonate deposits and general absence of foraminifera suggests an upwelling of anoxic saline groundwater under sea-level forcing, mixed with the overlying oxygenated fresh/brackish water, resulting in precipitation of iron oxide.

Circulating saline groundwater: ~6000 Cal yrs BP

A marine habitat was established ~6600 Cal yrs BP when saline groundwater completely inundated the Palm Cave benthos. The $\delta^{13}C_{org}$ values and C:N ratios of the organic matter indicates these habitats received regular inputs of marine organic matter at this time. The presence of marine organic matter is likely a result of increased circulation with adjacent lagoons as saline groundwater completely floods the Palm Cave System. This also resulted in a completely different suite of benthic foraminiferal communities.

The dominant taxa within the benthos at this time are consistent with other coastal marine environments (Javaux and Scott, 2003) and can be further divided into three assemblages that are likely distinguished based on total organic carbon. The first assemblage, Low-marine organic carbon assemblage, is characterized by low total organic carbon (mean: 2.2%) and marine taxa (e.g., *Spirophthalmidium emaciatum*, *Spirillina vivipara*, *Bolivina* spp., and *Rotaliella* spp.). This assemblage is comparable to previous research in the Palm Cave System that found *S. emaciatum* and Spirillinids associated with oligotrophic conditions in modern surface sediment samples (Chapter 3, this study). Additionally, *Bolivina* spp. indicates low-oxic conditions (Bernhard and Sen Gupta, 1999), likely associated with limited tidal flow due to the initial inundation of saline groundwater in the karst subterranean estuary benthos. Limited tidal flow also likely limited the flux of total organic carbon to the benthos. Alternatively, the Mid-marine organic carbon assemblage is characterized by increasing total organic carbon values (mean: 3.6%) and species richness (R=27.8), with similar dominant marine taxa. This suggests after marine conditions were established, sea-level continued to rise, which increased circulation,

thereby increasing the flux of total organic carbon to the sediments throughout the Palm Cave System.

Increased organic carbon deposition through time: ~3600 Cal yrs BP

A final shift in benthic foraminiferal taxa is observed in the High- marine organic carbon assemblage. This assemblage is characterized by the highest species richness (R=31) and diversity (*H*= 3). The dominant marine taxa include *Spirillina vivipara, Patellina* spp., *Miliolinella* spp., and *Quinqueloculina* spp. with lower abundance of *Spirophthalmidium emaciatum*. Previous research documented *S. emaciatum* as a dominant taxa in oligotrophic conditions, where is is not outcompeted by other marine, lagoonal miliolids (van Hengstum & Scott, 2011). Therefore, decreased *S. emaciatum* in the High- marine organic carbon assemblage likely suggests increased species diversity outcompetes *S. emaciatum* in response to increased increased total organic carbon. Additionally, increased total organic carbon likely supports the increased species diversity and abundant miliolids that are common to Bermuda's carbonate lagoons (Javaux & Scott, 2003).

CHAPTER V

CONCLUSIONS

Subterranean estuaries harbour a poorly understood, but globally dispersed anchialine ecosystem with diverse endemic cave-adapted fauna (Bishop et al., 2015; Iliffe and Kornicker, 2009; Stock et al., 1986). Interestingly, variability in geological, hydrological, and chemical characteristics has yielded a great variety of what are now considered anchialine settings, although not all settings are agreed upon by all researchers.

Anchialine ecosystems that are known to persist on non-karst landscapes, in water-filled pools and depressions on Hawaiian Islands, coastal tectonic faults and fissures in the Galapagos Islands, and flooded lava tubes in the Canary Islands (Brock et al., 1987; Iliffe, 1991; Santos, 2006; García et al., 2009), can be argued as anchialine ecosystems populating a volcanic subterranean estuary. The anchialine ecosystems in volcanic subterranean estuaries are beyond the scope of this work, but many ideas are developed in this dissertation that become fruitful hypotheses to test.

This research specifically addresses anchialine ecosystems within karst subterranean estuaries. Anchialine ecosystems within karst subterranean estuaries have been documented in cave conduits in the Caribbean and Mediterranean, and deep vertical shafts in Bahamas and Australia (Stock et al., 1986; Humpherys, 1999; Kornicker and Yager, 2002; Iliffe and Kornicker, 2009). Importantly some anchialine ecosystems exhibit obvious division of water masses (i.e., Yucatan, Mexico) while others exhibit a more homogenous environment dominated by the saline groundwater (i.e., submarine environment; Bermuda). Here we consider that karst subterranean estuaries are populated by an anchialine habitat continuum that spans, but does not strictly define, based on groundwater mass variability from the ocean to the terrestrial realm on a

carbonate landscape. While water mass characteristics have been given such importance to define habitats in the anchialine habitat continuum, benthic habitat variability has received less attention.

Previous research has highlighted the importance of salinity (van Hengstum and Scott, 2011; Radolovic et al., 2015; Riera et al., 2018; Romano et al., 2018) and nutrient supply (Fichez, 1990; Fichez, 1991; Ape et al., 2016) on meiofaunal communities (i.e., nematodes, crustaceans, polychaeta), while loss of biomass and diversity from outer to inner regions of KSEs of suspension and filter feeders (i.e., sponges, cnidarians, bryozoans, and tunicates) has been shown to be the result of light attenuation (Harmelin et al., 1985; Marti et al., 2004; Coombes et al., 2015), reduced tidal activity, and decreasing sediment size (Navarro-Barranco et al., 2013). However, if the karst subterranean estuary ecosystem is disrupted, due to natural or anthropogenic forcings (i.e., pollution, sea-level rise), faunal communities will shift, ultimately impacting ecosystem biodiversity and function.

This research addresses some basic questions to further understand karst subterranean estuary's benthic anchialine habitat variability over time and space: (*i*) how does organic carbon flux to the benthos impact benthic habitat variability in karst subterranean estuaries relative to other large-scale environmental variables (e.g., tidal exposure, ground water mass salinity), (*ii*) how do benthic habitats in a cave change and develop on a carbonate platform in response to sea-level forced vertical migration, and cave inundation, of a karst subterranean estuary since the last glacial maximum (~20,000 years ago), and (*iii*) how do benthic foraminifera document benthic habitat develop in a karst subterranean estuary since the last ice age?

In order to address these questions, this dissertation first systematically investigated modern benthic foraminiferal distributions occurring in eastern Bermudian karst subterranean

estuaries. Importantly, the paleoecological interpretation of benthic anchialine habitat variability depends on an understanding of the ecological processes operating at the present. Once the environmental controls for modern distributions could be constrained, core records were then used to identify habitat development and investigate environmental drivers over time.

As demonstrated in *Chapter II*, a primary finding of my research is that benthic anchialine habitat variability is driven by multiple environmental gradients within karst subterranean estuaries. Within Eastern Bermudian karst subterranean estuaries, benthic anchialine habitat variability is primarily driven by provenance of organic carbon (terrestrial vs. marine) accumulating in the benthos and secondarily by salinity, light, and tidal exposure. Within the dark regions of karst subterranean estuaries, where salinity, oxygen, darkness and lack of tidal exposure is constant, provenance of organic carbon is again, the main control of benthic foraminiferal distributions. The dominance of characteristic benthic foraminiferal taxa provides evidence that certain environmental conditions were present. These findings contribute to our understanding of benthic anchialine habitat variability within KSEs. Habitat variability is likely to be of particular importance because of the strong link between habitat and species diversity. Furthermore, habitat variation as a driver of functional composition and diversity suggests that habitat heterogeneity should be explicitly included within studies trying to predict the effect of species loss on ecosystem function.

Chapter III provides evidence of benthic anchialine habitat development in eastern Bermudian KSEs in response to Holocene sea-level rise. The results document the most complete record yet known of developmental succession in anchialine habitats in response to concomitant relative sea-level rise and vertical migration of a karst subterranean estuary since the last ice age in Bermuda. In addition, the results illuminate how sea-level rise can force

subsurface aquatic island fauna to experience a previously unknown bottleneck event. It is highly likely that this process impacted the evolutionary history of global subsurface aquatic island fauna during the Phanerozoic, and problematically, 21st century island-based marine ecosystem risk assessments are incomplete if this process is not regionally evaluated.

Chapter IV contributes to our understanding of the environmental controls on benthic anchialine habitat development the Palm Cave System. Specifically, how organic matter quantity and quality contribute to benthic habitat development. Benthic foraminiferal communities helped identify benthic anchialine habitat variability. Based on benthic foraminiferal distributions, from 9,500 to 7,000 Cal yrs BP, the karst subterranean estuary benthos was comparable to a fresh/brackish aquatic environment, dominated by terrestrial organic carbon and common marsh/brackish taxa (i.e., *Polysaccammina ipohalina*, *Tiphotrocha comprimata*). This suggests the meteoric lens, buoyed on top of the saline groundwater, had inundated the floor of the Palm Cave System, creating a fresh/brackish aquatic environment. From ~7000 Cal yrs BP to the present, marine organic matter and carbonate mud dominated the sediment, with abundant common marine/lagonal taxa (i.e., *Spirophthalmidium emaciatum*, *Spirillina vivipara*). These results suggest as sea-level continued to rise and marine water completely flooded the Bermuda carbonate platform, marine organic carbon contributed to benthic anchialine habitat development.

One of the key goals of my dissertation research was to expand the basic understanding of environmental impacts on benthic anchialine habitat variability by comparing benthic foraminiferal communities with environmental variables. Understanding that benthic anchialine habitat variability is driven by environmental gradients (i.e., nutrient supply, sediment grain size, light, tidal exposure) over time and space is important, considering urgently needed monitoring

of anchialine cave ecosystems, and the use of effective indicators, such as the benthic foraminifera studied here, could provide effective tools to assist marine cave conservation. Findings of my research are significant from an ecological point of view because they confirm that benthic anchialine habitat variability is controlled by important environmental gradients that also contribute to benthic anchialine habitat development over time. Important questions regarding other environmental gradients (i.e., pH, other nutrients, dissolved oxygen, temperature) impacting benthic habitat variability in karst subterranean estuaries remain unresolved. In addition, future studies should investigate linkages (coupling) between benthic and pelagic environmental conditions and their effect on benthic habitat variability, focus on different anchialine ecosystems (i.e., volcanic subterranean estuaries), improve the models for benthic habitat variability and change over time, and explore the effects of diverse environmental interactions within the karst subterranean estuaries and impacts on meiofaunal communities.

REFERENCES

Alavi, S. N. (1980). Micropalaeontological studies of Recent sediments from the Cilicia Basin (N.E. Mediterranean). Thesis, Univ. London, 230 pp. (unpublished)

Ali, J. R., & Aitchison, J. C. (2014). Exploring the combined role of eustasy and oceanic island thermal subsidence in shaping biodiversity on the Galápagos. Journal of Biogeography, 41(7), 1227-1241.

Aller, R. C. (2014). Sedimentary diagenesis, depositional environments, and benthic fluxes. In *Treatise on Geochemistry*, Vol. 8:*The Oceans and Marine Geochemistry*, ed. MJ Mottl, H Elderfield, pp. 293–334. Amsterdam: Elsevier. 2nd ed.

Aloulou, F., EllEuch B., & Kallel M. (2012). Benthic foraminiferal assemblages as pollution proxies in the northern coast of Gabes Gulf, Tunisia. Environmental Monitoring and Assessment, 184, 777–795. pmid:21476104

Altenbach, A. V., Pflaumann, U., Schiebel, R., Thies, A., Timm, S., & Trauth, M. (1999). Scaling percentages and distributional patterns of benthic foraminifera with flux rates of organic carbon. The Journal of Foraminiferal Research, 29(3), 173-185.

Alvarez, F., Iliffe, T. M., & Villalobos, J. L. (2005). New species of the genus *Typhlatya* (Decapoda: Atyidae) from anchialine caves in Mexico, the Bahamas, and Honduras. Journal of Crustacean Biology, 25(1), 81-94.

Alve, E., & Murray, J. W. (1999). Marginal marine environments of the Skagerrak and Kattegat: a baseline study of living (stained) benthic foraminiferal ecology. Palaeogeography, Palaeoclimatology, Palaeoecology, 146(1-4), 171-193.

Ape, F., Arigo, C., Gristina, M., Genovese, L., Di Franco, A., Di Lorenzo, M., & Mirto, S. (2016). Meiofaunal Diversity and Nematode Assemblages in Two Submarine Caves of a Mediterranean Marine Protected Area. Mediterranean Marine Science, 17(1), 202-215.

Armynot du Châtelet, É. A., Bout-Roumazeilles, V., Riboulleau, A., & Trentesaux, A. (2009). Sediment (grain size and clay mineralogy) and organic matter quality control on living benthic foraminifera. Revue de Micropaléontologie, 52(1), 75-84.

Armynot du Chatelet, E. A., Bout-Roumazeilles, V., Coccioni, R., Frontalini, F., Francescangeli, F., Margaritelli, G., & Tribovillard, N. (2016). Environmental control on a land–sea transitional setting: integrated sedimentological, geochemical and faunal approaches. Environmental Earth Sciences, 75(2), 123.

Ashmore, S., & Leatherman, S. P. (1984). Holocene sedimentation in Port Royal Bay, Bermuda. Marine Geology, 56(1-4), 289-298.

Bandy, O. L., Ingle Jr, J. C., & Resig, J. M. (1965). Foraminiferal trends, hyperion outfall, California 1. Limnology and Oceanography, 10(3), 314-332.

Bandy, O. L. (1964). Foraminiferal biofacies in sediments of Gulf of Batabano, Cuba, and their geologic significance. AAPG Bulletin, 48(10), 1666-1679.

Beddows, P.A., Smart, P.L., Whitaker, F.F. & Smith, S.L. (2005) in Hydrogeology and Biology of Post-Paleozoic Carbonate Aquifers. ed. J.B. Martin, C.M. Wicks, & I.D. Sasowky. Karst Waters Institute. 129-134.

Beddows, P.A., Smart, P.L., Whitaker, F.F. & Smith, S.L. (2007) Decoupled fresh-saline groundwater circulation of a coastal carbonate aquifer: Spatial patterns of temperature and specific electrical conductivity. Journal of Hydrology, 346, 18-32.

Belley, R., Snelgrove, P. V., Archambault, P., & Juniper, S. K. (2016). Environmental drivers of benthic flux variation and ecosystem functioning in Salish Sea and Northeast Pacific sediments. PloS One, 11(3), e0151110.

Berkeley, A., Perry, C. T., Smithers, S. G., & Horton, B. P. (2008). The spatial and vertical distribution of living (stained) benthic foraminifera from a tropical, intertidal environment, north Queensland, Australia. Marine Micropaleontology, 69(2), 240-261.

Bermúdez, P. J. (1949). Tertiary smaller foraminifera of the Dominican Republic (No. 25). Cushman Laboratory for Foraminiferal Research.

Bernhard, J. M., & Sen Gupta, B. K. (1999). Foraminifera of oxygen-depleted environments. In Modern foraminifera. Springer, Dordrecht, 201-216.

Bernhard, J. M. (1989). The distribution of benthic Foraminifera with respect to oxygen concentration and organic carbon levels in shallow-water Antarctic sediments. Limnology and Oceanography, 34(6), 1131-1141.

Bintanja, R., & Van de Wal, R. S. W. (2008). North American ice-sheet dynamics and the onset of 100,000-year glacial cycles. Nature, 454(7206), 869.

Bishop, R.E., Humphreys, W.F., Cukrov, N., Zic, V., Boxshall, G.A., Cukrov, M., Iliffe, T.M., Krsinic, F., Moore, W.S., Pohlman, J.W. & Sket, B. (2015) 'Anchialine' redefined as a subterranenan estuary in crevicular or cavernous geological setting. Journal of Crustacean Biology, 35, 511-514.

Boltovskoy, E., Scott, D. B., & Medioli, F. S. (1991). Morphological variations of benthic foraminiferal tests in response to changes in ecological parameters: a review. Journal of Paleontology, 65(2), 175-185.

Botello, A., Iliffe, T. M., Alvarez, F., Juan, C., Pons, J., & Jaume, D. (2013). Historical biogeography and phylogeny of Typhlatya cave shrimps (Decapoda: Atyidae) based on mitochondrial and nuclear data. Journal of Biogeography, 40(3), 594-607.

Bowman, T. E., & Iliffe, T. M. (1985). *Mictocaris halope*, a new unusual peracaridan crustacean from marine caves on Bermuda. Journal of Crustacean Biology, 5(1), 58-73.

Bradshaw, J. S. (1968). Environmental parameters and marsh foraminifera. Limnology and Oceanography, 13(1), 26-38.

Brankovits, D., Pohlman, J. W., Niemann, H., Leigh, M. B., Leewis, M. C., Becker, K. W., & Phillips, B. (2017). Methane-and dissolved organic carbon-fueled microbial loop supports a tropical subterranean estuary ecosystem. Nature Communications, 8(1), 1835.

Brankovits, D., Pohlman, J. W., Ganju, N. K., Iliffe, T. M., Lowell, N., Roth, E., & Lapham, L. L. (2018). Hydrologic controls of methane dynamics in karst subterranean estuaries. Global Biogeochemical Cycles, 32(12), 1759-1775.

Brett, M. T., Kainz, M. J., Taipale, S. J., & Seshan, H. (2009). Phytoplankton, not allochthonous carbon, sustains herbivorous zooplankton production. Proceedings of the National Academy of Sciences, 106(50), 21197-21201.

Bretz, J. H. (1960). Bermuda: A partially drowned, late mature, Pleistocene karst. Geological Society of America Bulletin, 71(12), 1729-1754.

Brock, R. E., Norris, J. E., Ziemann, D. A., & Lee, M. T. (1987). Characteristics of water quality in anchialine ponds of Kona, Hawaii Coast. Pacific Science, 41, 200-208.

Bussotti, S., Terlizzi, A., Fraschetti, S., Belmonte, G., & Boero, F. (2006). Spatial and temporal variability of sessile benthos in shallow Mediterranean marine caves. Marine Ecology Progress Series, 325, 109-119.

Calderón-Gutiérrez, F., Sánchez-Ortiz, C. A., & Huato-Soberanis, L. (2018). Ecological patterns in anchialine caves. PloS One, 13(11), e0202909.

Camacho, S., Moura, D., Connor, S., Scott, D., & Boski, T. (2015). Ecological zonation of benthic foraminifera in the lower Guadiana Estuary (southeastern Portugal). Marine Micropaleontology, 114, 1-18.

Cant, R. V., & Weech, P. S. (1986). A review of the factors affecting the development of Ghyben-Hertzberg lenses in the Bahamas. Journal of Hydrology, 84(3-4), 333-343.

Caralp, M. H. (1989). Size and morphology of the benthic foraminifer *Melonis barleeanum*; relationships with marine organic matter. The Journal of Foraminiferal Research, 19(3), 235-245.

Carman, K.W., 1933. The shallow-water foraminifera of Bermuda, Unpublished Ph.D. thesis, Massachusetts Institute of Technology.

Cearreta, A. (1988). Distribution and Ecology of benthic foraminifera. Revista Española de Paleontología, 3, 23-38.

Center, N.N.G.D. (2013). National Centers for Environmental Information, National Oceanic and Atmospheric Administration, https://data.noaa.gov.

Charette, M. A., & Sholkovitz, E. R. (2002). Oxidative precipitation of groundwater derived ferrous iron in the subterranean estuary of a coastal bay. Geophysical Research Letters, 29(10), 85-1.

Chevaldonné, P., & Lejeusne, C. (2003). Regional warming-induced species shift in north-west Mediterranean marine caves. Ecology Letters, 6(4), 371-379.

Clarke, K. R., Somerfield, P. J., & Gorley, R. N. (2008). Testing of null hypotheses in exploratory community analyses: similarity profiles and biota-environment linkage. Journal of Experimental Marine Biology and Ecology, 366(1-2), 56-69.

Collins, S. V., Reinhardt, E. G., Werner, C. L., Le Maillot, C., Devos, F., & Rissolo, D. (2015). Late Holocene mangrove development and onset of sedimentation in the Yax Chen cave system (Ox Bel Ha) Yucatan, Mexico: Implications for using cave sediments as a sea-level indicator. Palaeogeography, Palaeoclimatology, Palaeoecology, 438, 124-134.

Collins, S. V., Reinhardt, E. G., Rissolo, D., Chatters, J. C., Blank, A. N., & Erreguerena, P. L. (2015). Reconstructing water level in Hoyo Negro, Quintana Roo, Mexico, implications for early Paleoamerican and faunal access. Quaternary Science Reviews, 124, 68-83.

Coombes, M. A., La Marca, E. C., Naylor, L. A., Piccini, L., De Waele, J., & Sauro, F. (2015). The influence of light attenuation on the biogeomorphology of a marine karst cave: a case study of Puerto Princesa Underground River, Palawan, the Philippines. Geomorphology, 229, 125-133.

Corliss, B. H. (1991). Morphology and microhabitat preferences of benthic foraminifera from the northwest Atlantic Ocean. Marine Micropaleontology, 17(3-4), 195-236.

Curran, H. A., & White, B. (Eds.). (1995). Terrestrial and shallow marine geology of the Bahamas and Bermuda. Geological Society of America, 300

De'Ath, G. (2002). Multivariate regression trees: a new technique for modeling species–environment relationships. Ecology, 83(4), 1105-1117.

De'Ath, G., 2007. R Package "Mvpart": Multivariate Partitioning. Version 1.6-2. In: https://CRAN.R-project.org/package=mvpart.

Debenay, J. P., & Guillou, J. J. (2002). Ecological transitions indicated by foraminiferal assemblages in paralic environments. Estuaries, 25(6), 1107-1120.

Debenay, J. P., Tsakiridis, E., Soulard, R., & Grossel, H. (2001). Factors determining the distribution of foraminiferal assemblages in Port Joinville Harbor (Ile d'Yeu, France): the influence of pollution. Marine Micropaleontology, 43(1-2), 75-118.

Debenay, J. P., Guiral, D., & Parra, M. (2002). Ecological factors acting on the microfauna in mangrove swamps. The case of foraminiferal assemblages in French Guiana. Estuarine, Coastal and Shelf Science, 55(4), 509-533.

Deming, J. W., & Yager, P. L. (1992). Natural bacterial assemblages in deep-sea sediments: towards a global view. In Deep-sea food chains and the global carbon cycle (pp. 11-27). Springer, Dordrecht.

Den Dulk, M., Reichart, G. J., Van Heyst, S., Zachariasse, W. J., & Van der Zwaan, G. J. (2000). Benthic foraminifera as proxies of organic matter flux and bottom water oxygenation? A case history from the northern Arabian Sea. Palaeogeography, Palaeoclimatology, Palaeoecology, 161(3-4), 337-359.

Denitto, F., Terlizzi, A., & Belmonte, G. (2007). Settlement and primary succession in a shallow submarine cave: spatial and temporal benthic assemblage distinctness. Marine Ecology, 28, 35-46.

Denoyelle M., Geslin E., Jorissen F.J., Cazes L., & Galgani F. (2012) Innovative use of foraminifera in ecotoxicology: A marine chronic bioassay for testing potential toxicity of drilling muds. Ecological Indicators 12: 17–25. pmid:22901085

Dimarchopoulou, D., Gerovasileiou, V., & Voultsiadou, E. (2018). Spatial variability of sessile benthos in a semi-submerged marine cave of a remote Aegean Island (eastern Mediterranean Sea). Regional Studies in Marine Science, 17, 102-111.

Dissard, D., Nehrke, G., Reichart, G. J., & Bijma, J. (2010). Impact of seawater pCO2 on calcification and Mg/Ca and Sr/Ca ratios in benthic foraminifera calcite: results from culturing experiments with Ammonia tepida. Biogeosciences, 7, 81-93.

Diz, P., Francés, G., Costas, S., Souto, C., & Alejo, I. (2004). Distribution of benthic foraminifera in coarse sediments, Ría de Vigo, NW Iberian margin. The Journal of Foraminiferal Research, 34(4), 258-275.

Du Châtelet, É. A., Bout-Roumazeilles, V., Riboulleau, A., & Trentesaux, A. (2009). Sediment (grain size and clay mineralogy) and organic matter quality control on living benthic foraminifera. Revue de Micropaléontologie, 52(1), 75-84.

Du Châtelet, É. A., Bout-Roumazeilles, V., Coccioni, R., Frontalini, F., Francescangeli, F., Margaritelli, G., & Tribovillard, N. (2016). Environmental control on a land–sea transitional setting: integrated sedimentological, geochemical and faunal approaches. Environmental Earth Sciences, 75(2), 123.

Du Châtelet, É. A., Frontalini, F., & Francescangeli, F. (2018). Significance of replicates: Environmental and paleoenvironmental studies on benthic foraminifera and testate amoebae. Micropaleontology, 63(5), 257-274.

Dutton, A., Bard, E., Antonioli, F., Esat, T. M., Lambeck, K., & McCulloch, M. T. (2009). Phasing and amplitude of sea-level and climate change during the penultimate interglacial. Nature Geoscience, 2(5), 355.

Ellison, J. C. (1993). Mangrove retreat with rising sea-level, Bermuda. Estuarine, Coastal and Shelf Science, 37(1), 75-87.

Fernández-Palacios, J. M., Rijsdijk, K. F., Norder, S. J., Otto, R., de Nascimento, L., Fernández-Lugo, S., & Whittaker, R. J. (2016). Towards a glacial-sensitive model of island biogeography. Global Ecology and Biogeography, 25(7), 817-830.

Ferraro L., Sprovieri M., Alberico I., Lirer F., Prevedello L., & Marsella, E. (2006) Benthic foraminifera and heavy metals distribution: a case study from the Naples Harbour (Tyrrhenian Sea, Southern Italy). Environmental Pollution, 142(2), 274–87.

Fichez, R. (1990). Decrease in allochthonous organic inputs in dark submarine caves, connection with lowering in benthic community richness. Hydrobiologia, 207(1), 61-69.

Fichez, R. (1991). Suspended particulate organic matter in a Mediterranean submarine cave. Marine Biology, 108(1), 167-174.

Field, C. B., Barros, V., Stocker, T. F., & Dahe, Q. (Eds.). (2012). Managing the risks of extreme events and disasters to advance climate change adaptation: special report of the intergovernmental panel on climate change. Cambridge University Press.

Fisher, R.A., Corbet, A.S., & Williams, C.B. (1943). The relation between the number of species and the number of individuals in a random sample of an animal population. Journal of Animal Ecology, 12, 42-58.

Ford, D. & Williams, P.D. (2013). Karst Hydrogeology and Geomorphology. John Wiley & Sons, West Sussex

Fornós, J. J., Gines, J., & Gràcia, F. (2009). Present-day sedimentary facies in the coastal karst caves of Mallorca island (western Mediterranean). Journal of Cave and Karst Studies, 71(1), 86-99.

Fox, J. & Weisberg, S. (2011). An (Alavi) Companion to Applied Regression. In: Thousand Oaks CA: sage URL, 2nd ed., http://socserv.socsci.mcmaster.ca/jfox/Books/Companion.

Frail-Gauthier, J. L., Mudie, P. J., Simpson, A. G., & Scott, D. B. (2019). Mesocosm and Microcosm Experiments On the Feeding of Temperate Salt Marsh Foraminifera. Journal of Foraminiferal Research, 49(3), 259-274.

France, R. (1998). Estimating the assimilation of mangrove detritus by fiddler crabs in Laguna Joyuda, Puerto Rico, using dual stable isotopes. Journal of Tropical Ecology, 14(4), 413-425.

Frontalini, F. & Coccioni, R. (2011). Benthic foraminifera as bioindicators of pollution: a review of Italian research over the last three decades. Revue de Micropaleontolgie, 54, 115–127.

Frontalini, F., Buosi, C., Da Pelo, S., Coccioni, R., Cherchi, A., & Bucci, C. (2009). Benthic foraminifera as bio-indicators of trace element pollution in the heavily contaminated Santa Gilla lagoon (Cagliari, Italy). Marine Pollution Bulletin, 58(6), 858-877.

Frontalini, F., Margaritelli, G., Francescangeli, F., Rettori, R., & Du Châtelet, E. A. (2013). Benthic foraminiferal assemblages and biotopes in a coastal lake: the case study of Lake Varano (Southern Italy). Acta Protozoologica, (3, Special topic issue:" Protists as Bioindicators of Past and Present Environmental Conditions"), 147-160.

Gabriel, J. J., Reinhardt, E. G., Peros, M. C., Davidson, D. E., van Hengstum, P. J., & Beddows, P. A. (2009). Palaeoenvironmental evolution of Cenote Aktun Ha (Carwash) on the Yucatan Peninsula, Mexico and its response to Holocene sea-level rise. Journal of Paleolimnology, 42(2), 199-213.

Gandolfi, A., Todeschi, E. B. A., Van Doninck, K., Rossi, V., & Menozzi, P. (2001). Salinity tolerance of Darwinula stevensoni (Crustacea, Ostracoda). Italian Journal of Zoology, 68(1), 61-67.

García, A. M., Palmero, A. M., del Carmen Brito, M., Núñez, J., & Worsaae, K. (2009). Anchialine fauna of the Corona lava tube (Lanzarote, Canary Islands): diversity, endemism and distribution. Marine Biodiversity, 39(3), 169-182.

Garman, K. M., & Garey, J. R. (2005). The transition of a freshwater karst aquifer to an anoxic marine system. Estuaries, 28(5), 686-693.

Gehrels, W. R., & van de Plassche, O. (1999). The use *of Jadammina macrescens* (Brady) and *Balticammina pseudomacrescens* Brönnimann, Lutze and Whittaker (Protozoa: Foraminiferida) as sea-level indicators. Palaeogeography, Palaeoclimatology, Palaeoecology, 149(1-4), 89-101.

Gehrels, W. R. (1994). Determining relative sea-level change from salt-marsh foraminifera and plant zones on the coast of Maine, USA. Journal of Coastal Research, 990-1009.

Gehrels, W. R. (2000). Using foraminiferal transfer functions to produce high-resolution sea-level records from salt-marsh deposits, Maine, USA. The Holocene, 10(3), 367-376.

Gerovasileiou, V., & Voultsiadou, E. (2012). Marine caves of the Mediterranean Sea: a sponge biodiversity reservoir within a biodiversity hotspot. PLoS One, 7(7), e39873.

Gerovasileiou, V., Chintiroglou, C., Vafidis, D., Koutsoubas, D., Sini, M., Dailianis, T., & Voutsiadou, E. (2015). Census of biodiversity in marine caves of the eastern Mediterranean Sea. Mediterranean Marine Science, 16(1), 245-265.

Gerovasileiou, V., Dimitriadis, C., Arvanitidis, C., & Voultsiadou, E. (2017). Taxonomic and functional surrogates of sessile benthic diversity in Mediterranean marine caves. PloS One, 12(9), e0183707.

Gili, J. M., Riera, T., & Zabala, M. (1986). Physical and biological gradients in a submarine cave on the Western Mediterranean coast (north-east Spain). Marine Biology, 90(2), 291-297.

Gonneea, M. E., Charette, M. A., Liu, Q., Herrera-Silveira, J. A., & Morales-Ojeda, S. M. (2014). Trace element geochemistry of groundwater in a karst subterranean estuary (Yucatan Peninsula, Mexico). Geochimica et Cosmochimica Acta, 132, 31-49.

Gonzalez, B. C., Martínez, A., Borda, E., Iliffe, T. M., Fontaneto, D., & Worsaae, K. (2017). Genetic spatial structure of an anchialine cave annelid indicates connectivity within-but not between-islands of the Great Bahama Bank. Molecular Phylogenetics and Evolution, 109, 259-270.

Gooday, A. J., & Turley, C. M. (1990). Responses by benthic organisms to inputs of organic material to the ocean floor: a review. Philosophical Transactions of the Royal Society of London. Series A, Mathematical and Physical Sciences, 331(1616), 119-138.

Gooday, A. J., Levin, L. A., Linke, P., & Heeger, T. (1992). The role of benthic foraminifera in deep-sea food webs and carbon cycling. In Deep-sea food chains and the global carbon cycle. Springer, Dordrecht, 63-91.

Gooday, A. J. (1988). A response by benthic foraminifera to the deposition of phytodetritus in the deep sea. Nature, 332(6159), 70.

Gooday, A. J. (1993). Deep-sea benthic foraminiferal species which exploit phytodetritus: characteristic features and controls on distribution. Marine Micropaleontology, 22(3), 187-205.

Graf, G. (1989). Benthic-pelagic coupling in a deep-sea benthic community. Nature, 341(6241), 437.

Graham, M. H., 2003. Confronting multicollinearity in ecological multiple regression. Ecology, 84, 2809-2815.

Guilbault, J. P., Clague, J. J., & Lapointe, M. (1995). Amount of subsidence during a late Holocene earthquake—Evidence from fossil tidal marsh foraminifera at Vancouver Island, west coast of Canada. Palaeogeography, Palaeoclimatology, Palaeoecology, 118(1-2), 49-71.

Gulley, J. D., Mayer, A. S., Martin, J. B., & Bedekar, V. (2016). Sea level rise and inundation of island interiors: Assessing impacts of lake formation and evaporation on water resources in arid climates. Geophysical Research Letters, 43(18), 9712-9719.

Gupta, B. K. S., & Machain-Castillo, M. L. (1993). Benthic foraminifera in oxygen-poor habitats. Marine Micropaleontology, 20(3-4), 183-201.

Gustafsson, M., & Nordberg, K. (2000). Living (stained) benthic foraminifera and their response to the seasonal hydrographic cycle, periodic hypoxia and to primary production in Havstens Fjord on the Swedish west coast. Estuarine, Coastal and Shelf Science, 51(6), 743-761.

Haas, S., De Beer, D., Klatt, J. M., Fink, A., Rench, R. M., Hamilton, T. L., & Macalady, J. L. (2018). Low-light anoxygenic photosynthesis and Fe-S-biogeochemistry in a microbial mat. Frontiers in Microbiology, 9, 858.

Haig, D. W. (1988). Miliolid foraminifera from inner neritic sand and mud facies of the Papuan Lagoon, New Guinea. The Journal of Foraminiferal Research, 18(3), 203-236.

Hallam, A., & Wignall, P. B. (1999). Mass extinctions and sea-level changes. Earth-Science Reviews, 48(4), 217-250.

Hallock, P. (1985). Why are larger foraminifera large? Paleobiology, 11(2), 195-208.

Harmelin, J. G., Vacelet, J. & Vasseur, P. (1985). Les grottes sous-marines obscures: un milieu extrême et un remarquable biotope refuge. Téthys, 11, 214-229.

Harnik, P. G., Lotze, H. K., Anderson, S. C., Finkel, Z. V., Finnegan, S., Lindberg, D. R., & O'Dea, A. (2012). Extinctions in ancient and modern seas. Trends in Ecology & Evolution, 27(11), 608-617.

Haunold, T. G., Baal, C., & Piller, W. E. (1997). Benthic foraminiferal associations in the northern Bay of Safaga, Red Sea, Egypt. Marine Micropaleontology, 29(3-4), 185-210.

Hayward, B. W., & Hollis, C. J. (1994). Brackish foraminifera in New Zealand; a taxonomic and ecologic review. Micropaleontology, 40(3), 185-222.

Hayward, B. W., Grenfell, H., Cairns, G., & Smith, A. (1996). Environmental controls on benthic foraminiferal and thecamoebian associations in a New Zealand tidal inlet. The Journal of Foraminiferal Research, 26(2), 150-171.

Hayward, B. W. (1990). Foraminifera in nearshore sediments, Whale island, Bay of Plenty. Tane, 32, 93-99.

Hayward, B. W., Grenfell, H. R., & Scott, D. B. (1999). Tidal range of marsh foraminifera for determining former sea-level heights in New Zealand. New Zealand Journal of Geology and Geophysics, 42(3), 395-413.

He, Z., Li, X., Yang, M., Wang, X., Zhong, C., Duke, N. C., & Shi, S. (2018). Speciation with gene flow via cycles of isolation and migration: insights from multiple mangrove taxa. National Science Review, 6(2), 275-288.

Hearty, P. J., Olson, S. L., Kaufman, D. S., Edwards, R. L., & Cheng, H. (2004). Stratigraphy and geochronology of pitfall accumulations in caves and fissures, Bermuda. Quaternary Science Reviews, 23(9-10), 1151-1171.

Heiri, O., Lotter, A. F., & Lemcke, G. (2001). Loss on ignition as a method for estimating organic and carbonate content in sediments: reproducibility and comparability of results. Journal of paleolimnology, 25(1), 101-110.

Herguera, J. C., & Berger, W. (1991). Paleoproductivity from benthic foraminifera abundance: Glacial to postglacial change in the west-equatorial Pacific. Geology, 19(12), 1173-1176.

Hibbert, F. D., Williams, F. H., Fallon, S. J., & Rohling, E. J. (2018). A database of biological and geomorphological sea-level markers from the Last Glacial Maximum to present. Scientific data, 5.

Holland, S. M. (2012). Sea level change and the area of shallow-marine habitat: implications for marine biodiversity. Paleobiology, 38(2), 205-217.

Holme, N. A. (1961). The bottom fauna of the English Channel. Journal of the Marine Biological Association of the United Kingdom, 41(2), 397-461.

Holsinger, J. R. (1994). Pattern and process in the biogeography of subterranean amphipods. Hydrobiologia, 287(1), 131-145.

Holthuis, L. B. (1973). Caridean shrimps found in land-locked saltwater pools at four Indo-West Pacific localities (Sinai Peninsula, Funafuti Atoll, Maui and Hawaii Islands): with the description of one new genus and four new species. Zoologische Verhandelingen,128, 1-48.

Horton, B. P., & Murray, J. W. (2007). The roles of elevation and salinity as primary controls on living foraminiferal distributions: Cowpen Marsh, Tees Estuary, UK. Marine Micropaleontology, 63(3-4), 169-186.

Horton, B. P., Larcombe, P., Woodroffe, S. A., Whittaker, J. E., Wright, M. R., & Wynn, C. (2003). Contemporary foraminiferal distributions of a mangrove environment, Great Barrier Reef coastline, Australia: implications for sea-level reconstructions. Marine Geology, 198(3-4), 225-243.

Humphreys, W. (1999) Physico-chemical profile and energy fixation in Bundera Sinkhole, an anchialine remiped habitat in north-western Australia. Journal of the Royal Society of Western Australia, 82, 89-98.

Hunter, R. L., Webb, M. S., Iliffe, T. M., & Bremer, J. R. A. (2008). Phylogeny and historical biogeography of the cave-adapted shrimp genus *Typhlatya* (Atyidae) in the Caribbean Sea and western Atlantic. Journal of Biogeography, 35(1), 65-75.

Iliffe, T. M., & Kornicker, L. S. (2009). Worldwide diving discoveries of living fossil animals from the depths of anchialine and marine caves. Smithsonian Contributions to the Marine Sciences, (38).

Iliffe, T. M., Hart, C. W., & Manning, R. B. (1983). Biogeography and the caves of Bermuda. Nature, 302(5904), 141-142.

Iliffe, T. M., Kvitek, R., Blasco, S., Blasco, K., & Covill, R. (2011). Search for Bermuda's deep water caves. Hydrobiologia, 677(1), 157-168.

Iliffe, T. M. (1987). Observations on the biology and geology of anchialine caves. In Proceedings of the 3rd Symposium, Geology of Bahamas, 73-79.

Iliffe, T. M. (1991). Anchialine fauna of the Galápagos Islands. In Galapagos Marine Invertebrates. Springer, Boston, MA., 209-231.

Javaux, E. J., & Scott, D. B. (2003). Illustration of modern benthic foraminifera from Bermuda and remarks on distribution in other subtropical/tropical areas. Palaeontologia electronica, 6(4), 29.

Jorissen, F. J., de Stigter, H. C., & Widmark, J. G. (1995). A conceptual model explaining benthic foraminiferal microhabitats. Marine Micropaleontology, 26(1-4), 3-15.

Jorissen, F. J. (1999). Benthic foraminiferal microhabitats below the sediment-water interface. In Modern foraminifera. Springer, Dordrecht, 161-179.

Juggins, S. (2015). rioja: Analysis of Quaternary science data. R package version (0.8-3).

Jurado-Rivera, J. A., Pons, J., Alvarez, F., Botello, A., Humphreys, W. F., Page, T. J., & Jaume, D. (2017). Phylogenetic evidence that both ancient vicariance and dispersal have contributed to the biogeographic patterns of anchialine cave shrimps. Scientific Reports, 7(1), 2852.

Kaiho, K. (1994). Benthic foraminiferal dissolved-oxygen index and dissolved-oxygen levels in the modern ocean. Geology, 22(8), 719-722.

Kitamura, A., Hiramoto, M., Kase, T., Yamamoto, N., Amemiya, M., & Ohashi, S. (2007). Changes in cavernicolous bivalve assemblages and environments within a submarine cave in the Okinawa Islands during the last 5,000 years. Paleontological Research, 11(2), 163-183.

Klaus, J. S., Lutz, B. P., McNeill, D. F., Budd, A. F., Johnson, K. G., & Ishman, S. E. (2011). Rise and fall of Pliocene free-living corals in the Caribbean. Geology, 39(4), 375-378.

Kornicker, L. S., & Iliffe, T. M. (1989). Ostracoda (Myodocopina, Cladocopina, Halocypridina) from anchialine caves in Bermuda. Smithsonian Contributions Zoology, (470), 1-47.

Kornicker, L. S., & Yager, J. (2002). Description of Spelaeoecia saturno, a new species from an anchialine cave in Cuba, (Crustacea: Ostracoda: Myodocopa: Halocyprididae). Proceedings of the Biological Society of Washington, 115(1), 153-170.

Kovacs, S. E., Reinhardt, E. G., Chatters, J. C., Rissolo, D., Schwarcz, H. P., Collins, S. V., & Erreguerena, P. L. (2017). Calcite raft geochemistry as a hydrological proxy for Holocene aquifer conditions in Hoyo Negro and Ich Balam (Sac Actun Cave System), Quintana Roo, Mexico. Quaternary Science Reviews, 175, 97-111.

Kuhn, G. (1984). Sedimentations-Geschichte der Bermuda North Lagoon im Holozän (Doctoral dissertation, Geologisch-Paläontologisches Institut der Universität).

Kuhnt, T., Schmiedl, G., Ehrmann, W., Hamann, Y., & Hemleben, C. (2007). Deep-sea ecosystem variability of the Aegean Sea during the past 22 kyr as revealed by Benthic Foraminifera. Marine Micropaleontology, 64(3-4), 141-162.

Külköylüoğlu, O., & Vinyard, G. L. (2000). Distribution and ecology of freshwater Ostracoda (Crustacea) collected from springs of Nevada, Idaho, and Oregon: a preliminary study. Western North American Naturalist, 60(3), 6.

Külköylüoğlu, O. (2004). On the usage of ostracods (Crustacea) as bioindicator species in different aquatic habitats in the Bolu region, Turkey. Ecological Indicators, 4(2), 139-147.

Lamb, A. L., Wilson, G. P., & Leng, M. J. (2006). A review of coastal palaeoclimate and relative sea-level reconstructions using δ13C and C/N ratios in organic material. Earth-Science Reviews, 75(1-4), 29-57.

Land, L.S., MacKenzie, F.T., & Gould, S.J. (1967). The Pleistocene history of Bermuda. Geological Society of America Bulletin, 78, 993-1006.

Langer, M. R., & Hottinger, L. (2000). Biogeography of selected" larger" foraminifera. Micropaleontology, 46, 105-126.

Langer, M. R. (1993). Epiphytic foraminifera. Marine Micropaleontology, 20(3-4), 235-265.

Lea, D. W. (2003). Elemental and Isotopic Proxies of Past Ocean Temperatures. Treatise on Geochemistry, 6.

Lee, J. J., Tietjen, J. H., Mastropaolo, C., & Rubin, H. (1977). Food quality and the heterogeneous spatial distribution of meiofauna. Helgoländer Wissenschaftliche Meeresuntersuchungen, 30(1), 272.

Legendre, P., & Legendre, L. (1998). Numerical ecology: developments in environmental modelling. Elsevier, Amsterdam, 63-75.

Legg, D. A., Sutton, M. D., & Edgecombe, G. D. (2013). Arthropod fossil data increase congruence of morphological and molecular phylogenies. Nature Communications, 4, 2485.

León, L. F., Morales, F. M., & Fernández, M. M. (2014). Sea level change as a forcing function of anchialine cave environment's readjustment in the humid tropics of the Gulf of Mexico and the Caribbean. Environmental Research Journal, 8(1).

Leutenegger, S. (1984). Symbiosis in benthic foraminifera; specificity and host adaptations. The Journal of Foraminiferal Research, 14(1), 16-35.

Levinton, J. S., Bianchi, T. S., & Stewart, S. (1984). What is the role of particulate organic matter in benthic invertebrate nutrition? Bulletin of marine science, 35(3), 270-282.

Levinton, J. (1972). Stability and trophic structure in deposit-feeding and suspension-feeding communities. The American Naturalist, 106(950), 472-486.

Li, W. X., Lundberg, J., Dickin, A. P., Ford, D. C., Schwarcz, H. P., McNutt, R., & Williams, D. (1989). High-precision mass-spectrometric uranium-series dating of cave deposits and implications for palaeoclimate studies. Nature, 339(6225), 534.

Lins, L., Guilini, K., Veit-Köhler, G., Hauquier, F., Alves, R. D. S., Esteves, A. M., & Vanreusel, A. (2014). The link between meiofauna and surface productivity in the Southern Ocean. Deep Sea Research Part II: Topical Studies in Oceanography, 108, 60-68.

Lipps JH (1983) Biotic interactions in benthic foraminifera. In: Tevesz MJS, Mc Call PL (eds) Biotic interactions in recent and fossil benthic communities. Plenum Press, New-York, pp 331–373. pmid:17734912

Lisiecki, L. E. (2010). Links between eccentricity forcing and the 100,000-year glacial cycle. Nature geoscience, 3(5), 349.

Little, S. N., & van Hengstum, P. J. (2019). Intertidal and subtidal benthic foraminifera in flooded caves: Implications for reconstructing coastal karst aquifers and cave paleoenvironments. Marine Micropaleontology, 149, 19-34.

Loeblich, A. R., & Tappan, H. (1987). Foraminiferal genera and their classification. Springer.

Loubere, P., & Fariduddin, M. (1999). Benthic foraminifera and the flux of organic carbon to the seabed. In Modern foraminifera, Springer, Dordrecht, 181-199.

Loubere, P. (1996). The surface ocean productivity and bottom water oxygen signals in deep water benthic foraminiferal assemblages. Marine Micropaleontology, 28(3-4), 247-261.

Love, R., Milne, G. A., Tarasov, L., Engelhart, S. E., Hijma, M. P., Latychev, K., & Törnqvist, T. E. (2016). The contribution of glacial isostatic adjustment to projections of sea-level change along the Atlantic and Gulf coasts of North America. Earth's Future, 4(10), 440-464.

Ludt, W. B., & Rocha, L. A. (2015). Shifting seas: the impacts of Pleistocene sea-level fluctuations on the evolution of tropical marine taxa. Journal of Biogeography, 42(1), 25-38.

Lundberg, J., & Ford, D. C. (1994). Late Pleistocene sea level change in the Bahamas from mass spectrometric U-series dating of submerged speleothem. Quaternary Science Reviews, 13(1), 1-14.

Maddocks, R. F., & Iliffe, T. M. (1986). Podocopid ostracoda of Bermudian caves. Stygologia, 2(1-2), 26-76.

Maddocks, R. F., & Iliffe, T. M. (1991). Anchialine podocopid Ostracoda of the Galapagos Islands. Zoological Journal of the Linnean Society, 103(1), 75-99.

Mallon, J., Glock, N., & Schönfeld, J. (2012). The response of benthic foraminifera to low-oxygen conditions of the Peruvian oxygen minimum zone. In Anoxia. Springer, Dordrecht, 305-321.

Martí, R., Uriz, M. J., Ballesteros, E., & Turon, X. (2004). Benthic assemblages in two Mediterranean caves: species diversity and coverage as a function of abiotic parameters and geographic distance. Journal of the Marine Biological Association of the United Kingdom, 84(3), 557-572.

Martin, J. B., Gulley, J., & Spellman, P. (2012). Tidal pumping of water between Bahamian blue holes, aquifers, and the ocean. Journal of Hydrology, 416, 28-38.

Martins, M. V. A., Silva, F., Laut, L. L., Frontalini, F., Clemente, I. M., Miranda, P., & Dias, J. M. A. (2015). Response of benthic foraminifera to organic matter quantity and quality and bioavailable concentrations of metals in Aveiro Lagoon (Portugal). PLoS One, 10(2), e0118077.

Matera, N. J., & Lee, J. J. (1972). Environmental factors affecting the standing crop of foraminifera in sublittoral and psammolittoral communities of a Long Island salt marsh. Marine Biology, 14(2), 89-103.

McCauley, D. J., Pinsky, M. L., Palumbi, S. R., Estes, J. A., Joyce, F. H., & Warner, R. R. (2015). Marine defaunation: Animal loss in the global ocean. Science, 347(6219), 1255641.

McCrone, A. W., & Schafer, C. (1966). Geochemical and sedimentary environments of foraminifera in the Hudson River estuary, New York. Micropaleontology, 505-509.

McIntyre, C. P., Roberts, M.L., Burton, J.R., McNichol, A.P., Burke, A., Robinson, L.F., von Reden, K.F, & Jenkins, W.J. (2011). Rapid radiocarbon (14C) analysis of coral and carbonate samples using a continuous-flow accelerator mass spectrometry system. Paleoceanography, 26, 6.

Mejía-Ortíz, L. M., Yanez, G., & López-Mejía, M. (2007). Echinoderms in an anchialine cave in Mexico. Marine Ecology, 28, 31-34.

Mendes, I., Gonzalez, R., Dias, J. M. A., Lobo, F., & Martins, V. (2004). Factors influencing recent benthic foraminifera distribution on the Guadiana shelf (Southwestern Iberia). Marine Micropaleontology, 51(1-2), 171-192.

Menning, D. M., Wynn, J. G., & Garey, J. R. (2015). Karst estuaries are governed by interactions between inland hydrological conditions and sea level. Journal of Hydrology, 527, 718-733.

Metcalfe, C. D., Beddows, P. A., Bouchot, G. G., Metcalfe, T. L., Li, H., & Van Lavieren, H. (2011). Contaminants in the coastal karst aquifer system along the Caribbean coast of the Yucatan Peninsula, Mexico. Environmental pollution, 159(4), 991-997.

Miller, K. G., Kominz, M. A., Browning, J. V., Wright, J. D., Mountain, G. S., Katz, M. E., & Pekar, S. F. (2005). The Phanerozoic record of global sea-level change. Science, 310(5752), 1293-1298.

Milne, G. A., & Peros, M. (2013). Data–model comparison of Holocene sea-level change in the circum-Caribbean region. Global and Planetary Change, 107, 119-131.

Mojtahid, M., Jorissen, F., Lansard, B., Fontanier, C., Bombled, B., & Rabouille, C. (2009). Spatial distribution of live benthic foraminifera in the Rhône prodelta: Faunal response to a continental–marine organic matter gradient. Marine Micropaleontology, 70(3-4), 177-200.

Moore, W. S. (1999). The subterranean estuary: a reaction zone of ground water and sea water. Marine Chemistry, 65(1-2), 111-125.

Moritsch, M. M., Pakes, M. J., & Lindberg, D. R. (2014). How might sea level change affect arthropod biodiversity in anchialine caves: a comparison of Remipedia and Atyidae taxa (Arthropoda: Altocrustacea). Organisms Diversity & Evolution, 14(2), 225-235.

Muhs, D. R., Budahn, J. R., Prospero, J. M., Skipp, G., & Herwitz, S. R. (2012). Soil genesis on the island of Bermuda in the Quaternary: The importance of African dust transport and deposition. Journal of Geophysical Research: Earth Surface, 117(F3).

Murray, J. W. (1988). Neogene bottom water-masses and benthic foraminifera in the NE Atlantic Ocean. Journal of the Geological Society, 145(1), 125-132.

Murray, J.W. (1991). Ecology and paleoecology of benthic foraminifera. Essex: Longman Scientific & Technical books.

Murray, J. W. (2001). The niche of benthic foraminifera, critical thresholds and proxies. Marine Micropaleontology, 41(1-2), 1-7.

Murray, J. W. (2006). Ecology and applications of benthic foraminifera. Cambridge University Press.

Mylroie, J. E., & Carew, J. L. (1995). Karst development on carbonate islands. D.A Budd, P.M Harris, A Saller (Eds.), Unconformities and Porosity in Carbonate Strata, American Association of Petroleum Geologists. Memoir, 3, 55-76

Mylroie, J. E., Carew, J. L., & Vacher, H. L. (1995). Karst development in the Bahamas and Bermuda. Geological Society of America Special Papers, 300, 251-267.

Navarro-Barranco, C., Guerra-García, J. M., Sánchez-Tocino, L., Jiménez-Prada, P., Cea, S., & García-Gómez, J. C. (2013). Soft-bottom diversity patterns in marine caves; lessons from crustacean community. Journal of experimental marine biology and ecology, 446, 22-28.

Neiber, M. T., Hartke, T. R., Stemme, T., Bergmann, A., Rust, J., Iliffe, T. M., & Koenemann, S. (2011). Global biodiversity and phylogenetic evaluation of Remipedia (Crustacea). PLoS One, 6(5), e19627.

Nepote, E., Bianchi, C. N., Morri, C., Ferrari, M., & Montefalcone, M. (2017). Impact of a harbour construction on the benthic community of two shallow marine caves. Marine Pollution Bulletin, 114(1), 35-45.

Neumann, A. C. (1965). Processes of recent carbonate sedimentation in Harrington Sound, Bermuda. Bulletin of Marine Science, 15(4), 987-1035.

Neumann, A. C. (1971). Quaternary sea-level data from Bermuda. Quaternaria, 14, 41-43.

Odum, W. E. (1988). Comparative ecology of tidal freshwater and salt marshes. Annual review of Ecology and Systematics, 19(1), 147-176.

Ohga, T., & Kitazato, H. (1997). Seasonal changes in bathyal foraminiferal populations in response to the flux of organic matter (Sagami Bay, Japan). Terra Nova, 9(1), 33-37.

Oksanen, J., Blanchet, F. G., Kindt, R., Legendre, P., Minchin, P. R., O'hara, R. B., & Oksanen, M. J. (2013). Package 'vegan'. Community ecology package, version, 2(9).

Olesen, J., Meland, K., Glenner, H., van Hengstum, P. J., & Iliffe, T. M. (2017). *Xibalbanus cozumelensis*, a new species of Remipedia (Crustacea) from Cozumel, Mexico, and a molecular phylogeny of Xibalbanus on the Yucatán Peninsula. European Journal of Taxonomy, 316, 1-27.

Omori, A., Kitamura, A., Fujita, K., Honda, K., & Yamamoto, N. (2010). Reconstruction of light conditions within a submarine cave during the past 7000 years based on the temporal and spatial distribution of algal symbiont-bearing large benthic foraminifers. Palaeogeography, Palaeoclimatology, Palaeoecology, 292(3-4), 443-452.

Orpin, A. R., Haig, D. W., & Woolfe, K. J. (1999). Sedimentary and foraminiferal facies in Exmouth Gulf, in arid tropical northwestern Australia. Australian Journal of Earth Sciences, 46(4), 607-621.

Ozarko, D. L., Patterson, R. T., & Williams, H. F. L. (1997). Marsh Foraminifera from Nanaimo, British Columbia (Canada); implications of infaunal habitat and taphonomic biasing. The Journal of Foraminiferal Research, 27(1), 51-68.

Palmer, A. N., Palmer, M. V., & Queen, J. M. (1977). Geology and origin of the caves of Bermuda. In Proceeding of the 7Th International Speleological Congress, Sheffield, 336-339.

Papadopoulou, A., & Knowles, L. L. (2017). Linking micro- and macroevolutionary perspectives to evaluate the role of Quaternary sea-level oscillations in island diversification. Evolution, 71(12), 2901-2917.

Parravicini, V., Guidetti, P., Morri, C., Montefalcone, M., Donato, M., & Bianchi, C. N. (2010). Consequences of sea water temperature anomalies on a Mediterranean submarine cave ecosystem. Estuarine, Coastal and Shelf Science, 86(2), 276-282.

Patterson, R. T., & Fishbein, E. (1989). Re-examination of the statistical methods used to determine the number of point counts needed for micropaleontological quantitative research. Journal of Paleontology, 63(2), 245-248.

Peltier, W. R. (2004). Global glacial isostasy and the surface of the ice-age Earth: the ICE-5G (VM2) model and GRACE. Annual Review of Earth and Planetary Sciences, 32, 111-149.

Peters, S. E. (2008). Environmental determinants of extinction selectivity in the fossil record. Nature, 454(7204), 626.

Pfannkuche, O. (1993). Benthic response to the sedimentation of particulate organic matter at the BIOTRANS station, 47 N, 20 W. Deep Sea Research Part II: topical studies in oceanography, 40(1-2), 135-149.

Piehler, M. F., & Smyth, A. R. (2011). Habitat-specific distinctions in estuarine denitrification affect both ecosystem function and services. Ecosphere, 2(1), 1-17.

Pimiento, C., Griffin, J. N., Clements, C. F., Silvestro, D., Varela, S., Uhen, M. D., & Jaramillo, C. (2017). The Pliocene marine megafauna extinction and its impact on functional diversity. Nature Ecology & Evolution, 1(8), 1100.

Pirsson, L. V. (1914). Geology of Bermuda Island; the igneous platform. American journal of Science, (225), 189-206.

Pohlman, J. W., Iliffe, T. M., & Cifuentes, L. A. (1997). A stable isotope study of organic cycling and the ecology of an anchialine cave ecosystem. Marine Ecology Progress Series, 155, 17-27.

Porter, M. L. (2007). Subterranean biogeography: what have we learned from molecular techniques. Journal of Cave and Karst Studies, 69(1), 179-186.

Radolović, M., Bakran-Petricioli, T., Petricioli, D., Surić, M., & Perica, D. (2015). Biological response to geochemical and hydrological processes in a shallow submarine cave. Mediterranean Marine Science, 16(2), 305-324.

Rastorgueff, P. A., Harmelin-Vivien, M., Richard, P., & Chevaldonné, P. (2011). Feeding strategies and resource partitioning mitigate the effects of oligotrophy for marine cave mysids. Marine Ecology Progress Series, 440, 163-176.

Rastorgueff, P. A., Bellan-Santini, D., Bianchi, C. N., Bussotti, S., Chevaldonné, P., Guidetti, P., & Ruitton, S. (2015). An ecosystem-based approach to evaluate the ecological quality of Mediterranean undersea caves. Ecological Indicators, 54, 137-152.

Redfield, A. C. (1967). Postglacial change in sea level in the western North Atlantic Ocean. Science, 157(3789), 687-692.

Regier, J. C., Shultz, J. W., Zwick, A., Hussey, A., Ball, B., Wetzer, R., & Cunningham, C. W. (2010). Arthropod relationships revealed by phylogenomic analysis of nuclear protein-coding sequences. Nature, 463(7284), 1079.

Reimer, P. J., Bard, E., Bayliss, A., & Beck, J.W. (2013). IntCal13 and Marine13 radiocarbon age calibration curves 0-50,000 years Cal BP. Radiocarbon, 55, 1869-1887.

Richards, D. A., Smart, P. L., & Edwards, R. L. (1994). Maximum sea levels for the last glacial period from U-series ages of submerged speleothems. Nature, 367(6461), 357.

Riedl, R., & Ozretić, B. (1969). Hydrobiology of marginal caves. Part I. General problems and introduction. Internationale Revue der gesamten Hydrobiologie und Hydrographie, 54(5), 661-683.

Riera, R., Monterroso, Ó., Núñez, J., & Martínez, A. (2018). Distribution of meiofaunal abundances in a marine cave complex with secondary openings and freshwater filtrations. Marine Biodiversity, 48(1), 203-215.

Riveiros, N. V., Babalola, A. O., Boudreau, R. E., Patterson, R. T., Roe, H. M., & Doherty, C. (2007). Modern distribution of salt marsh foraminifera and thecamoebians in the Seymour–Belize Inlet Complex, British Columbia, Canada. Marine Geology, 242(1-3), 39-63.

Rohling, E. J., Foster, G. L., Grant, K. M., Marino, G., Roberts, A. P., Tamisiea, M. E., & Williams, F. (2014). Sea-level and deep-sea-temperature variability over the past 5.3 million years. Nature, 508(7497), 477.

Romano, E., Bergamin, L., Pierfranceschi, G., Provenzani, C., & Marassich, A. (2018). The distribution of benthic foraminifera in Bel Torrente submarine cave (Sardinia, Italy) and their environmental significance. Marine Environmental Research, 133, 114-127.

Ross, C. A. (1972). Biology and ecology of Marginopora vertebralis (Foraminiferida), Great Barrier Reef. The Journal of Protozoology, 19(1), 181-192.

Rosso, A., Sanfilippo, R., Ruggieri, R., Maniscalco, R., & Vertino, A. (2015). Exceptional record of submarine cave communities from the Pleistocene of Sicily (Italy). Lethaia, 48(1), 133-144.

Roy, M., Martin, J. B., Cherrier, J., Cable, J. E., & Smith, C. G. (2010). Influence of sea level rise on iron diagenesis in an east Florida subterranean estuary. Geochimica et Cosmochimica Acta, 74(19), 5560-5573.

Roy, M., Martin, J. B., Cable, J. E., & Smith, C. G. (2013). Variations of iron flux and organic carbon remineralization in a subterranean estuary caused by inter-annual variations in recharge. Geochimica et Cosmochimica Acta, 103, 301-315.

RStudio, 2016. RStudio: integrated Development Environment for R. Boston, MA. Version 1.1.383. In: http://www.rstudio.org/.

Ruiz, F., González-Regalado, M. L., Pendón, J. G., Abad, M., Olías, M., & Muñoz, J. M. (2005). Correlation between foraminifera and sedimentary environments in recent estuaries of southwestern Spain: applications to Holocene reconstructions. Quaternary International, 140, 21-36.

Sanders, H. L. (1968). Marine benthic diversity: a comparative study. The American Naturalist, 102(925), 243-282.

Santoro, A.E., Francis, C.A., de Sieyes, N.R. and Boehm, A.B. (2008) Shifts in the relative abundance of ammonia-oxidizing bacteria and archaea across physicochemical gradients in a subterranean estuary. Environmental Microbiology, 10, 1068-1079.

Santos, I. R. S., Burnett, W. C., Chanton, J., Mwashote, B., Suryaputra, I. G., & Dittmar, T. (2008). Nutrient biogeochemistry in a Gulf of Mexico subterranean estuary and groundwater-derived fluxes to the coastal ocean. Limnology and Oceanography, 53(2), 705-718.

Santos, S. R. (2006). Patterns of genetic connectivity among anchialine habitats: a case study of the endemic Hawaiian shrimp *Halocaridina rubra* on the island of Hawaii. Molecular Ecology, 15(10), 2699-2718.

Sanz, S., & Platvoet, D. (1995). New perspectives on the evolution of the genus *Typhlatya* (Crustacea). Contributions to Zoology, 65, 79-99.

Schmiedl, G., Mackensen, A., & Müller, P. J. (1997). Recent benthic foraminifera from the eastern South Atlantic Ocean: dependence on food supply and water masses. Marine micropaleontology, 32(3-4), 249-287.

Schmiedl, G., Mitschele, A., Beck, S., Emeis, K. C., Hemleben, C., Schulz, H., & Weldeab, S. (2003). Benthic foraminiferal record of ecosystem variability in the eastern Mediterranean Sea during times of sapropel S5 and S6 deposition. Palaeogeography, Palaeoclimatology, Palaeoecology, 190, 139-164.

Schmitter-Soto, J. J., Comín, F. A., Escobar-Briones, E., Herrera-Silveira, J., Alcocer, J., Suárez-Morales, E., & Steinich, B. (2002). Hydrogeochemical and biological characteristics of cenotes in the Yucatan Peninsula (SE Mexico). Hydrobiologia, 467(1-3), 215-228.

Schnitker, D. (1967) Variation in test morphology of *Triloculina linneiana* d'Orbigny in laboratory cultures. Contributions of the Cushman Foundation for Foraminiferal Research, 18, 84-86.

Schönfeld, J., Alve, E., Geslin, E., Jorissen, F., Korsun, S., & Spezzaferri, S. (2012). The FOBIMO (FOraminiferal Bio-MOnitoring) initiative—towards a formalised protocol for benthic foraminiferal monitoring studies. Marine Micropaleontology, (94–95), 1–13.

Schönfeld, J. (2002). A new benthic foraminiferal proxy for near-bottom current velocities in the Gulf of Cadiz, northeastern Atlantic Ocean. Deep Sea Research Part I: Oceanographic Research Papers, 49(10), 1853-1875.

Schwentner, M., Combosch, D. J., Nelson, J. P., & Giribet, G. (2017). A phylogenomic solution to the origin of insects by resolving crustacean-hexapod relationships. Current Biology, 27(12), 1818-1824.

Scott, D. B., & Hermelin, J. O. R. (1993). A device for precision splitting of micropaleontological samples in liquid suspension. Journal of Paleontology, 67(1), 151-154.

Scott, D. S., & Medioli, F. S. (1978). Vertical zonations of marsh foraminifera as accurate indicators of former sea-levels. Nature, 272(5653), 528.

Scott, D. B., Schnack, E. J., Ferrero, L., Espinosa, M., & Barbosa, C. F. (1990). Recent marsh foraminifera from the east coast of South America: comparison to the northern hemisphere. In Paleoecology, Biostratigraphy, Paleoceanography and Taxonomy of Agglutinated Foraminifera. Springer, Dordrecht, 717-737.

Scottt, D. B., Collinst, E. S., Dugganf, J., Asioli, A., Saito, T., & Hasegawa, S. (1996). Pacific Rim marsh foraminiferal distributions: implications for sea-level studies. Journal of Coastal Research, 850-861.

Scott, D. B. (1976). Brackish-water foraminifera from southern California and description of *Polysaccammina ipohalina* n. gen., n. sp. The Journal of Foraminiferal Research, 6(4), 312-321.

Seiglie, G. A. (1968). Foraminiferal assemblages as indicators of high organic carbon content in sediments and of polluted waters. AAPG Bulletin, 52(11), 2231-2241.

Sen Gupta, B. K. & Machain-Castillo, M. L. (1993). Benthic foraminifera in oxygen-poor habitats. Marine Micropaleontology, 20(3-4), 183-201.

Sen Gupta B.K. (1999) Foraminifera in marginal marine environments. In: Modern Foraminifera. Springer, Dordrecht

Setty, M. G., & Nigam, R. (1982). Foraminiferal assemblages and organic carbon relationship in benthic marine ecosystem of western Indian continental shelf. Indian Journal of Marine Sciences, 11, 225-232.

Shinn, E. A., Reich, C. D., Locker, S. D., & Hine, A. C. (1996). A giant sediment trap in the Florida Keys. Journal of Coastal Research, 953-959.

Sket, B., & Iliffe, T. M. (1980). Cave fauna of Bermuda. Internationale Revue der gesamten Hydrobiologie und Hydrographie, 65(6), 871-882.

Smart, C. W., King, S. C., Gooday, A. J., Murray, J. W., & Thomas, E. (1994). A benthic foraminiferal proxy of pulsed organic matter paleofluxes. Marine Micropaleontology, 23(2), 89-99.

Sobczak, W. V., Cloern, J. E., Jassby, A. D., & Müller-Solger, A. B. (2002). Bioavailability of organic matter in a highly disturbed estuary: The role of detrital and algal resources. Proceedings of the National Academy of Sciences, 99(12), 8101-8105.

Sperazza, M., Moore, J. N., & Hendrix, M. S. (2004). High-resolution particle size analysis of naturally occurring very fine-grained sediment through laser diffractometry. Journal of Sedimentary Research, 74(5), 736-743.

Spiteri, C., Regnier, P., Slomp, C. P., & Charette, M. A. (2006). pH-Dependent iron oxide precipitation in a subterranean estuary. Journal of Geochemical Exploration, 88(1-3), 399-403.

Steadman, D. W., Franz, R., Morgan, G. S., Albury, N. A., Kakuk, B., Broad, K., & Jarzen, D. M. (2007). Exceptionally well preserved late Quaternary plant and vertebrate fossils from a blue hole on Abaco, The Bahamas. Proceedings of the National Academy of Sciences, 104(50), 19897-19902.

Steinthorsdottir, M., & Håkansson, E. (2017). Endo-and epilithic faunal succession in a Pliocene–Pleistocene cave on Rhodes, Greece: record of a transgression. Palaeontology, 60(5), 663-681.

Stock, J.H., Iliffe, T.M. & Williams, D. (1986). The concept anchialine reconsidered. Stygologia, 2, 90-92.

Stock, J.H. (1980). Regression model evolution as exemplified by the genus *Pseudoniphargus* (Amphipoda). Bijdragen tot de Dierkunde, 50, 105-144.

Stoffer, J. L. (2013). A Hydrological Model of Harrington Sound, Bermuda and its Surrounding Cave Systems. Doctoral dissertation. Texas A&M University at Galveston.

Suárez-Morales, E., Reid, J. W., Fiers, F., & Iliffe, T. M. (2004). Historical biogeography and distribution of the freshwater cyclopine copepods (Copepoda, Cyclopoida, Cyclopinae) of the Yucatan Peninsula, Mexico. Journal of Biogeography, 31(7), 1051-1063.

Suhr, S. B., Pond, D. W., Gooday, A. J., & Smith, C. R. (2003). Selective feeding by benthic foraminifera on phytodetritus on the western Antarctic Peninsula shelf: evidence from fatty acid biomarker analysis. Marine Ecology Progress Series, 262, 153-162.

Surić, M., Juračić, M., Horvatinčić, N., & Bronić, I. K. (2005). Late Pleistocene–Holocene sea-level rise and the pattern of coastal karst inundation: records from submerged speleothems along the Eastern Adriatic Coast (Croatia). Marine Geology, 214(1-3), 163-175.

Tarasov, L., Dyke, A. S., Neal, R. M., & Peltier, W. R. (2012). A data-calibrated distribution of deglacial chronologies for the North American ice complex from glaciological modeling. Earth and Planetary Science Letters, 315, 30-40.

Thomas, E., & Varekamp, J. C. (1991). Paleo-environmental analyses of marsh sequences (Clinton, Connecticut): evidence for punctuated rise in relative sea level during the latest Holocene. Journal of Coastal Research, 125-158.

Thornton, S. F., & McManus, J. (1994). Application of organic carbon and nitrogen stable isotope and C/N ratios as source indicators of organic matter provenance in estuarine systems: evidence from the Tay Estuary, Scotland. Estuarine, Coastal and Shelf Science, 38(3), 219-233.

Trezzi, G., Garcia-Orellana, J., Rodellas, V., Santos-Echeandia, J., Tovar-Sánchez, A., Garcia-Solsona, E., & Masqué, P. (2016). Submarine groundwater discharge: a significant source of dissolved trace metals to the North Western Mediterranean Sea. Marine Chemistry, 186, 90-100.

Vacher, H. L., & Wallis, T. N. (1992). Comparative hydrogeology of fresh-water lenses of Bermuda and Great Exuma Island, Bahamas. Groundwater, 30(1), 15-20.

Vacher, H. L., Rowe, M. P., & Quinn, T. (1997). Geology and hydrogeology of Bermuda. In Geology and hydrogeology of carbonate islands. Elsevier, Amsterdam, 54, 35-90.

Valentine, J. W., & Jablonski, D. (1991). Biotic effects of sea level change: the Pleistocene test. Journal of Geophysical Research: Solid Earth, 96(B4), 6873-6878.

van Hengstum, P. J., & Scott, D. B. (2011). Ecology of foraminifera and habitat variability in an underwater cave: distinguishing anchialine versus submarine cave environments. The Journal of Foraminiferal Research, 41(3), 201-229.

van Hengstum, P. J., & Scott, D. B. (2012). Sea-level rise and coastal circulation controlled Holocene groundwater development in Bermuda and caused a meteoric lens to collapse 1600 years ago. Marine Micropaleontology, 90, 29-43.

van Hengstum, P. J., Reinhardt, E. G., Beddows, P. A., Huang, R. J., & Gabriel, J. J. (2008). Thecamoebians (testate amoebae) and foraminifera from three anchialine cenotes in Mexico: Low salinity (1.5–4.5 psu) faunal transitions. The Journal of Foraminiferal Research, 38(4), 305-317.

van Hengstum, P. J., Scott, D. B., & Javaux, E. J. (2009). Foraminifera in elevated Bermudian caves provide further evidence for+ 21 m eustatic sea level during Marine Isotope Stage 11. Quaternary Science Reviews, 28(19-20), 1850-1860.

van Hengstum, P. J., Reinhardt, E. G., Beddows, P. A., & Gabriel, J. J. (2010). Linkages between Holocene paleoclimate and paleohydrogeology preserved in a Yucatan underwater cave. Quaternary Science Reviews, 29(19-20), 2788-2798.

van Hengstum, P. J., Scott, D. B., Gröcke, D. R., & Charette, M. A. (2011). Sea level controls sedimentation and environments in coastal caves and sinkholes. Marine Geology, 286(1-4), 35-50.

van Hengstum, P. J., Donnelly, J. P., Kingston, A. W., Williams, B. E., Scott, D. B., Reinhardt, E. G., & Patterson, W. P. (2015). Low-frequency storminess signal at Bermuda linked to cooling events in the North Atlantic region. Paleoceanography, 30(2), 52-76.

van Hengstum, P. J., Donnelly, J. P., Fall, P. L., Toomey, M. R., Albury, N. A., & Kakuk, B. (2016). The intertropical convergence zone modulates intense hurricane strikes on the western North Atlantic margin. Scientific Reports, 6, 21728.

Vollbrecht, R. D. (1996). Postglazialer Anstieg des Meeresspiegels, paläoklima und hydrographie, aufgezeichnet in sedimenten der Bermuda inshore waters.

Waelbroeck, C., Labeyrie, L., Michel, E., Duplessy, J. C., McManus, J. F., Lambeck, K., & Labracherie, M. (2002). Sea-level and deep water temperature changes derived from benthic foraminifera isotopic records. Quaternary Science Reviews, 21(1-3), 295-305.

Walker, L. R., & Del Moral, R. (2003). Primary succession and ecosystem rehabilitation. Cambridge University Press.

Weigelt, P., Steinbauer, M. J., Cabral, J. S., & Kreft, H. (2016). Late Quaternary climate change shapes island biodiversity. Nature, 532(7597), 99.

Whitaker, F. F., & Smart, P. L. (1990). Active circulation of saline ground waters in carbonate platforms: Evidence from the Great Bahama Bank. Geology, 18(3), 200-203.

Whitaker, D., & Christman, M. (2014). clustsig: Significant Cluster Analysis. R package version, 1.

White, W. B. (2007). Cave sediments and paleoclimate. Journal of Cave and Karst studies, 69(1), 76-93.

Williams, R. H., McGee, D., Kinsley, C. W., Ridley, D. A., Hu, S., Fedorov, A., & deMenocal, P. B. (2016). Glacial to Holocene changes in trans-Atlantic Saharan dust transport and dust-climate feedbacks. Science Advances, 2(11), e1600445.

Yager, J. (1981). Remipedia, a new class of Crustacea from a marine cave in the Bahamas. Journal of Crustacean Biology, 328-333.

Yager, J. (2013). *Speleonectes cokei*, new species of Remipedia (Crustacea: Speleonectidae) from a submerged ocean cave near Caye Chapel, Belize. Zootaxa, 3710(4), 354-362.

Yamamoto, N., Kitamura, A., Ohmori, A., Morishima, Y., Toyofuku, T., & Ohashi, S. (2009). Long-term changes in sediment type and cavernicolous bivalve assemblages in Daidokutsu submarine cave, Okinawa Islands: evidence from a new core extending over the past 7,000 years. Coral Reefs, 28(4), 967-976.

Yılmaz, F., & Külköylüoğlu, O. (2006). Tolerance, optimum ranges, and ecological requirements of freshwater Ostracoda (Crustacea) in Lake Aladağ (Bolu, Turkey). Ecological Research, 21(2), 165-173.

Zabala, M., Riera, T., Gili, J. M., Barange, M., Lobo, A., & Peñuelas, J. (1989). Water flow, trophic depletion, and benthic macrofauna impoverishment in a submarine cave from the Western Mediterranean. Marine Ecology, 10(3), 271-287.

APPENDIX A

BERMUDA SEA-LEVEL POINTS

Index No.	Sample Identification Code	General Locaiton in Bermuda	Lab number	Original Source	Origin of GPS Position Information	Depth of sample (mbsl)	Latitude	Longitude	Material dated	Specified Environmental Indicator	SL Indicator Type (This Work)	Conventional ^{14}C age	Conventional	error	$\delta^{13}C_{org}$	Calibration Curve	1s Minimum, Calibrated yrs. BP_{1950}	1s Maximum, Calibrated yrs. BP_{1950}	Probability	2s Minimum, Calibrated yrs. BP_{1950}	2s Maximum, Calibrated yrs. BP_{1950}	Probability	Highest Probability 1s Midpoint	Highest Probability 1s Uncertainty	Highest Probability 2s Midpoint	Highest Probability 2s Uncertainty
1	ACN #D12	Devonshire Marsh	ML 559	Neumann (1971)	Not specified in Vollbrecht (1996), so a central position in Devonshire Marsh estimated from Google Earth	3.4	32.307686	-64.755452	freshwater peat	No data	terrestrial limiting	3815 ±95	3815	95	N/A	IntCal13	4089	4300	0.783	3962	4440	0.98	4194.5	105.5	4201	239
2	ACN #D9	Devonshire Marsh	ML 556	Neumann (1971)	Not specified in Vollbrecht (1996), so a central position in Devonshire Marsh estimated from Google Earth	5.8	32.307686	-64.755452	freshwater peat	No data	terrestrial limiting	4585 ±100	4585	100	N/A	IntCal13	5053	5189	0.412	4967	5487	0.943	5121	68	5227	260
3	ACN #D11	Devonshire Marsh	ML 555	Neumann (1971)	Not specified in Vollbrecht (1996), so a central position in Devonshire Marsh estimated from Google Earth	7.4	32.307686	-64.755452	freshwater peat	No data	terrestrial limiting	5070 ±100	5070	100	N/A	IntCal13	5713	5917	0.976	5594	6002	0.999	5815	102	5798	204
4	ACN #D1	Devonshire Marsh	ML 553	Neumann (1971)	Not specified in Vollbrecht (1996), so a central position in Devonshire Marsh estimated from Google Earth	8.9	32.307686	-64.755452	freshwater peat	No data	terrestrial limiting	6000 ±110	6000	110	N/A	IntCal13	6716	6980	0.959	6618	7164	0.989	6848	132	6891	273
5	ACN #D5	Devonshire Marsh	Ml 552	Neumann (1971)	Not specified in Vollbrecht (1996), so a central position in Devonshire Marsh estimated from Google Earth	10.7	32.307686	-64.755452	freshwater peat	No data	terrestrial limiting	6510 ±110	6510	110	N/A	IntCal13	7316	7508	0.981	7242	7591	0.986	7412	96	7416.5	174.5
6	ACN #D4	Devonshire Marsh	ML 550	Neumann (1971)	Not specified in Vollbrecht (1996), so a central position in Devonshire Marsh estimated from Google Earth	12.5	32.307686	-64.755452	freshwater peat	No data	terrestrial limiting	6970 ±120	6970	120	N/A	IntCal13	7690	7874	0.848	7594	8000	1	7782	92	7797	203
7	GS 01: 1.22-1.28	Great Sound	KI-1997	Vollbrecht (1996)	Estimated from Appendix in Vollbrect (1996)	12.6	32.296135	-64.830826	freshwater peat	No data	terrestrial limiting	7250 ±90	7250	90	-27.2	IntCal13	7997	8165	1	7929	8218	0.946	8081	84	8073.5	144.5
8	GS 02: 5.94-6.01	Great Sound	KI-1998	Vollbrecht (1996)	Estimated from Appendix in Vollbrect (1996)	27.1	32.280491	-64.846911	freshwater peat	No data	terrestrial limiting	9150 ±210	9150	210	-27.9	IntCal13	10132	10605	0.861	9677	10823	0.967	10368.5	236.5	10250	573
9	ACN #HS	Harrington Sound	ML 69-2A	Vollbrecht (1996)	Not specified in Vollbrecht (1996), so a central position in Harrington Sound estimated from Google Earth	4.4	32.33217	-64.719905	freshwater peat	No data	terrestrial limiting	4994 ±80	4994	80	N/A	IntCal13	5644	5761	0.658	5601	5903	1	5702.5	58.5	5752	151
10	ACN #HS	Harrington Sound	ML 69-3A	Vollbrecht (1996)	Not specified in Vollbrecht (1996), so a central position in Harrington Sound estimated from Google Earth	4.7	32.33217	-64.719905	freshwater peat	No data	terrestrial limiting	4760 ±100	4760	100	N/A	IntCal13	5447	5593	0.742	5293	5719	1	5520	73	5506	213

11	HS-TB 02/2: 1.35-1.4	Harrington Sound	KI-2045.02	Vollbrecht (1996)	Estimated from Appendix in Vollbrect (1996)	4.7	32.32442222	-64.7398861	freshwater peat	No data	terrestrial limiting	3830 ±95	3830	95	-26.4	IntCal13	4146	4359	0.801	3971	4446	0.975	4252.5	106.5	4208.5	237.5
12	HS-TI: 1.8-1.85	Harrington Sound	KI-2117.02	Vollbrecht (1996)	Estimated from Appendix in Vollbrect (1996)	5.5	32.33430556	-64.7260472	freshwater peat	No data	terrestrial limiting	4990 ±65	4990	65	-29	IntCal13	5646	5755	0.722	5606	5798	0.712	5700.5	54.5	5702	96
13	ACN #HS	Harrington Sound	ML-69-13A	Vollbrecht (1996)	Not specified in Vollbrecht (1996), so a central position in Harrington Sound estimated from Google Earth	5.6	32.33217	-64.719905	freshwater peat	No data	terrestrial limiting	4787 ±105	4787	105	N/A	IntCal13	5447	5608	0.776	5298	5745	1	5527.5	80.5	5521.5	223.5
14	HS-TB/1: 0.85-0.90	Harrington Sound	KI-2044	Vollbrecht (1996)	Estimated from Appendix in Vollbrect (1996)	7	32.32479444	-64.7376861	freshwater peat	No data	terrestrial limiting	5800 ±80	5800	80	-27.7	IntCal13	6493	6677	0.996	6413	6757	0.984	6585	92	6585	172
15	ACN #HS	Harrington Sound	ML 69-12A	Vollbrecht (1996)	Not specified in Vollbrecht (1996), so a central position in Harrington Sound estimated from Google Earth	7.6	32.33217	-64.719905	freshwater peat	No data	terrestrial limiting	5829 ±110	5829	110	N/A	IntCal13	6494	6749	0.992	6399	6911	1	6621.5	127.5	6655	256
16	ACN #HS	Harrington Sound	ML 69-16A	Vollbrecht (1996)	Not specified in Vollbrecht (1996), so a central position in Harrington Sound estimated from Google Earth	9.4	32.33217	-64.719905	freshwater peat	No data	terrestrial limiting	6785 ±120	6785	120	N/A	IntCal13	7560	7748	0.914	7435	7853	0.994	7654	94	7644	209
17	ACN #HS	Harrington Sound	ML 69-17B	Vollbrecht (1996)	Not specified in Vollbrecht (1996), so a central position in Harrington Sound estimated from Google Earth	11.2	32.33217	-64.719905	freshwater peat	No data	terrestrial limiting	6800 ±120	6800	120	N/A	IntCal13	7565	7763	0.942	7458	7866	0.981	7664	99	7662	204
18	ACN #HS	Harrington Sound	ML 69-17A	Vollbrecht (1996)	Not specified in Vollbrecht (1996), so a central position in Harrington Sound estimated from Google Earth	11.4	32.33217	-64.719905	freshwater peat	No data	terrestrial limiting	7221 ±110	7221	110	N/A	IntCal13	7957	8164	1	7838	8223	0.947	8060.5	103.5	8030.5	192.5
19	HS-PH/2: 3.45-3.5	Harrington Sound	KI-3408	Vollbrecht (1996)	Estimated from Appendix in Vollbrect (1996)	12.3	32.33470278	-64.731125	freshwater peat	No data	terrestrial limiting	6850 ±100	6850	100	-28.9	IntCal13	7605	7787	0.987	7562	7873	0.95	7696	91	7717.5	155.5
20	ACN #HS	Harrington Sound	ML 69-18C	Vollbrecht (1996)	Not specified in Vollbrecht (1996), so a central position in Harrington Sound estimated from Google Earth	13	32.33217	-64.719905	freshwater peat	No data	terrestrial limiting	7280 ±100	7280	100	N/A	IntCal13	7996	8184	0.986	7938	8327	1	8090	94	8132.5	194.5
21	ACN #HS	Harrington Sound	ML 69-18A	Vollbrecht (1996)	Not specified in Vollbrecht (1996), so a central position in Harrington Sound estimated from Google Earth	13.2	32.33217	-64.719905	freshwater peat	No data	terrestrial limiting	7360 ±160	7360	160	N/A	IntCal13	8027	8328	1	7915	8453	0.979	8177.5	150.5	8184	269
22	8450ACN #HS	Harrington Sound	ML 69-19A	Vollbrecht (1996)	Not specified in Vollbrecht (1996), so a central position in Harrington Sound estimated from Google Earth	15.1	32.33217	-64.719905	freshwater peat	No data	terrestrial limiting	7709 ±140	7709	140	N/A	IntCal13	8360	8649	0.99	8294	8810	0.896	8504.5	144.5	8552	258
23	ACN #HS	Harrington Sound	ML 69-20A	Vollbrecht (1996)	Not specified in Vollbrecht (1996), so a central position in Harrington Sound estimated from Google Earth	17.3	32.33217	-64.719905	freshwater peat	No data	terrestrial limiting	7400 ±135	7400	135	N/A	IntCal13	8153	8360	0.817	7956	8429	1	8256.5	103.5	8192.5	236.5
24	ACN #HS	Harrington Sound	ML 69-15A	Vollbrecht (1996)	Not specified in Vollbrecht (1996), so a central position in Harrington Sound estimated from Google Earth	17.4	32.33217	-64.719905	freshwater peat	No data	terrestrial limiting	7880 ±100	7880	100	N/A	IntCal13	8584	8789	0.72	8510	8999	0.977	8686.5	102.5	8754.5	244.5

25	ACN #HS	Harrington Sound	ML 69-22A	Vollbrecht (1996)	Not specified in Vollbrecht (1996), so a central position in Harrington Sound estimated from Google Earth	17.9	32.33217	-64.719905	freshwater peat	No data	terrestrial limiting	8833 ±140	8833	140	N/A	IntCal13	9731	9965	0.565	9552	10208	1	9848	117	9880	328
26	ACN #HS	Harrington Sound	ML 69-27B	Vollbrecht (1996)	Not specified in Vollbrecht (1996), so a central position in Harrington Sound estimated from Google Earth	18.3	32.33217	-64.719905	freshwater peat	No data	terrestrial limiting	8030 ±140	8030	140	N/A	IntCal13	8648	9033	0.943	8544	9305	0.997	8840.5	192.5	8924.5	380.5
27	ACN #HS	Harrington Sound	ML 69-27A	Vollbrecht (1996)	Not specified in Vollbrecht (1996), so a central position in Harrington Sound estimated from Google Earth	18.6	32.33217	-64.719905	freshwater peat	No data	terrestrial limiting	8785 ±140	8785	140	N/A	IntCal13	9599	9939	0.827	9541	10189	1	9769	170	9865	324
28	ACN #HS	Harrington Sound	ML 69-24A	Vollbrecht (1996)	Not specified in Vollbrecht (1996), so a central position in Harrington Sound estimated from Google Earth	19.2	32.33217	-64.719905	freshwater peat	No data	terrestrial limiting	8195 ±100	8195	100	N/A	IntCal13	9021	9282	1	8974	9463	0.977	9151.5	130.5	9218.5	244.5
29	HS-MR 05/2: 0.8-0.85	Harrington Sound	KI-2121	Vollbrecht (1996)	Estimated from Appendix in Vollbrect (1996)	19.8	32.33066667	-64.7186028	freshwater peat	No data	terrestrial limiting	8900 ±160	8900	160	-27.9	IntCal13	9767	10204	1	9543	10299	0.989	9985.5	218.5	9921	378
30	HS-MLB 02/2:2.2-2.26	Harrington Sound	KI-2120	Vollbrecht (1996)	Estimated from Appendix in Vollbrect (1996)	19.9	32.33863611	-64.7267861	freshwater peat	No data	terrestrial limiting	8760 ±125	8760	125	-30.1	IntCal13	9556	9918	0.954	9541	10164	1	9737	181	9852.5	311.5
31	HS-MR 08: 1.8-1.85	Harrington Sound	KI-2111.01	Vollbrecht (1996)	Estimated from Appendix in Vollbrect (1996)	20.3	32.33463333	-64.7132611	freshwater peat	No data	terrestrial limiting	8900 ±100	8900	100	-28.3	IntCal13	9887	10195	0.978	9679	10235	1	10041	154	9957	278
32	Unlabeled	Harrington Sound	ML-186	Redfield (1967)	Given the Depth, Devil's Hole in Harrington Sound is the assumed position	20.7	32.323903	-64.719874	freshwater peat	No data	terrestrial limiting	9145 ±150	9145	150	N/A	IntCal13	10182	10523	0.965	9887	10727	0.996	10352.5	170.5	10307	420
33	HS-CB 03: 2.59-2.64	Harrington Sound	KI-2119	Vollbrecht (1996)	Estimated from Appendix in Vollbrect (1996)	21.6	32.33749167	-64.7192389	freshwater peat	No data	terrestrial limiting	8800 ±100	8800	100	-28.5	IntCal13	9672	9945	0.769	9579	10161	0.985	9808.5	136.5	9870	291
34	HS-CD 02: 3.45-3.5	Harrington Sound	KI-2118	Vollbrecht (1996)	Estimated from Appendix in Vollbrect (1996)	21.9	32.33795833	-64.7078139	freshwater peat	No data	terrestrial limiting	9410 ±170	9410	170	-28	IntCal13	10414	10813	0.784	10253	11148	1	10613.5	199.5	10700.5	447.5
35	HS-CB 05/2: 3.75-3.80	Harrington Sound	KI-3932.38	Vollbrecht (1996)	Estimated from Appendix in Vollbrect (1996)	22.2	32.34195833	-64.7139389	freshwater peat	No data	terrestrial limiting	9370 ±95	9370	95	-28.7	IntCal13	10484	10725	0.921	10266	10796	0.947	10604.5	120.5	10531	265
36	HS-MR 07: 1.24-1.29	Harrington Sound	KI-2113	Vollbrecht (1996)	Estimated from Appendix in Vollbrect (1996)	22.3	32.33019722	-64.7206167	freshwater peat	No data	terrestrial limiting	9440 ±110	9440	110	-28.2	IntCal13	10514	10794	0.803	10398	11135	1	10654	140	10766.5	368.5
37	HS-SP 01: 392-3.98	Harrington Sound	KI-1800.03	Vollbrecht (1996)	Estimated from Appendix in Vollbrect (1996)	23	32.333575	-64.7119722	freshwater peat	No data	terrestrial limiting	9940 ±170	9940	170	-25.4	IntCal13	11208	11722	0.979	11068	12082	0.968	11465	257	11575	507
38	HS-PT 02: 1.10-1.15	Harrington Sound	KI-2112	Vollbrecht (1996)	Estimated from Appendix in Vollbrect (1996)	23.2	32.32978056	-64.7185528	freshwater peat	No data	terrestrial limiting	9150 ±165	9150	165	-28.2	IntCal13	10167	10579	1	9769	10752	1	10373	206	10260.5	491.5
39	HS-PT 01: 1.71-1.76	Harrington Sound	KI-1733.01	Vollbrecht (1996)	Estimated from Appendix in Vollbrect (1996)	23.2	32.32978056	-64.7185528	freshwater peat	No data	terrestrial limiting	9640 ±95	9640	95	-27.3	IntCal13	10793	10965	0.552	10720	11219	1	10879	86	10969.5	249.5
40	ACN #HS 78ft	Harrington Sound	ML 526	Vollbrecht (1996)	Not specified in Vollbrecht (1996), so a central position in Harrington Sound estimated from Google Earth	23.8	32.33217	-64.719905	freshwater peat	No data	terrestrial limiting	9180 ±140	9180	140	N/A	IntCal13	10223	10521	0.974	10116	10731	0.951	10372	149	10423.5	307.5

41	HS-GP (24.3): 2.39-2.43	Harrington Sound	KI-1732.01	Vollbrecht (1996)	Estimated from Appendix in Vollbrect (1996)	23.9	32.32819444	-64.7231194	freshwater peat	No data	terrestrial limiting	9020 ±115	9020	115	-25.3	IntCal13	10113	10275	0.556	9761	10437	0.981	10194	81	10099	338
42	HS-GP (01.4): 3.25-3.3	Harrington Sound	KI-1732.02	Vollbrecht (1996)	Estimated from Appendix in Vollbrect (1996)	24.8	32.32819444	-64.7231194	freshwater peat	No data	terrestrial limiting	9720 ±100	9720	100	-26.3	IntCal13	11070	11243	0.71	10742	11292	0.997	11156.5	86.5	11017	275
43	HS-CS/1: 2.85-2.90	Harrington Sound	KI-2114	Vollbrecht (1996)	Estimated from Appendix in Vollbrect (1996)	24.8	32.33146111	-64.7218556	freshwater peat	No data	terrestrial limiting	9450 ±170	9450	170	-29.5	IntCal13	10505	10879	0.735	10287	11180	1	10692	187	10733.5	446.5
44	HS-CD 01: 4.15-4.20	Harrington Sound	KI-2116	Vollbrecht (1996)	Estimated from Appendix in Vollbrect (1996)	24.8	32.337525	-64.7078806	freshwater peat	No data	terrestrial limiting	10130 ±90	10130	90	-29.4	IntCal13	11604	11988	0.952	11340	12076	1	11796	192	11708	368
45	HS-SP 04: 5.72-5.75	Harrington Sound	Beta-88712	Vollbrecht (1996)	Estimated from Appendix in Vollbrect (1996)	26.8	32.32954167	-64.7174306	freshwater peat	No data	terrestrial limiting	9730 ±60	9730	60	-29.3	IntCal13	11108	11227	1	11068	11251	0.841	11167.5	59.5	11159.5	91.5
46	HS-SP 03: 5.78-5.82	Harrington Sound	KI-2172	Vollbrecht (1996)	Estimated from Appendix in Vollbrect (1996)	27	32.32919722	-64.7168528	freshwater peat	No data	terrestrial limiting	9750 ±120	9750	120	-29.1	IntCal13	11067	11274	0.684	10713	11409	0.975	11170.5	103.5	11061	348
47	HS-PB 01: 6.75-6.78	Harrington Sound	KI-2171	Vollbrecht (1996)	Estimated from Appendix in Vollbrect (1996)	27.3	32.32768333	-64.7276944	freshwater peat	No data	terrestrial limiting	10110 ±110	10110	110	-29	IntCal13	11596	11845	0.567	11271	12081	1	11720.5	124.5	11676	405
48	ACN #ML1	Mangrove Lake	ML 557	Vollbrecht (1996)	Estimate of Position from Google Earth	5	32.325734	-64.708029	freshwater peat	fern-sedge peat (Vollbrecht, 1996, Table 2)	terrestrial limiting	4120 ±100	4120	100	N/A	IntCal13	4527	4727	0.751	4408	4865	1	4627	100	4636.5	228.5
49	Unlabeled	Mangrove Lake	Unlabeled	Watts and Hansen (1986)	Estimate of position based on description in paper and Google Earth	18	32.325827	-64.707423	freshwater peat	pollen, *Typha latifolia* (See Watts and Hanson, 1986)	terrestrial limiting	9260 ± 200	9260	200	N/A	IntCal13	10218	10730	1	10113	11129	0.949	10474	256	10621	508
50	ACN #P1	Pembroke Marsh	ML 547	Vollbrecht (1996)	Not specified in Vollbrecht (1996), so a central position in Pembroke Marsh estimated from Google Earth	14.5	32.301239	-64.782209	freshwater peat	Sedge Rootlets (Vollbrecht, 1996, Table 2)	terrestrial limiting	7630 ±120	7630	120	N/A	IntCal13	8336	8559	1	8175	8654	0.992	8447.5	111.5	8414.5	239.5
51	ACN #P2	Pembroke Marsh	ML 546	Vollbrecht (1996)	Not specified in Vollbrecht (1996), so a central position in Pembroke Marsh estimated from Google Earth	16.9	32.301239	-64.782209	freshwater peat	Sedge Rootlets (Vollbrecht, 1996, Table 2)	terrestrial limiting	8530 ±130	8530	130	N/A	IntCal13	9403	9685	0.975	9234	9906	0.982	9544	141	9570	336
52	PR o3/2: 5.46-5.49	Port Royal Bay	KI-2000	Vollbrecht (1996)	Estimated from Appendix in Vollbrect (1996)	20.8	32.26416	-64.855092	freshwater peat	No data	terrestrial limiting	8890 ±70	8890	70	-27.9	IntCal13	9911	10165	1	9736	10201	1	10038	127	9968.5	232.5
53	Unlabeled	Port Royal Bay	Unlabeled	Ashmore and Leatherman (1984)	Estimated using Google Earth and Fig 1 in MG paper	25.2	32.261899	-64.853756	freshwater peat	Fern (*Osmunda*), and sedge (Ashmore and Leatherman, 1984)	terrestrial limiting	9590 ±100	9552	89	N/A	IntCal13	10772	11102	1	10659	11202	0.998	10937	165	10930.5	271.5
54	PR 01/1, 4.07-4.1	Port Royal Bay	KI-1999	Vollbrecht (1996)	Estimated from Appendix in Vollbrect (1996)	26.7	32.262654	-64.856715	freshwater peat	No data	terrestrial limiting	9400 ±85	9400	85	-28.8	IntCal13	10508	10742	1	10383	10869	0.914	10625	117	10626	243
55	Unlabeled	Shelly Bay, North Shore	I-1683	Redfield 1967	Estimated using Google Earth	1.7	32.331638	-64.742539	freshwater peat	No data	terrestrial limiting	1850 ±110	1850	110	N/A	IntCal13	1690	1897	0.855	1532	2013	0.99	1793.5	103.5	1772.5	240.5
56	Unlabeled	Shelly Bay, North Shore	I-1684	Redfield 1967	Estimated using Google Earth	2.3	32.331638	-64.742539	freshwater peat	No data	terrestrial limiting	1820 ±120	1820	120	N/A	IntCal13	1609	1880	1	1516	2006	0.97	1744.5	135.5	1761	245
57	ACN #FR	St. George's Harbour	ML 549	Vollbrecht (1996)	Not specified in Vollbrecht (1996), so a central position in St Georges' Harbour estimated from Google Earth	9.9	32.374306	-64.679036	basal brackish peat	*Rhizophora mangle* (Vollbrecht, 1996, Table 2)	**index**	6070 ±110	6070	110	N/A	IntCal13	6787	7028	0.839	6673	7179	0.98	6907.5	120.5	6926	253
58	ACN #TC	St. George's Harbour	ML 551	Vollbrecht (1996)	Not specified in Vollbrecht (1996), so a central position in St Georges' Harbour estimated from Google Earth	12.3	32.374306	-64.679036	freshwater peat	Wax Myrtle (Vollbrecht,, 1996, Table 2)	terrestrial limiting	7460 ±120	7460	120	N/A	IntCal13	8173	8389	1	8011	8458	0.995	8281	108	8234.5	223.5
59	SGH 02: 6.14-6.22	St. George's Harbour	KI-2001	Vollbrecht (1996)	Estimated from Appendix in Vollbrect (1996)	20.1	32.377759	-64.675211	freshwater peat	No data	terrestrial limiting	8780 ±100	8780	100	-29.1	IntCal13	9605	9922	0.897	9553	9970	0.77	9763.5	158.5	9761.5	208.5
60	Unlabeled	Long Bay, Somerset Bermuda	I-1685	Redfield 1967	Estimate of position from Google Earth	0.5	32.305502	-64.872838	freshwater peat	No data	terrestrial limiting	880 ±120	880	120	N/A	IntCal13	725	914	0.942	645	1009	0.969	819.5	94.5	827	182
61	Unlabeled	Long Bay, Somerset Bermuda	I-1969	Redfield 1967	Estimate of position from Google Earth	0.6	32.305502	-64.872838	freshwater peat	No data	terrestrial limiting	1210 ±95	1210	95	N/A	IntCal13	1056	1191	0.689	955	1295	1	1123.5	67.5	1125	170

62	Unlabeled	Long Bay, Somerset Bermuda	I-1764	Redfield 1967	Estimate of position from Google Earth	1	32.305502	-64.872838	freshwater peat	No data	terrestrial limiting	1510 ±110	1510	110	N/A	IntCal13	1314	1445	0.66	1255	1628	0.974	1379.5	65.5	1441.5	186.5
63	Unlabeled	Long Bay, Somerset Bermuda	I-1971	Redfield 1967	Estimate of position from Google Earth	1.3	32.305502	-64.872838	freshwater peat	No data	terrestrial limiting	2440 ±110	2440	110	N/A	IntCal13	2358	2540	0.636	2306	2758	0.983	2449	91	2532	226
64	Unlabeled	Long Bay, Somerset Bermuda	I-1973	Redfield 1967	Estimate of position from Google Earth	1.7	32.305502	-64.872838	freshwater peat	No data	terrestrial limiting	2530 ±100	2530	100	N/A	IntCal13	2489	2748	1	2350	2787	1	2618.5	129.5	2568.5	218.5
65	Unlabeled	Long Bay, Somerset Bermuda	I-1975	Redfield 1967	Estimate of position from Google Earth	2	32.305502	-64.872838	freshwater peat	No data	terrestrial limiting	2690 ±90	2690	90	N/A	IntCal13	2740	2887	0.952	2690	3037	0.933	2813.5	73.5	2863.5	173.5
66	Unlabeled	Long Bay, Somerset Bermuda	I-1686	Redfield 1967	Estimate of position from Google Earth	2.3	32.305502	-64.872838	freshwater peat	No data	terrestrial limiting	3900 ±120	3900	120	N/A	IntCal13	4151	4446	0.897	3979	4645	0.975	4298.5	147.5	4312	333
67	Unlabeled	Long Bay, Somerset Bermuda	I-1762	Redfield 1967	Estimate of position from Google Earth	3.1	32.305502	-64.872838	freshwater peat	No data	terrestrial limiting	3600 ±120	3600	120	N/A	IntCal13	3817	4014	0.647	3588	4241	1	3915.5	98.5	3914.5	326.5
68	Unlabeled	Long Bay, Somerset Bermuda	I-1763	Redfield 1967	Estimate of position from Google Earth	3.2	32.305502	-64.872838	freshwater peat	No data	terrestrial limiting	3930 ±120	3930	120	N/A	IntCal13	4223	4525	0.896	4073	4659	0.922	4374	151	4366	293
69	NL 031/4: 4.73-4.81	North Lagoon	KI-1991.02	Kuhn (1984)	Gischler and Kuhn (2018)	26.1	32.443	-64.643	freshwater peat	No data	terrestrial limiting	9700 ±90	9700	90	-28.5	IntCal13	11070	11228	0.68	10761	11247	1	11149	79	11004	243
70	NL 039: 1.5-1.6	North Lagoon	KI-1992	Kuhn (1984)	Gischler and Kuhn (2018)	19.6	32.328	-64.89	freshwater peat	No data	terrestrial limiting	7870 ±95	7870	95	-27.8	IntCal13	8552	8782	0.817	8510	8995	0.974	8667	115	8752.5	242.5
71	NL 040: 4.78-4.81	North Lagoon	KI-1993.04	Kuhn (1984)	Gischler and Kuhn (2018)	23	32.443	-64.798	freshwater peat	No data	terrestrial limiting	9230 ±150	9230	150	-31.3	IntCal13	10238	10579	1	10126	10796	0.955	10408.5	170.5	10461	335
72	NL 048: 2.31-2.35	North Lagoon	KI-1994.02	Kuhn (1984)	Gischler and Kuhn (2018)	17	32.33	-64.75	freshwater peat	No data	terrestrial limiting	8710 ±80	8710	80	-27.1	IntCal13	9548	9780	0.989	9531	9936	0.965	9664	116	9733.5	202.5
73	NL049: 1.07-1.12	North Lagoon	KI-1995	Kuhn (1984)	Gischler and Kuhn (2018)	3.1	32.3	-64.87	freshwater peat	No data	terrestrial limiting	3980 ±55	3980	55	-24.3	IntCal13	4404	4527	0.942	4248	4578	0.995	4465.5	61.5	4413	165
74	NL051: 2.83-2.87	North Lagoon	KI-1996.04	Kuhn (1984)	Gischler and Kuhn (2018)	14.6	32.307	-64.876	freshwater peat	No data	terrestrial limiting	8010 ±95	8010	95	-28.8	IntCal13	8725	9011	1	8596	9128	1	8868	143	8862	266
75	NL 054: 4.52-4.57	North Lagoon	KI-2585.02	Vollbrecht (1996)	Estimated from Appendix in Vollbrect (1996)	19.1	32.36262	-64.71724	freshwater peat	No data	terrestrial limiting	9010 ±125	9010	125	-28.5	IntCal13	9909	10274	1	9729	10438	0.977	10091.5	182.5	10083.5	354.5
76	NL 055/2: 5.5-5.54	North Lagoon	KI-2586.03	Vollbrecht (1996)	Estimated from Appendix in Vollbrect (1996)	18.3	32.36187	-64.716751	freshwater peat	No data	terrestrial limiting	8800 ±120	8800	120	-28.1	IntCal13	9664	9949	0.735	9555	10174	1	9806.5	142.5	9864.5	309.5
77	MS-C6	Mill Share	GX-21542	Javaux (1999)	Not specified in Javaux (1999), so a central position in the wetland was chosen	2.71	32.294518	-64.801283	mangrove peat	No data	impacted by autocompaction	2940 ±60	2940	60	N/A	IntCal13	2997	3175	1	2924	3251	0.976	3086	89	3087.5	163.5
78	DC06	Mill Share	GX-21545	Javaux (1999)	Not specified in Javaux (1999), so a central position in the wetland was chosen	2.9	32.294518	-64.801283	basal brackish peat	No data	terrestrial limiting	2930 ±60	2930	60	N/A	IntCal13	2992	3167	1	2921	3243	0.977	3079.5	87.5	3082	161
79	C05	Mill Share	GX-21543	Javaux (1999)	Not specified in Javaux (1999), so a central position in the wetland was chosen	2.32	32.294518	-64.801283	basal brackish peat	No data	terrestrial limiting	1070 ±60	1070	60	N/A	IntCal13	930	1009	0.733	905	1151	0.952	969.5	39.5	1028	123
80	C02	Mill Share	GX-21544	Javaux (1999)	Not specified in Javaux (1999), so a central position in the wetland was chosen	1.37	32.294518	-64.801283	mangrove peat	No data	impacted by autocompaction	510 ±55	510	55	N/A	IntCal13	505	555	0.857	477	569	0.722	530	25	523	46
81	DC05	Mills Creek	GX-21546	Javaux (1999)	Not specified in Javaux (1999), so a central position in the wetland was chosen	4.45	32.300589	-64.80162	basal brackish peat	No data	terrestrial limiting	2940 ±60	2940	60	N/A	IntCal13	2997	3175	1	2924	3251	0.976	3086	89	3087.5	163.5
82	DC05	Hungry Bay	GX-21547	Javaux (1999)	Not specified in Javaux (1999), so a central position in the wetland was chosen	1.65	32.290241	-64.758863	basal brackish peat	No data	terrestrial limiting	2010 ±50	2010	50	N/A	IntCal13	1893	2004	0.978	1869	2114	1	1948.5	55.5	1991.5	122.5
83	HB1-9	Hungry Bay	not given (Beta)	Ellison (1993)	Estimated using Google Earth and Fig 3 from paper	5.55	32.290233	-64.759236	mangrove peat	Terrestrial marshes did not exist in Hungy Bay (at HB-1) prior to 2000 years ago (Ellison, 1996)	terrestrial limiting	4870 ±90	4870	90	-27	IntCal13	5577	5718	0.756	5447	5761	0.892	5647.5	70.5	5604	157
84	HB2-1	Hungry Bay	not given (Beta)	Ellison (1993)	Estimated using Google Earth and Fig 3 from paper	5.45	32.291561	-64.758066	mangrove peat	Terrestrial marshes did not exist in Hungy Bay prior to 2000 years ago (Ellison, 1996)	terrestrial limiting	4940 ±100	4940	100	-27.6	IntCal13	5588	5753	0.852	5573	5912	0.933	5670.5	82.5	5742.5	169.5

85	HB5-2	Hungry Bay	not given (Beta)	Ellison (1993)	Estimated using Google Earth and Fig 3 from paper	2.25	32.28906	-64.75989	mangrove peat	Terrestrial marshes did not exist in Hungy Bay prior to 2000 years ago (Ellison, 1996)	terrestrial limiting	3990 ±110	3990	110	-27.4	IntCal13	4285	4587	0.895	4216	4729	0.871	4436	151	4472.5	256.5
86	HB1-1	Hungry Bay	not given (Beta)	Ellison (1993)	Estimated using Google Earth and Fig 3 from paper	0.65	32.290233	-64.759236	mangrove peat	*Rhizophora mangle* (Ellison, 1993, Global Ecology and Biogeography Letters)	terrestrial limiting	390 ±90	390	90	-25.1	IntCal13	425	510	0.555	282	556	0.977	467.5	42.5	419	137
87	HB1-2	Hungry Bay	not given (Beta)	Ellison (1993)	Estimated using Google Earth and Fig 3 from paper	1.45	32.290233	-64.759236	mangrove peat	*Rhizophora mangle* (Ellison, 1993, Global Ecology and Biogeography Letters)	terrestrial limiting	1080 ±80	1080	80	-26.4	IntCal13	920	1080	0.968	892	1182	0.913	1000	80	1037	145
88	HB1-3	Hungry Bay	not given (Beta)	Ellison (1993)	Estimated using Google Earth and Fig 3 from paper	2.45	32.290233	-64.759236	mangrove peat	Terrestrial marshes did not exist in Hungy Bay prior to 2000 years ago (Ellison, 1996)	terrestrial limiting	2090 ±90	2090	90	-21	IntCal13	1946	2154	0.932	1881	2311	1	2050	104	2096	215
89	HB1-4	Hungry Bay	not given (Beta)	Ellison (1993)	Estimated using Google Earth and Fig 3 from paper	3.45	32.290233	-64.759236	mangrove peat	Terrestrial marshes did not exist in Hungy Bay prior to 2000 years ago (Ellison, 1996)	terrestrial limiting	2740 ±110	2740	110	-26.9	IntCal13	2749	2966	1	2697	3171	0.97	2857.5	108.5	2934	237
90	HB1-6	Hungry Bay	not given (Beta)	Ellison (1993)	Estimated using Google Earth and Fig 3 from paper	4.45	32.290233	-64.759236	mangrove peat	Terrestrial marshes did not exist in Hungy Bay prior to 2000 years ago (Ellison, 1996)	terrestrial limiting	3880 ±100	3880	100	-26.5	IntCal13	4152	4424	1	3985	4537	0.991	4288	136	4261	276
91	HB2-2	Hungry Bay	not given (Beta)	Ellison (1993)	Estimated using Google Earth and Fig 3 from paper	0.85	32.291561	-64.758066	mangrove peat	Terrestrial marshes did not exist in Hungy Bay at HB-2 prior to 750 years ago (Ellison, 1996)	terrestrial limiting	730 ±80	730	80	-25.3	IntCal13	639	735	0.828	541	796	0.992	687	48	668.5	127.5
92	HB4-1	Hungry Bay	not given (Beta)	Ellison (1993)	Estimated using Google Earth and Fig 3 from paper	0.23	32.289378	-64.759618	mangrove peat	Mangrove peat (Ellison, 1993, Global Ecology and Biogeography Letters)	terrestrial limiting	750 ±60	750	60	-25.3	IntCal13	658	733	1	634	790	0.921	695.5	37.5	712	78
93	HB5-1	Hungry Bay	not given (Beta)	Ellison (1993)	Estimated using Google Earth and Fig 3 from paper	0.35	32.28906	-64.75989	mangrove peat	Mangrove peat (Ellison, 1993, Global Ecology and Biogeography Letters)	terrestrial limiting	1460 ±60	1460	60	-22.3	IntCal13	1303	1396	1	1285	1423	0.86	1349.5	46.5	1354	69
94	DC04	Hungry Bay	UGAMS-4589	van Hengstum et al (2011)	Not specified in van Hengstum (2011), a northeastern position in the wetland was chosen	2.57	32.291685	-64.757743	mangrove peat	Terrestrial marshes did not exist in Hungy Bay prior to 2000 years ago (Ellison, 1996)	terrestrial limiting	2580 ± 20	2580	20	-26.1	IntCal13	2731	2748	1	2720	2751	1	2739.5	8.5	2735.5	15.5
95	DC05	Hungry Bay	UGAMS-4590	van Hengstum et al (2011)	Not specified in van Hengstum (2011), a northeastern position in the wetland was chosen	1.19	32.291685	-64.757743	mangrove peat	Dr. David B. Scott examined marsh foraminifera in these samples	terrestrial limiting	810 ± 20	810	20	-23.3	IntCal13	698	730	1	684	748	0.978	714	16	716	32
96	DC06	Hungry Bay	UGAMS-4591	van Hengstum et al (2011)	Not specified in van Hengstum (2011), a northeastern position in the wetland was chosen	0.85	32.291685	-64.757743	mangrove peat	Dr. David B. Scott examined marsh foraminifera in these samples	terrestrial limiting	230 ± 20	230	20	-24.7	IntCal13	285	298	0.613	280	306	0.573	291.5	6.5	293	13

97	DC17	Hungry Bay	UGAMS-4592	van Hengstum et al (2011)	Not specified in van Hengstum (2011), a northeastern position in the wetland was chosen	0.7	32.291685	-64.757743	mangrove peat	Dr. David B. Scott examined marsh foraminifera in these samples	terrestrial limiting	530 ± 20	530	20	-24.2	IntCal13	525	544	1	516	554	0.937	534.5	9.5	535	19
98	DC18	Hungry Bay	UGAMS-4593	van Hengstum et al (2011)	Not specified in van Hengstum (2011), a northeastern position in the wetland was chosen	0.6	32.291685	-64.757743	mangrove peat	Dr. David B. Scott examined marsh foraminifera in these samples	terrestrial limiting	490 ± 20	490	20	-24.2	IntCal13	513	529	1	507	537	1	521	8	522	15
99	DC13	Hungry Bay	UGAMS-4594	van Hengstum et al (2011)	Not specified in van Hengstum (2011), a northeastern position in the wetland was chosen	1.96	32.291685	-64.757743	mangrove peat	Terrestrial marshes did not exist in Hungy Bay prior to 2000 years ago (Ellison, 1996)	terrestrial limiting	3240 ± 25	3240	25	-25.6	IntCal13	3443	3480	0.68	3392	3511	882	3461.5	18.5	3451.5	59.5
100	DC14	Hungry Bay	UGAMS-4595	van Hengstum et al (2011)	Not specified in van Hengstum (2011), a northeastern position in the wetland was chosen	1.82	32.291685	-64.757743	mangrove peat	Terrestrial marshes did not exist in Hungy Bay prior to 2000 years ago (Ellison, 1996)	terrestrial limiting	2800 ± 25	2800	25	-25.6	IntCal13	2865	2929	0.976	2844	2965	0.994	2897	32	2904.5	60.5
101	DC15	Hungry Bay	UGAMS-4596	van Hengstum et al (2011)	Not specified in van Hengstum (2011), a northeastern position in the wetland was chosen	2.02	32.291685	-64.757743	mangrove peat	Terrestrial marshes did not exist in Hungy Bay prior to 2000 years ago (Ellison, 1996)	terrestrial limiting	3110 ± 30	3110	30	-25.3	IntCal13	3331	3373	0.565	3237	3386	1	3352	21	3311.5	74.5
102	DC07	Hungry Bay	UGAMS-4597	van Hengstum et al (2011)	Not specified in van Hengstum (2011), a northeastern position in the wetland was chosen	3.44	32.291685	-64.757743	mangrove peat	Terrestrial marshes did not exist in Hungy Bay prior to 2000 years ago (Ellison, 1996)	terrestrial limiting	3630 ± 25	36330	25	-26.1	IntCal13	3906	3874	1	3867	3990	0.943	3890	-16	3928.5	61.5
103	DCC8B	Hungry Bay	OS-72328	van Hengstum et al (2011)	Not specified in van Hengstum (2011), a northeastern position in the wetland was chosen	2.01	32.291685	-64.757743	mangrove peat	Terrestrial marshes did not exist in Hungy Bay prior to 2000 years ago (Ellison, 1996)	terrestrial limiting	2490 ± 45	2490	45	-26.4	IntCal13	2491	2643	0.788	2424	2738	0.971	2567	76	2581	157
104	GB-Core 5, 31.25 cm	Green Bay Cave	OS-78019	van Hengstum et al (2011)	Estimated from Google Earth, based on overlays of underwater cave surveys and maps	2.25	32.32609	-64.739467	marine sediment	bivalve	marine limiting	2040 ± 25	2040	25	-0.57	IntCal13	1949	2007	0.827	1926	2063	0.958	1978	29	1994.5	68.5
105	GB-Core 9, 37.5 cm	Green Bay Cave	OS-81364	van Hengstum et al (2011)	Estimated from Google Earth, based on overlays of underwater cave surveys and maps	2.25	32.326145	-64.739456	marine sediment	bivalve	marine limiting	2000 ± 25	2000	25	0.29	IntCal13	1926	1988	1	1892	1997	1	1957	31	1944.5	52.5
106	GB-Core 11, 37.25 cm	Green Bay Cave	OS-81365	van Hengstum et al (2011)	Estimated from Google Earth, based on overlays of underwater cave surveys and maps	2.25	32.326306	-64.739394	marine sediment	bivalve	marine limiting	2020 ± 25	2020	25	0.29	IntCal13	1942	1996	0.963	1898	2009	0.947	1969	27	1953.5	55.5
107	GB-Core 5, 51.5 cm	Green Bay Cave	OS-80321	van Hengstum et al (2011)	Estimated from Google Earth, based on overlays of underwater cave surveys and maps	14.3	32.32609	-64.739467	sediment	marine foraminifera, ostracodes, calcite rafts	marine limiting	6800 ± 25	6800	25	-0.14	IntCal13	7619	7664	1	7594	7676	1	7641.5	22.5	7635	41
108	GB-Core 5, 61.25 cm	Green Bay Cave	OS-79218	van Hengstum et al (2011)	Estimated from Google Earth, based on overlays of underwater cave surveys and maps	20.8	32.32609	-64.739467	sediment	marine foraminfera, ostracodes, calcite rafts	marine limiting	7160 ± 65	7160	65	-1.59	IntCal13	7931	8032	0.951	7915	8073	0.778	7981.5	50.5	7994	79

109	GB-Core 9, 59.5 cm	Green Bay Cave	OS-81373	van Hengstum et al (2011)	Estimated from Google Earth, based on overlays of underwater cave surveys and maps	14.3	32.326145	-64.739456	sediment	marine foraminifera, ostracodes, calcite rafts	marine limiting	6700 ± 35	6700	35	-0.72	IntCal13	7562	7595	0.685	7494	7622	1	7578.5	16.5	7558	64
110	GB-Core 11, 46.75 cm	Green Bay Cave	OS-81369	van Hengstum et al (2011)	Estimated from Google Earth, based on overlays of underwater cave surveys and maps	20.7	32.326306	-64.739394	sediment	marine foraminifera, ostracodes, calcite rafts	marine limiting	7210 ± 40	7210	40	-0.93	IntCal13	7964	8047	1	7955	8071	0.802	8005.5	41.5	8013	58
111	SM-C15_79-80 cm	Palm Cave System	OS-129829	this work	Estimated from Google Earth, based on overlays of underwater cave surveys and maps	22.7	32.345361°	-64.711628°	sediment	brackish foraminifera (*Polysaccamina ipohalina, Entzia macrescens*)	marine limiting	8710 ± 35	8710	35	-26.8	IntCal13	9584	9697	0.945	9548	9782	0.996	9640.5	56.5	9665	117
112	SM-C14_86-87 cm	Palm Cave System	OS-135568	this work	Estimated from Google Earth, based on overlays of underwater cave surveys and maps	21.6	32.345039	-64.711257	sediment	brackish foraminifera (*Polysaccamina ipohalina, Entzia macrescens*)	marine limiting	8740 ± 30	8740	30	-24.7	IntCal13	9583	9827	0.831	9540	9955	0.881	9705	122	9747.5	207.5
113	SM-C10_174-175 cm	Palm Cave System	OS-122745	this work	Estimated from Google Earth, based on overlays of underwater cave surveys and maps	22.4	32.344779	-64.711037	sediment	brackish foraminifera (*Polysaccamina ipohalina, Entzia macrescens*)	marine limiting	8680 ± 35	8680	35	-23.7	IntCal13	9556	9634	0.828	9554	9704	0.998	9595	39	9629	75

Notes:

(1) Brackish peat verified by salt marsh foraminifera (Javaux, 1993) or botanical remains (Vollbrecht, 1996 and Ellison, 1993). However, we (this study) consider all the "basal peat" data previously reported from Hungry Bay as "Freshwater Peat", based on the extensive work of Kemp et al., (2019, Open Quaternary, doi.org/10.5334/oq.49.)

(2) Older ages without $d^{13}C$ values (not reported by original authors) reported may be offset by an additional few hundred years because a $d^{13}C$-correction could not be preformed.

(3) A maximum vertical uncertainty estimate (most conservative) on basal mangrove peat depth of Vollbrecht (1996) is the maximum 1.2 m tidal range in Bermuda

(4) Sample Index points 80-83 were $d^{13}C$-corrected (Javaux, 1999, p. 283), although $d^{13}C$ values not reported in original publication (the thesis).

(5) Table only includes samples collected from <30 m bsl.